Electronic Thesis and Dissertation Repository

12-15-2021 12:00 PM

Seizure Detection Using Deep Learning, Information Theoretic Measures and Factor Graphs

Bahareh Salafian, *The University of Western Ontario*

Supervisor: Farsad, Nariman, *The University of Western Ontario*
: De Ribaupierre, Sandrine, *The University of Western Ontario*
A thesis submitted in partial fulfillment of the requirements for the Master of Science degree in Biomedical Engineering
© Bahareh Salafian 2021

Recommended Citation

Abstract

Epilepsy is a common neurological disorder that disrupts normal electrical activity in the brain causing severe impact on patients' daily lives. Accurate seizure detection based on long-term time-series electroencephalogram (EEG) signals has gained vital importance for epileptic seizure diagnosis. However, visual analysis of these recordings is a time-consuming task for neurologists. Therefore, the purpose of this thesis is to propose an automatic hybrid model-based/data-driven algorithm that exploits inter-channel and temporal correlations. Hence, we use mutual information (MI) estimator to compute correlation between EEG channels as spatial features and employ a carefully designed 1D convolutional neural network (CNN) to extract additional information from raw EEGs. Then, seizure probabilities from combined features of MI estimator and CNN are applied to factor graphs to learn factor nodes. The performance of the algorithm is evaluated through measuring different parameters as well as comparing with previous studies. On CHB-MIT dataset, our generalized algorithm achieves state-of-the-art performance.

Keywords: Epilepsy, seizure detection, EEG, deep learning, 1D CNN, mutual information, factor graph

Summary for Lay Audience

Epilepsy is a common neurological disorder affecting about 50 million people worldwide. This disease is usually accompanied by the transient occurrence of signs or symptoms due to abnormal excessive electrical activity in the brain that may cause seizures. Our brain is constantly generating electrical pulses transmitted by neurons to control our movement, thoughts, and memories. In normal situations, neurons are firing independently or in small groups; however, during an epileptic seizure, many neurons fire simultaneously, 500 times faster than normal. The extensive sudden discharges in neural brain activity due to epileptic seizures scrambles the 'messages' that the brain sends out to the rest of the body. This can lead to life-threatening consequences such as involuntary movements, sensations, and emotions and may cause a temporary loss of awareness and even death. As such, early detection of epileptic seizures can significantly improve quality of life for patients experiencing epileptic seizures. The most common technique used to diagnose seizures is reviewing scalp electroencephalogram (EEG) signals by a neurologist. Visually scanning the recordings, however, is a time-consuming process due to contamination by physiological and non-physiological resources as well as the similarity of seizure spikes to normal EEG waveforms. As such, we have developed an automatic and generalized algorithm for seizure detection. To implement this approach, we capture two important underlying features that exist during seizure times, including computing inter-channel correlation among different EEG channels and temporal correlations between consecutive blocks. The first feature stems from the fact that when the seizure occurs in one or more parts of the brain, it propagates to other regions. This manifests itself as highly non-linear correlations among channels recording. The second property achieves due to spanning the seizure over multiple EEG blocks. Therefore, the thesis aims to propose a hybrid model-based/data-driven algorithm to exploit spatial and temporal correlations. The main two components in this algorithm are a neural mutual information estimator to compute inter-channel correlation and factor graph inference to exploit temporal correlations at reduced complexity. On the CHB-MIT dataset, our method obtains the best performance results compared to prior works.

Acknowledgements

I would like to express my sincerest gratitude to my supervisors, Dr. Sandrine De Ribaupierre and Dr. Nariman Farsad whose guidance and continuous support have been invaluable throughout my graduate studies. I am really grateful to have had the opportunity to work with these two amazing mentors. I would like to thank Dr. De Ribaupierre for the time she always took from her busy schedule to guide me with her clinical knowledge and research expertise during this thesis. I would like to express my deepest gratitude to Dr. Farsad for being a dedicated, patient and caring supervisor. His encouraging leadership style with his continuous optimism and motivational gratitude has made my Master's studies much more memorable and enjoyable experience. I was very fortunate to work with Dr. De Ribaupierre and Dr. Farsad and from both of them, I have learned how wonderful mentorship looks like and I will carry this with me to move forward in my research career.

I would also like to thank my advisory committee members, Dr. Roy Eagleson and Dr. Lyle Muller for their feedback and insights. Their constructive criticism and comments has helped me to follow the right direction and successfully complete my dissertation. I have also had the opportunity to collaborate with Dr. Nir Shlezinger and Eyal Fishel Ben from Ben-Gurion University of the Negev. I am really appreciative for their contribution to the factor graph study within this thesis. I would like to acknowledge my amazing lab mates at LIA Lab for their time they spent to improve my presentation skills. It has been an honor for me to work along side such a talented and collaborative team.

Finally, I would like to say huge thank you to my family. I am grateful to my brother for his happy distractions to rest my mind outside of the research. A special thank goes to my parents for allowing me to freely pursue my academic goals and dreams in Canada and always supporting me during tough time in my life. Thank you Mom and Dad for constantly encouraging me to be a happy, strong and hard working person. This journey would not have been possible without your support.

Co-Authorship Statement

Studies in this thesis are performed by collaboration of various researchers. The individual contributions are listed below:

Chapter 1: Bahareh Salafian—wrote manuscript; Sandrine De Ribaupierre—reviewed and revised manuscript; Nariman Farsad—reviewed and revised manuscript.

Chapter 2: Bahareh Salafian—study design, data analysis, performed experiments, wrote manuscript; Eyal Fishel Ben—study design, data analysis, performed experiments, wrote factor graph section; Nir Shlezinger—study design,reviewed and revised manuscript; Sandrine De Ribaupierre—reviewed and revised manuscript; Nariman Farsad—study design,reviewed and revised manuscript.

Chapter 3: Bahareh Salafian—study design, data analysis, performed experiments, wrote manuscript; Eyal Fishel Ben—study design, data analysis, performed experiments, wrote factor graph section; Nir Shlezinger—study design,reviewed and revised manuscript; Sandrine De Ribaupierre—reviewed and revised manuscript; Nariman Farsad—study design,reviewed and revised manuscript.

Chapter 4: Bahareh Salafian—study design, data analysis, performed experiments, wrote manuscript; Eyal Fishel Ben—study design, data analysis, performed experiments; Nir Shlezinger—study design,reviewed and revised manuscript; Sandrine De Ribaupierre—reviewed and revised manuscript; Nariman Farsad—study design,reviewed and revised manuscript.

Chapter 5: Bahareh Salafian—wrote manuscript; Sandrine De Ribaupierre—reviewed and revised manuscript; Nariman Farsad—reviewed and revised manuscript.

Contents

List of Figures

List of Tables

List of Abbreviations

EEG electroencephalogram

EOG electrooculogram

HMM Hidden Markov model

DL Deep learning

DNN deep neural network

CNN convolutional neural network

DWT discrete wavelet transform

RNN recurrent neural network

FLOPs floating point operations

MI mutual information

LSTM Long-Short Term Memory

SVM support vector machine

KL Kulback-Leibler

MICAL Mutual Information-based CNN-Aided Learned factor graphs

MAP maximum a-posteriori probability

RBF radial basis function

EDF European Data Format

Chapter 1

Introduction

1.1 Epilepsy

Epilepsy is a chronic neurological disorder that, according to World Health Organization, affects 50 million people worldwide [1]. This disease is usually accompanied by the transient occurrence of signs or symptoms resulting from abnormal excessive electrical activity in the brain that may cause seizures [22]. The brain is constantly generating electrical pulses transmitted by neurons to control our movement, thoughts, and memories. Neurons are responsible for transmitting an electrical pulse and sending 'messages' to nearby neurons and the rest of the body through neurotransmitters. In a normal state, neurons are firing in a small group to perform a task; however, during an epileptic seizure, many neurons fire at the same time – as many as 500 times a second, much faster than normal[1]. The extensive sudden discharges in neural brain activity due to epileptic seizures scrambles the 'messages' that the brain sends out to the rest of the body. This can lead to life-threatening consequences such as involuntary movements, sensations, and emotions and may cause a temporary loss of awareness and even death [65]. The number of epileptic seizures varies from person to person; some patients rarely experience seizures, while others may have hundreds of seizures per day. It should be noted that having a single seizure cannot be interpreted as epilepsy. A person is considered to have epilepsy when two or more unprovoked seizures occur within 24 hours. Depending on what

---

[1]https://www.ninds.nih.gov/Disorders/Patient-Caregiver-Education/Hope-Through-Research/Epilepsies-and-Seizures-Hope-Through

part of the brain causes the seizures, epileptic seizures are categorized into two main groups: focal and generalized seizures, and there are many different types of seizures described under these two categories [71]. Focal seizures start in one area of the brain, and they are defined based on the region where the seizure originates. However, generalized seizures result from abnormal neural activity that rapidly appear on both sides of the brain [71]. Epilepsy has various causes such as genetic mutations, brain tumors, head trauma, or abnormalities of brain development. However, for most cases, the underlying cause of epilepsy is unknown [39].

Seizure detection is essential in the neurologist's toolbox for deciding on suitable treatment options. Currently, this task is mainly performed by neurologists, which can be very time-consuming and prone to errors, and based on the previous study, it can lead to a 30% misdiagnosis rate [8]. An automated seizure detection system can alleviate this, allow for more long-term monitoring of patients, and better guidance in choosing the correct treatment options. In this thesis, we focus on automated seizure detection systems and propose a novel algorithm based on a combination of techniques from signal processing, information theory, and machine learning that achieves excellent detection performance and generalizability compared to prior work in this domain.

The rest of this chapter is organized as follows. In the remainder of this section, we discuss the diagnostic tests for epilepsy. Then in the next section, we describe the automated seizure detection systems and tools and methods applied in this domain. In Section 1.3, we describe the classification and detection techniques used for the seizure detection problem in the past. Finally, we end the chapter by presenting the research objectives and the overview of the rest of the thesis.

1.1.1 Diagnostic Tests for Epileptic Seizure

1.1.1.1 Experimental Tests

There are many different tests used to evaluate if a person has a form of epilepsy and, if so, what type of seizures the patient is suffering from. Using medical history, the doctor can use past illnesses or symptoms related to seizures as well as any family history for diagnosing epilepsy [54]. In some cases, blood tests show the metabolic or genetic disorders that might

be associated with the seizures [58, 39]. Other underlying health conditions such as infections, lead poisoning, anemia, and diabetes could also be the triggers of epileptic seizures [39]. Measuring motor abilities, behavior, and intellectual abilities through developmental, neurological, and behavioral tests can also help determine the type of epilepsy and how it is affecting the individual [26, 87].

1.1.1.2 Imaging and Monitoring

Imaging and monitoring are among the most common tools for detecting epileptic seizures. They are used to infer electrical activity and specify abnormal structures of the brain that lead to seizures. A magnetoencephalogram (MEG) [85] is a non-invasive medical tool that measures the magnetic fields generated by electrical currents in the brain. MEG helps identify surface abnormalities in brain activity. This method is mainly used in surgical procedures to remove focal areas of seizure while preventing brain function interference [85]. Brain scans including computed tomography (CT) [66], positron emission tomography (PET) [70] and magnetic resonance imaging (MRI) [46] are widely used in observing epileptic seizures. CT and MRI can be used to capture scans of the structural abnormalities in the brain, such as tumors or cysts that may lead to a seizure. A type of MRI called functional MRI (fMRI) [66] can measure the changes in blood flow to check functional abnormalities as a result of epileptic seizures. An expert can utilize PET to identify brain areas with abnormal metabolism even after the seizure stops. Single-photon emission computed tomography (SPECT) [15] is sometimes used to localize the epileptogenic zone(EZ) as precisely as possible and to define overlap between the EZ and eloquent cortex. Monitoring brain activity signal through EEG is the most common method in seizure detection [74].

The discovery of electrical properties of the brain was first stimulated by Richard Caton (1842–1926), a Liverpool physiologist, by recording electrical activity from the brains of animals using a sensitive galvanometer. This accomplishment indicated fluctuations in activity during sleep and the absence of activity following death. In 1902, Hans Berger (1873–1941), a German psychiatrist, used a capillary electrometer resulted in detecting EEG from the cortical surface of the dog, as had others before him. Berger believed that psychic function in the human would be expected to release metabolic energy in the form of localized heat and electrical

currents, leading to the understanding of normal and disturbed mental processes. Therefore, he recorded the first human EEGs in 1924. Fisher and Lowenback first discovered epileptiform spikes in 1934. One year later, Gibbs, and Lennox's team, demonstrated interictal epileptiform discharges and 3-Hz spike-wave patterns during clinical seizures. In 1936, Gibbs and Jasper described focal interictal spikes. The first clinical EEG laboratories were established in the United States in the 1930s and 40s, and in 1947, the American EEG Society, after the American Clinical Neurophysiology Society, was founded [73].

Currently, there are two main groups of EEG recording techniques: scalp EEG and invasive EEG [93]. During scalp EEG acquisition, multiple electrodes are attached to the scalp of individuals and are connected to a monitoring device using wires [93]. The position of each electrode is determined based on the International 10/20 system [4] and indicated by letters and numbers. As shown in Fig.1.1, letters represent the area of the brain under electrodes, e.g., F for frontal lobe and T for temporal lobe. Also, even numbers refer to the right side of the head and odd numbers denote the left side of the head. Invasive EEG also known as electrocorticography (ECoG) provides direct measurement of the brain electrical activity by implanting electrodes on the cortex [86]. These signals are usually recorded in conjunction with video monitoring of the patient. This technique is mainly employed when a patient is diagnosed with refractory epilepsy to determine the seizure onset zone that needs to be removed through surgery [86]. Since about 70% of patients with epileptic seizures can be treated successfully by anti-epileptic drugs while approximately 7% to 8% of cases require surgical resection, scalp EEG has been the most preferred method used in epilepsy applications due to its non-invasiveness and cost-benefit ratio [52].

Seizure detection generally consists of three steps: 1. signal acquisition, 2. signal processing, 3. feature extraction and classification. In the rest of this chapter, we first describe the advantages of having an automated seizure detection system and the motivation behind the proposed algorithm. In Subsection 1.2.2 to 1.3.1, we describe signal processing and machine learning techniques used in prior work for automatic seizure detection.
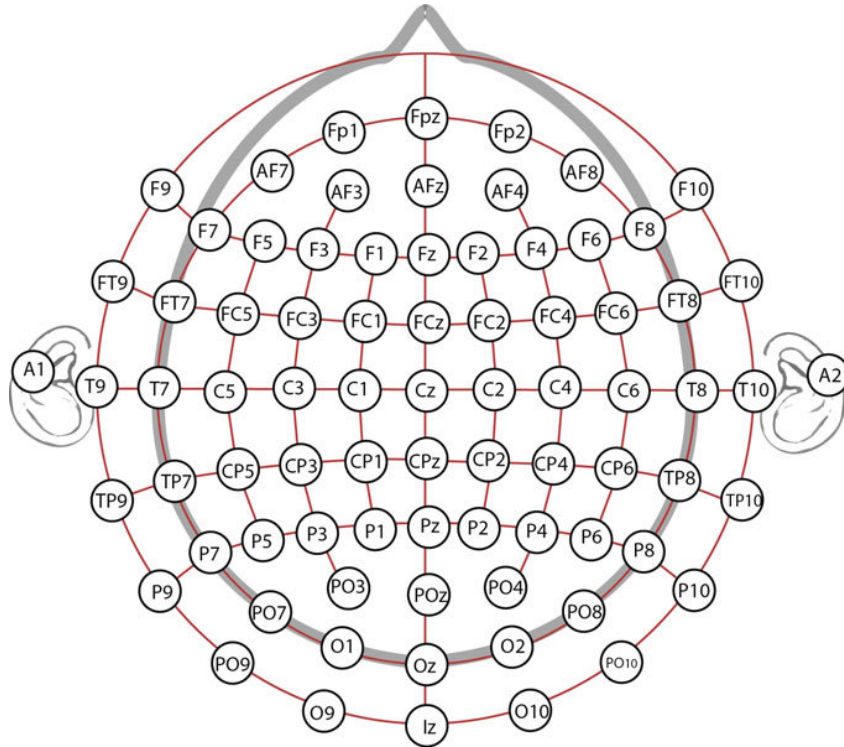
Figure 1.1: Electrode Placement according to the International 10-20 System[61].

1.2 Automated Seizure Detection System

1.2.1 Motivation

This thesis presents a novel automated seizure detection based on a hybrid model-based and data-driven approach. As mentioned in Subsection 1.1.1.2, an epileptic seizure is a critical clinical problem, and EEG is one of the most important tools to study epileptic seizure and capture changes in electrical brain activity that could indicate the seizure. The diagnosis of epileptic seizure usually depends on manual inspection of EEG by doctors, which is a time-consuming and error-prone procedure. Therefore, having automated seizure detection can enable long-term patient monitoring, decrease diagnosis time, and enable doctors to suggest more suitable treatment options for patients with epileptic seizures. Currently, some seizure tracking research relies on patients or families to report the number of seizures. However, in several cases, patients report only about half of their seizures that occur during the wakefulness and even less during sleep [30]. As such, automated seizure detection can provide more accurate seizure quantification and helps experts to select treatment more objectively and to better guide

research in this domain.

Prior detection approaches are sometimes based on limited features manually extracted by neurologists, which do not work well for detecting seizure patterns in EEG signal across a large population [91]. Moreover, existing machine learning and deep learning (DL) detection methods are not capable of capturing both spatial and temporal information effectively and efficiently for generalizability across patients [40, 36, 11, 63, 50].

To overcome these limitations, a system for automated seizure detection, called MICAL is proposed in this thesis. This algorithm has three main novelties:

1. Unlike prior work, our carefully designed CNN extracts features from raw EEG signals that can capture 1 second of data as a receptive field. In contrast to 2D CNN used in previous study [11], our architecture can combine all measurements from different EEG channels at a given time instance and operates on the raw signals with minimal pre-processing.

2. When a seizure occurs as sharp wave discharges in one or more EEG channels, it affects patterns of other channel's recordings. As such, the neural MI estimator used in this study computes instantaneous dependencies among EEG channels capturing the inter-channel correlations during the seizure. To the best of our knowledge, this is the first time that MI is used for estimating the correlation between EEG channels, which can then be used as features for the detection of seizures. One of the benefits of the neural MI estimator used in the proposed algorithm over traditional methods such as cross-correlation is that it can measure correlation even in the presence of a highly non-linear relationship between EEG channels.

3. The previous items capture the signal level features and inter-channel correlations as an extra feature for seizure detection. However, there are also temporal correlations in EEG signals. To capture the temporal correlations, factor graph inference is applied on the features extracted by the 1D CNN and MI estimator to learn factor nodes. Using HMM and message passing over factor graphs, a final estimate of seizure start and end time is obtained in a computationally efficient manner. Note that in our algorithm MI is used to

capture the inter-channel correlations, while factor graph is used to capture the temporal correlations in the EEG recordings.

In Subsection 1.2.2, we first explain previous signal processing techniques specifically applied to EEG recordings in order to remove various noises and interferences. We then, in Subsection 1.3.1 discuss different algorithms that have been already explored for seizure classification and detection.

1.2.2 Signal processing

As explained in Subsection 1.1.1.2, EEG shows electrical activity in the brain and is used as a tool in epileptic seizure diagnosis and choosing suitable treatments. However, EEGs are prone to be contaminated by undesired artifacts. The artifacts can be due to recording instruments such as bad electrodes, line noise, and high electrode impedance [25], or can be caused by physiological artifacts such as eye movements, eye blinks, cardiac activity, and muscle activity, which are typically more complicated to remove [19]. The existence of such artifacts can interfere with neural information, which can lead to misdiagnosing epileptic seizures [37]. In the following sections, we describe some of the techniques for artifact removal, specifically physiologic artifacts.

1.2.2.1 Regression

Ocular artifacts due to eye movements and blinks are one of the sources of artifacts that contaminate EEG recordings. The origin of this artifact is due to the significant difference in potential between the cornea and the retina. Ocular artifacts result in shifting electric fields that propagate across the whole head, which can be much larger than the electrical activity produced by the brain. The electrooculogram (EOG) signals obtained through electrodes located near the eyes can be employed to estimate and remove ocular interference. Regression techniques are the most common methods for estimating and removing ocular artifacts [44]. This method can be used in both time and frequency domains, and it relies on the assumption that the observed signal in each EEG channel is the sum of the artifact-free EEG recording and artifacts

cause by eye movement [76]. Hence, the regression method aims to find the coefficients which characterize the spread of EOG in EEG signal. This can be formulated as:

$$EEG_{cor} = EEG_{raw} - \gamma F(HEOG) - \delta F(VEOG), \tag{1.1}$$

where, γ and δ are estimated parameters between reference channels and EEG channels and EEG_{cor} and EEG_{raw} denote denoised and raw EEG signals, respectively. HEOG and VEOG represent the recordings from horizontal and vertical EOG channels. Regression-based denoised filtering has two steps. First, a calibration phase determines the value of the coefficients. Then, noise components are estimated and removed in the second phase.

1.2.2.2 Wavelet Transform (WT)

The wavelet-based technique is another denoising method that has been proposed for EEG signals [35]. Unlike windowed representation in short time Fourier transform, WT can provide smooth representation. Hence, it could capture fine details, sudden changes, and similarities in EEG signals. WT transforms the recording into time as well as frequency domain. This strategy involves three main phases: 1) decomposing the signal through selected mother wavelet and level of decomposition, 2) applying a threshold on the resultant coefficients, and 3) reconstructing the corrected EEG signal. The WT is based on a time-variant decomposition, which means it is possible to choose different filter settings (e.g., wavelet coefficients) for different time intervals. The WT can be represented as the following integral:

$$W_x(u, s) = \int_{-\infty}^{\infty} x(t)\, \Phi_{u,s}(t)\, dx \tag{1.2}$$

In (1.2), the input signal $x(t)$ is correlated with the wavelet with translation parameter u and dilation parameter s. This transform converts the signal into coefficients representing more time resolution at higher frequencies and more frequency resolution at lower frequencies. Although this technique can be applied in real-time, choosing the threshold is a complicated process.

1.2.2.3 Principle Component Analysis (PCA)

PCA is one of the most popular and simplest denoising algorithms for blind source separation [47]. In the case of EEG denoising, PCA can be used to divide signals into a smaller number of artificial variables called principal components (PCs). The objective of PCA is to reduce the dimensionality of the dataset while keeping the variations present in the dataset. PCs are uncorrelated, spatially orthogonal, and ordered such that the first few components capture most of the variations that exist in the original feature variables [69]. PCA is performed by eigenvalue decomposition of the data covariance matrix, typically after the mean centering of the data. Mathematically, PCA transforms a set of n correlated variables $X = (x_1, x_2, \ldots, x_n)$ into a set of uncorrelated variables (PCs) $(p_1, p_2, \ldots, p_n)$. While PCA algorithm is simple, it decomposes the signals into uncorrelated but not necessarily independent components. Thus it is not able to deal with higher-order statistical dependencies, which might exist between EEG samples. Finally, this method does not work well when EEGs have comparable amplitudes.

1.2.2.4 Independent Component Analysis (ICA)

The ICA-based denoising technique can be viewed as a modified version of PCA since it decomposes the signal into independent components (ICs) using higher-order statistics. ICA assumes that signal sources are instantaneously linear mixtures of cerebral and artifactual sources. Once ICs are obtained from original signals, the denoised signal is reconstructed by removing ICs containing artifacts [69]. ICA is usually performed under the following assumptions:

- Source signals are statistically independent of each other and are instantaneously mixed.

- The dimension of the observation signal must be greater than or equal to the source signal.

- The sources are non-Gaussian, or only one source is Gaussian.

However, the acquisition of EEG signals is not usually linear under the instantaneous mixture assumption. Moreover, sources are not known in advance and can potentially exhibit Gaussian-

like distribution. Another limitation is that ICA operates in time-space, whereas artifacts have narrow frequency ranges.

1.2.2.5 Filtering Methods

Numerous filtering algorithms have been proposed for artifact removal from EEG signals. Below we describe two commonly used filtering approaches for artifact removal.

- The first approach is based on basic low-pass, high-pass, band-pass, and notch filters. For example, the notch filter is used to remove power-line noise wires, light fluorescent, and other artifacts caused by equipment that can interfere with EEG records [57].

- The second approach is based on adaptive filters. An adaptive filter estimates the interfering signals in the EEG recording using an iterative algorithm [55]. While adaptive filters can efficiently remove linear interferences, removing nonlinear interferences using adaptive filters results in high computational complexity.

1.3   Classification and Detecting Epileptic Seizure

In seizure detection problem, there are few basic terms as follows:

- Ictal state which is the time when the seizure occurs (from start to end).

- Preictal state is a period just before a seizure occurs.

- Interictal state refers to the period between seizures.

- Postictal state is a period just after the seizure ends.

For this thesis, seizure detection refers to identifying ictal intervals from EEG recordings of patients with epileptic seizures. One common way to analyze EEG signals for seizure detection is visually scanning the recordings by experienced neurologists. However, this process is time-consuming, inefficient, and is prone to human error, especially when there are long-term recordings [8]. In addition, this process is an expert-dependent process due to the subjective

nature of the analysis and various interictal spikes morphology. Another challenge in reviewing EEGs is their similarity to the artifacts caused by patient's movements. Therefore, to overcome the limitations associated with EEG monitoring, automatic seizure detection algorithms have been extensively explored. These techniques can be categorized into spike detection, feature engineering, and non-feature-based design. We begin this section by describing two popular classification architectures, followed by presenting different seizure detection methods used in prior work.

1.3.1 Classification architectures

One of the most important methods used for seizure detection is classification using machine learning. We describe two common machine learning techniques, support vector machine (SVM) and deep learning models, used in prior work below.

1.3.1.1 Support Vector Machine (SVM)

The support vector machine [60] is a model used for classification, which aims to find an optimal hyperplane used as a decision boundary to distinguish between different classes. The optimal hyperplane is selected such that it maximizes the margin to each class (i.e., the distance from the hyperplane to the nearest sample from each class) [60]. Conventional linear SVM is not helpful for problems such as seizure detection where the data may not be linearly-separable. In this scenario, kernel methods can be used to lift the signal to a higher dimensional space where the seizure and non-seizure states are linearly-separable. For example, the radial basis function (RBF) kernel has been used in [42] with SVM for seizure detection. The SVM is a binary classifier that can be extended to the multiclass SVM when the seizure detection output is categorized into more than two groups. One approach for multiclass SVM is using error-correcting output codes (ECOC) adopted from digital communication [82].

1.3.1.2 Deep Learning

DL architectures can learn a hierarchical feature representation automatically by providing sufficient input data [79]. Recent advances in DL architectures has motivated their application in

biology and medicine, for example in plant-phenotyping [59], analysis of ECG signals [84], assessment of ultrasound images of breast lesions [13], classification of skin lesions [17], or diagnosing breast cancer [27]. DL has two widely used architectures, convolutional neural networks (CNNs) and recurrent neural networks (RNNs). We describe each of these architectures below.

CNN Many layered neural network architectures such as CNNs are biologically-inspired models. One of the early works that inspired this layered approach is the work of Hubel and Wiesel's on the cat's visual cortex. By mapping the flow of visual information from the retina to the thalamus and the cortex, Hubel and Wiesel figured out that mammals visually perceive the world around them using a layered architecture of neurons in the brain. This observation was inspirational in using multiple layers in artificial neural networks such as CNN [31, 43]. The structure of the CNNs allows them to learn various types of features ranging from low-level features such as edges to higher-level features such as object parts and ultimately the entire shapes. The CNN consists of three main layers: convolutional layer, pooling layer, and fully connected (FC) layer.

1. **Convolutional layer** is the core block in a CNN. It consists of one or more filters (kernels) that are convolved with input data, e.g. images or EEG recordings, to extract features from the input data. Mathematically, the convolution operation is represented as follows [2]:

$$y_k = \sum_{n=0}^{N-1} x_n \times h_{k-n} \tag{1.3}$$

where x is input data, h is the filter, and y is the output, and N represents the number of elements in x. The subscript represents the indices. For example, x_n is indicative of the n_{th} element of the vector x.

2. **Pooling layer** also known as a down-sampling layer, is used for dimensionality reduction to decrease the number of elements in the input. Similar to the convolutional layer, a window is slided across the signal. Two main types of pooling layers include max-pooling and average-pooling. In max pooling, the maximum value of the signal in each

window is selected as the output. In average polling, the average value within the window is selected as the output. Max-pooling is more common than Average-pooling as it reduces computational complexity and prevents overfitting.

3. **Fully connected layer** is the last few layers of a CNN. It takes the features learned by the previous convolutional layers as input and performs classification based on these features. The last fully-connected layer in the network is typically a *sigmoid* function for a binary classification problem and a *softmax* activation function for a multi-class classification problem.

RNN Although CNNs are suitable for learning hierarchical representations, they have a limitation when samples are distributed dependently (e.g., in sequential data). Therefore, recurrent neural networks (RNN)s were introduced to pass information across sequences and model sequential data with temporal dependencies at multiple scales [51]. The input and the output for an RNN is typically a sequence. For instance, a sequence input can be denoted by $(x_{(1)}, x_{(2)}, \cdots, x_{(T)})$ where each $x_{(t)}$ is a real-valued vector. That is, an input sequence consists of data points from a discrete sequence, where $x_{(t)}$ is the input corresponding to the sequence step indexed by t. RNNs are feedforward neural networks connected by the inclusion of edges that span adjacent time steps that leads to establishing temporal dynamic behavior in the model. In this procedure, a feedforward neural network refers to the network where the output of higher layers is computed by setting the values of lower layers. In other words, the information flows in one direction, and connections between nodes do not form a cycle [51]. Like feedforward neural networks, RNNs may not have cycles among standard edges. However, those edges that connect adjacent time steps called recurrent edges may exhibit cycles, including cycles of length one that are self-connections from a node to itself across time [16]. The following equations represent the main principle behind RNN structure.

$$h_{(t)} = \sigma(W_{hx}x_{(t)} + W_{hh}h_{(t-1)} + b_h) \tag{1.4}$$
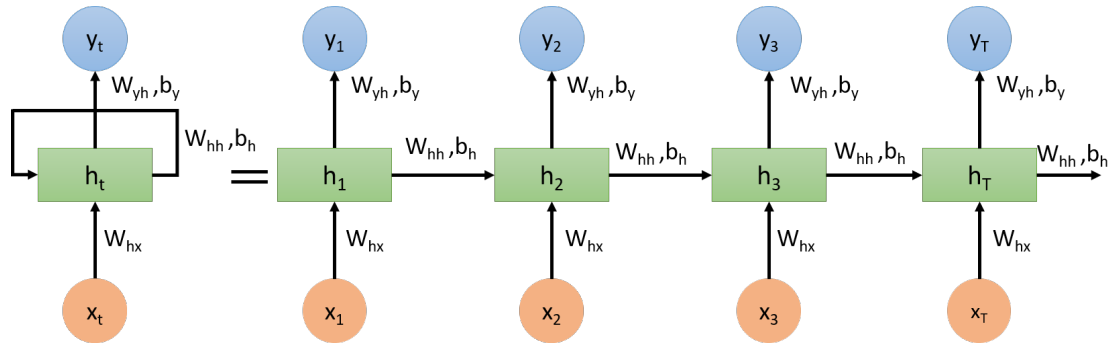
Figure 1.2: RNN structure.

$$\hat{y}_{(t)} = softmax(W_{yh}h_{(t)} + b_y). \tag{1.5}$$

Here W_{hx} is the matrix of conventional weights between the input and the hidden layer, and W_{hh} is the matrix of recurrent weights between the hidden layer and itself at adjacent time steps. The vectors b_h and b_y are bias parameters that allow each node to learn an offset.

Training an RNN is usually based on using forward pass evaluating a loss function that measures the error between the true label and the output, and a backward pass that updates the parameters to minimize the loss. Fig.1.2 provides visualization of an RNN architecture. First, the input is processed through the hidden layers for a single time step. Then, the estimated label is calculated in the last layer, and the total loss is computed. The derivatives are calculated during backward propagation to update the weights such that the loss is minimized. Since RNNs also can keep information from the past sequences during backpropagation, the gradients also move backward in time [9]. Therefore, long sequences can result in a deep RNN, which is prone to vanishing gradients or exploding gradients. The former occurs when derivatives at each step are small and become smaller as we move backward during backpropagation. This is because multiplying small gradients close to zero results in even smaller gradients. The gradients explode when the derivatives at each time step are too large. Therefore, as the gradients move backward, they get larger because multiplying numbers larger than one results in a larger gradient. Both vanishing and exploding gradients can stop the optimization from reaching a suitable local minimum and learning a good set of parameters.

To overcome some of the limitations of the vanilla RNNs, gated RNN can be used. We now describe the two most popular gated recurrent units, the Long short-term memory (LSTM), and the Gated Recurrent Units (GRU).

- **Long short-term memory (LSTM)**: was introduced to overcome the vanishing gradient problem [51]. Similar to a standard RNN, this model contains a hidden layer, but each node is substituted by an intermediate type of storage called a memory cell. In order to store the information and control the memory cell, LSTM uses a gating mechanism. Fig.1.3 shows the structure of an LSTM. We now describe the components of the LSTM below.

  1. Activation Functions: The *tanh* and *sigmoid* are two non-linear activation functions that regulate the flow of information in the LSTM cell. *Tanh* is used to ensure that the values flowing through the network are between -1 and 1. When values are passed through different transformations, some of them may become enormous and cause others to seem insignificant. Therefore, *tanh* avoids information fading. *Sigmoid* is used in the gates of the LSTM. Unlike *tanh*, it limits the values between 0 (to forget the information) and 1 (to update the information). *Sigmoid* helps the network learn, which information can be forgotten and which information must be kept from one time step to another. In fig.1.3, *sigmoid* is shown by red circles and *tanh* by blue circles.

  2. Input gate: The input gate updates the cell state. First, the current input and previous hidden state are concatenated and are passed through a fully-connected layer with a *sigmoid* activation function to select important information. Next, another fully connected layer with *tanh* activation function is applied to the current input x_t and previous hidden state h_{t-1}. Then output generated from both activation functions is used for point-wise multiplication, which results in adding information to the cell state. Mathematically this is represented by:

$$i_t = \sigma(W_i[h_{t-1}, x_t] + b_i) \tag{1.6}$$

$$\tilde{C}_t = tanh(W_C[h_{t-1}, x_t] + b_C) \tag{1.7}$$

where, i_t is input gate at timestep t, W_i and W_C are the weights, and b_i and b_C are the bias terms.

3. Forget gate: The forget gate is used to remove information from the cell state. First, the current input x_t and the previous hidden state h_{t-1} are concatenated and passed through a fully-connected layer with a *sigmoid* activation function. Based on the generated value, which is between 0 and 1, forget gate decides which the parts of the old cell state to remove (i.e., the parts corresponding to values that are close to zero). This is represented mathematically as,

$$f_t = \sigma(W_f[h_{t-1}, x_t] + b_f) \tag{1.8}$$

where, f_t is forget gate at time step t, W_f is the weight, and b_f is the bias. The value of f_t will be later used by the cell for point-wise multiplication.

4. Cell state: After the forget and input gates, the next step is to update the cell state according to the output of these gates. First, the previous cell state C_{t-1} is multiplied by the output of the forget gate f_t. Then, i_t and $\tilde{C}_t$ are used to further update the new cell state C_t. The following equation summarizes this process:

$$C_t = f_t * C_{t-1} + i_t * \tilde{C}_t \tag{1.9}$$

5. Output gate: As explained earlier, the hidden state contains information about previous inputs. The output gate decides the value of the next hidden state. First, the values of the previous hidden state and current input are concatenated and passed through a fully-connected layer with a *sigmoid* activation function. Then, a *tanh* function is applied to the new cell state C_t, and a pint-wise multiplication between the outputs of both functions is performed to determine the new hidden state. Math-

ematically this can represented as:

$$o_t = \sigma(W_o[h_{t-1}, x_t] + b_o) \tag{1.10}$$

$$h_t = o_t * \tanh(C_t) \tag{1.11}$$

where, o_t indicates output gate. Ultimately, the new hidden state and new cell state are passed to the next time step.

- **Gated Recurrent Units (GRU)**: Fig1.4 shows the structure of a GRU. This architecture is similar to the LSTM, but it has only two gates instead of three: a reset gate and an update gate. It also does not have a cell state. Mathematically the GRU can represented as:

$$u_t = \sigma(W_u[h_{t-1}, x_t] + b_u) \tag{1.12}$$

$$r_t = \sigma(W_r[h_{t-1}, x_t] + b_r) \tag{1.13}$$

$$\hat{h}_t = \tanh(W_h[x_t + r_t * h_{t-1}] + b_h) \tag{1.14}$$

$$h_t = (1 - u_t) * h_{t-1} + u_t * \hat{h}_t \tag{1.15}$$

where u_t and r_t represent update gate and reset gate, respectively. $\hat{h}_t$ indicates current memory content and h_t is output memory content.

GRU has less training time and uses less memory compared to LSTM as it has two gates instead of three gates. However, LSTM is more suitable for sequences with long-term
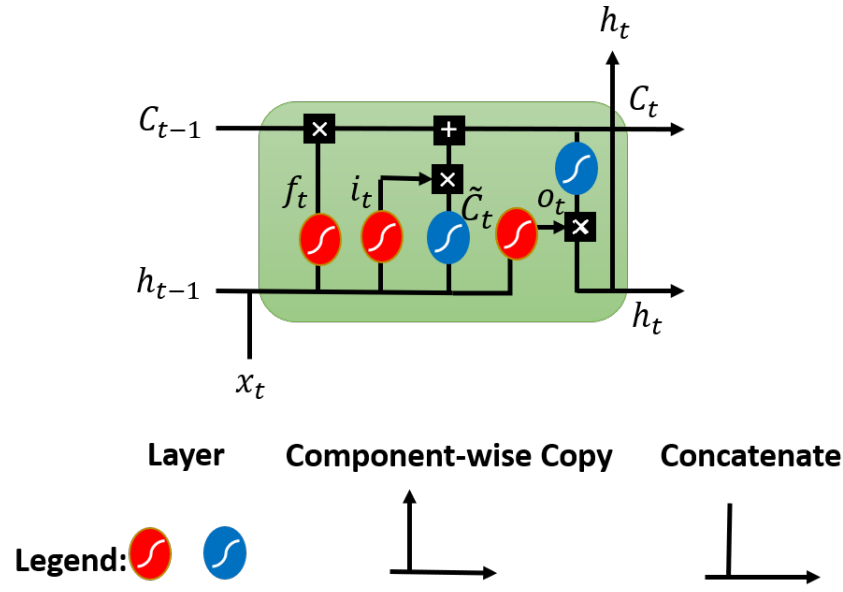
Figure 1.3: LSTM architecture with all gates and memory cell.

dependencies [90].

1.3.2 Spike Detection

A number of spike detection methods have been previously developed. These methods focus on detecting the presence of interictal spikes in the multichannel EEG recording with high sensitivity and selectivity [81]. They are divided into different categories: template matching, mimetic analysis, power spectral analysis, wavelet analysis, and artificial neural networks (ANNs). We now describe each of these methods below.

- Template matching is one of the most popular approaches for pattern recognition. This technique is proposed to match parts of the observed signal with a predefined template to measure shape similarity between measured signal and the template. A threshold is then applied to the similarity score for detection of the spikes [68, 89].

- In mimetic method, for seizure detection, each EEG channel is broken into segments. The sequences are then characterized as seizure or no seizure based on specific amplitude and duration relative to the background activity that are provided by the expertise of a neurologist [28, 29].
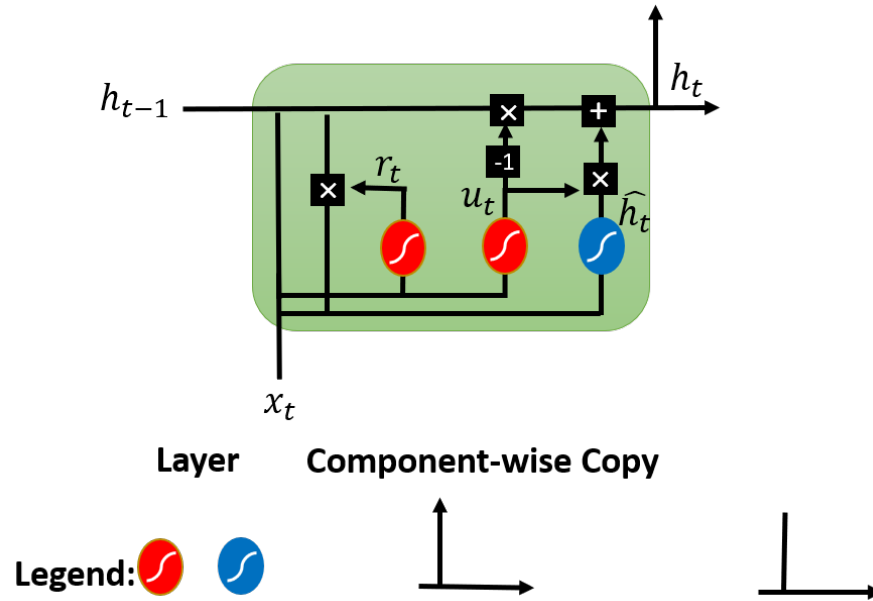
Figure 1.4: GRU architecture

- The seizure spike detection-based power spectral density proposed by Exarchos et al. [18] contains four stages. The first step eliminates low background activity and then detects transient events in the EEG recordings. Next, in the clustering stage, transient events detected in the EEG recordings converted to the prototype transient events. During this process, clustering assigns each transient event to a cluster based on a procedure that emulates the process that the neurologists follow during the examination of EEG recordings. Then, some features, specifically the power spectrum density (PSD) of each prototype transient event, are extracted. In the third stage, the continuous-valued features are transformed into discrete ones using a discretization technique. Finally, the classification association rule mining approach extracts rules for classifying the new transient events. .

- Wavelet analysis in [33] uses discrete wavelet transform to decompose signals into different sub-bands. To select a basis function that matches spike's shape or frequency characteristics, the cross-correlation between a known epileptic spike and various wavelet bases available in the MATLAB wavelet toolbox was computed. Then, after discrete wavelet decomposition, an adapted threshold was first applied to wavelet coefficients, and seizure spikes were detected by wavelet coefficients reconstruction.

- Artificial neural network (ANN) is one of the most promising approaches in EEG spike detection. In this technique the ANN can be used on raw EEG spikes [45, 24] or extracted features [3] from spikes.

Generally, spike detection methods mainly depend upon the expert definition of EEG features that describe a spike such as slope, duration, height, and sharpness. However, these measures are not sufficient to represent epileptic seizure spikes due to difference of opinion among experts definition of spikes as well as similarity of spikes to normal waves or background noise. Therefore, spike detection approaches can result in high false detection rates [92].

1.3.3 Feature-Based Design

There are a number of features that influence seizure detection performance. Several features used in prior work are: time-domain features, frequency-domain features, time and frequency features (discretely), and time-frequency domain features (simultaneously). We now describe each of these methods below.

Time-domain analysis Since biosignals are non-stationary and time-domain analysis works with stationary signals, the first step for performing this technique is considering the signal as multiple stationary segments. Existing works have employed slope sign change, Willison amplitude, and Lyapunov exponents. Lyapunov exponents is used in time-series data as a measure of the dynamics of the series [83]. Willison amplitude counts the number of times the absolute value of the difference between consecutive samples exceeds a predetermined threshold value. In [83] Lyapunov exponent is used as a feature along with neural networks for seizure detection. Khorshidtalab et al. [41] used a modified Willison amplitude and slope sign change as features and used the SVM and a fuzzy C-means classifiers for seizure detection based on these features. In [78], other features such as first-line length and energy features were extracted in the time domain and used with K-Nearest Neighbour (KNN), linear discriminant analysis (LDA), and quadratic discriminant analysis (QDA) classifiers for seizure detection.

Frequency-domain analysis Several algorithms are used for extracting features in the frequency domain from EEG recordings: fast Fourier transform (FFT), Eigenvector decomposi-

tion, and Autoregressive (AR) models. In [49], FFT was used to extract features for seizure detection. In that work, first the EEG signal was partitioned into five sub-band frequencies using FFT, and then PCA was used to find a linear combination of frequency features with the maximum variance. The Eigenvector decomposition technique is used to calculate signal frequency and power from artifact-dominated measurements. Power spectral density (PSD) is typically employed to extract frequency features in this method. The eigendecomposition can then be applied on the PSD even in artifact corrupted signal for feature extraction. This method works specifically well in the presence of signals with many distinctive sinusoids embedded in noise [7]. However, this technique does not perform well for small eigenvalues resulting in a relatively poor statistical accuracy. AR methods also rely on the PSD of the EEG for extracting features using a parametric approach [7]. The two most popular techniques for estimation of AR models are the Yule-Walker and Burg's techniques [75, 20].

Time and frequency features   Prior works have also considered using both time and frequency features for seizure detection. Iscan et al. [34] used combined time and frequency features for the classification of healthy patients and epileptic patients based on EEG recordings. Time-domain features were extracted by using cross-correlation and frequency-domain features by computing the PSD. Srinivasan et al. [72] considered three frequency-domain features (dominant frequency, average power in the primary energy zone, and normalized spectral entropy) and two time-domain features (spike rhythmicity and relative spike amplitude) to detect the seizure.

Time-frequency domain analysis   Time-frequency domain analysis extract features from a signal in both time and frequency domains simultaneously. Time-frequency distribution (TFD) and wavelet transform analysis (WT) are two main techniques used for this task [42]. The goal of TFD is to design a joint function of time and frequency that describes the energy density and intensity of a signal in both domains simultaneously [14]. Boashash et al. [10] used TFD features on multi-channel recordings along with channel fusion and feature fusion for seizure detection. In contrast to short-time Fourier transform (STFT) that uses a fixed window size, WT utilizes short windows at high frequencies and long windows at low frequencies. Further-

more, WT is based on applying mother wavelets that can be scaled and shifted to correlate with anomalies or events embedded in the signal [56]. WT methods are categorized into Continuous Wavelet Transforms (CWT) and Discrete Wavelet Transform (DWT). In CWT, the coefficients are calculated for a continuous variation (infinitesimal increments) for both translation and dilation factors, whereas DWT processes the input signals with finite impulse response filters [21]. Many prior works have used WT for feature extraction for seizure detection. Subasi et al. [74] developed a dynamic wavelet network using DWT to decompose EEGs into the frequency sub-bands. Then, a neural network uses these features as input to classify healthy and epileptic patients. Rosso et al. [62] introduced a new tool based on wavelet entropy using orthogonal discrete wavelet transform (ODWT). ODWT has three parameters: relative wavelet energy, wavelet entropy (WE), and relative wavelet entropy (RWE). The relative wavelet energy provides information about the relative energy associated with different frequency bands present in the EEG and their corresponding degree of importance. The WE carries information about the degree of order/disorder associated with a multi-frequency signal response, and the RWE measures the degree of similarity between different segments of the signal.

1.3.4   Deep learning-based feature extraction

In most of the techniques described thus far, a classifier, for instance, SVM, was employed on the features extracted from EEG recordings of patients. However, it is unclear if manually extracting features is the best approach to seizure detection. Therefore, recent studies are focused on using DL algorithms as they can learn the relevant features on their own, and they can perform nonlinear classification [95]. Note that these are two distinct features of the neural networks, and it is still possible to use manually extracted features with neural networks for improved performance due to the nonlinear classification capabilities of these models. The authors in [67] generated three different features based on Fourier, wavelet, and empirical mode decomposition transforms. A 2D CNN made up of two convolutional layers and three fully-connected layers for classification was then applied to these features. They achieved the best results when using Fourier transform. A wavelet-based deep learning approach was described in [6], where DWT was used to extract time-frequency domain features in five sub-band fre-

quencies. All predefined coefficients were supplied as the input to a 2D CNN architecture for seizure detection. Turk et al. [80] proposed a seizure detection algorithm using CWT based on Morlet Continuous Wave and the scalogram images for each EEG segment. A 2D CNN structure was used to learn the properties of these scalogram images and classify the seizure state. In [12, 23], time-frequency features were used along with a 1D CNN. In the proposed method, first, the DWT of signals was evaluated. Then an architecture comprised of multiple CNN filters and a fully-connected softmax layer was used for classifying the seizure state.

1.3.5   Non-feature Based Design

Extracting features from raw EEG recordings, which is also known as feature engineering, requires careful engineering and considerable domain expertise. The extracted feature vector must be highly related to the classification task [48]. However, this strategy is difficult as various types of patterns appear during seizure [42]. Moreover, many artifacts in the signal can have structures similar to the seizure patterns. Unlike feature engineering algorithms, deep-learning models learn the relevant features independently. The two main DL architectures which are used directly on raw EEG data for seizure detection applications are the CNN and the RNN. Below, we summarize some previous studies based on these two architectures.

1.3.5.1   Convolutional Neural Network (CNN)

This class of DL models are extensively used for epileptic seizure detection using EEG signals. In [38], after using a notch filter to remove 60 Hz noise from EEG signals of five patients, a 1D CNN was employed to detect interictal epileptiform spikes due to seizures. Acharya et al. [2] applied a 3-layer CNN architecture to the normalized EEG signals for seizure detection, while a 2D CNN architecture was used in [53]. Boonyakitanont et al. [11] proposed a detection scheme using raw EEG records divided into 4-second blocks followed by using a deep 2D CNN architecture to learn the features from EEG signals. They showed state-of-the-art performance for detection accuracy via per-patient training based on metrics such as F1 score, accuracy, sensitivity, and specificity.

1.3.5.2 Recurrent neural networks

Although CNNs are popular for seizure detection, these models are not able to exploit temporal correlations in the recordings. Hence, many recent studies have been focused on using the RNN architecture [88, 94]. Hussein et al. [32] used a deep recurrent neural network, particularly an LSTM for seizure detection on segmented seizure recordings. Aristizabal et al. [5] developed another LSTM-based seizure detection technique, while [77] used the GRU for seizure state classification. Roy et al. [64] proposed an architecture termed ChronoNet formed by stacking multiple 1D convolution layers followed by GRU layers where each 1D convolution layer uses multiple filters of exponentially varying lengths. [79] also considered a combination of CNN structure with an RNN model. In their study, five different archetypes including 1D CNNs, 2D CNNs, LSTMs, 1D CNNs with LSTMs and 2D CNNs with LSTMs were implemented. Their evaluation results indicated that the model consisting of 2D CNNs with LSTMs showed the best performance.

1.4 Research Objectives and Hypothesis

The challenges of previous works motivate us to have a reliable seizure detection system. The objectives of this work are as follows:

- Propose a system which can generalize across patients without the need for per patient training.

- The proposed system must be computationally efficient for use in real-time seizure detection.

- The proposed method should exploiting temporal correlation between consecutive EEG blocks to improve performance.

- The proposed method should also capture inter-channel correlations during seizure, which can further improve performance.

The corresponding hypotheses are as follows:

- Factor graph inference thanks to HMM and sum-product algorithms is able to capture temporal correlation for seizure detection at a reduced complexity compared to RNNs.

- MI estimation can capture the inter-channel correlations and help improve the performance of seizure detection algorithms.

1.5 Thesis Overview

This thesis is written in an integrated article format where each abovementioned objective is pursued in each chapter.

Chapter 2 describes a computationally efficient hybrid model-based/data-driven approach to seizure detection, using CNNs and factor graph inference. It is demonstrated that the proposed algorithm can capture temporal correlation at reduced complexity compared to prior works and RNNs. We also demonstrate that our approach can achieve a better performance compared to prior work.

Chapter 3 investigates the effect of MI estimations for capturing the inter-channel correlations. This chapter shows MI is a promising measure to compute instantaneous dependencies among EEG channels at the beginning and during seizure.

Chapter 4 provides more details about the techniques presented in previous chapter. It also combines all the proposed methods together and presents a more comprehensive evaluation. A 6-fold-leave-4-patients-out evaluation is used to demonstrate the generalizability the our algorithm.

Chapter 5 is the concluding chapter of the thesis that highlights the findings corresponding to studies detailed in each chapter as well as strengths and limitations of our proposed technique. It also describes future research directions in seizure detection, prediction, and classifications.

References

[1] Epilepsy. `https://www.who.int/news-room/fact-sheets/detail/epilepsy`.

[2] U Rajendra Acharya, Shu Lih Oh, Yuki Hagiwara, Jen Hong Tan, and Hojjat Adeli. Deep convolutional neural network for the automated detection and diagnosis of seizure using eeg signals. *Computers in biology and medicine*, 100:270–278, 2018.

[3] Nurettin Acir, Ibrahim Oztura, Mehmet Kuntalp, Baris Baklan, and Cuneyt Guzelis. Automatic detection of epileptiform events in eeg by a three-stage procedure based on artificial neural networks. *IEEE Transactions on Biomedical Engineering*, 52(1):30–40, 2004.

[4] Nabeel Ahammad, Thasneem Fathima, and Paul Joseph. Detection of epileptic seizure event and onset using eeg. *BioMed research international*, 2014, 2014.

[5] David Ahmedt-Aristizabal, Clinton Fookes, Kien Nguyen, and Sridha Sridharan. Deep classification of epileptic signals. In *2018 40th Annual International Conference of the IEEE Engineering in Medicine and Biology Society (EMBC)*, pages 332–335. IEEE, 2018.

[6] Rohan Akut. Wavelet based deep learning approach for epilepsy detection. *Health information science and systems*, 7(1):1–9, 2019.

[7] Amjed S Al-Fahoum and Ausilah A Al-Fraihat. Methods of eeg signal features extraction using linear analysis in frequency and time-frequency domains. *International Scholarly Research Notices*, 2014, 2014.

[8] Selim R Benbadis. Errors in eegs and the misdiagnosis of epilepsy: importance, causes, consequences, and proposed remedies. *Epilepsy & Behavior*, 11(3):257–262, 2007.

[9] Yoshua Bengio, Patrice Simard, and Paolo Frasconi. Learning long-term dependencies with gradient descent is difficult. *IEEE transactions on neural networks*, 5(2):157–166, 1994.

[10] Boualem Boashash and Samir Ouelha. Automatic signal abnormality detection using time-frequency features and machine learning: A newborn eeg seizure case study. *Knowledge-Based Systems*, 106:38–50, 2016.

[11] Poomipat Boonyakitanont, Apiwat Lek-uthai, Krisnachai Chomtho, and Jitkomut Songsiri. A Comparison of Deep Neural Networks for Seizure Detection in EEG Signals. *bioRxiv*, page 702654, 2019. Publisher: Cold Spring Harbor Laboratory.

[12] Xuhui Chen, Jinlong Ji, Tianxi Ji, and Pan Li. Cost-sensitive deep active learning for epileptic seizure detection. In *Proceedings of the 2018 ACM International Conference on Bioinformatics, Computational Biology, and Health Informatics*, pages 226–235, 2018.

[13] Jie-Zhi Cheng, Dong Ni, Yi-Hong Chou, Jing Qin, Chui-Mei Tiu, Yeun-Chung Chang, Chiun-Sheng Huang, Dinggang Shen, and Chung-Ming Chen. Computer-aided diagnosis with deep learning architecture: applications to breast lesions in us images and pulmonary nodules in ct scans. *Scientific reports*, 6(1):1–13, 2016.

[14] Leon Cohen. Time-frequency distributions-a review. *Proceedings of the IEEE*, 77(7):941–981, 1989.

[15] Michael D Devous, Ronald A Thisted, Gillian F Morgan, Robert F Leroy, and Christopher C Rowe. Spect brain imaging in epilepsy: a meta-analysis. In *Database of Abstracts of Reviews of Effects (DARE): Quality-assessed Reviews [Internet]*. Centre for Reviews and Dissemination (UK), 1998.

[16] Jelena Djuris, Svetlana Ibric, and Zorica Djuric. Neural computing in pharmaceutical products and process development. In *Computer-Aided Applications in Pharmaceutical Technology*, pages 91–175. Elsevier, 2013.

[17] Andre Esteva, Brett Kuprel, Roberto A Novoa, Justin Ko, Susan M Swetter, Helen M Blau, and Sebastian Thrun. Dermatologist-level classification of skin cancer with deep neural networks. *nature*, 542(7639):115–118, 2017.

[18] Themis P Exarchos, Alexandros T Tzallas, Dimitrios I Fotiadis, Spiros Konitsiotis, and Sotirios Giannopoulos. Eeg transient event detection and classification using association rules. *IEEE Transactions on Information Technology in Biomedicine*, 10(3):451–457, 2006.

[19] Mehrdad Fatourechi, Ali Bashashati, Rabab K Ward, and Gary E Birch. Emg and eog artifacts in brain computer interface systems: A survey. *Clinical neurophysiology*, 118(3):480–494, 2007.

[20] Oliver Faust, RU Acharya, Alastair R Allen, and CM Lin. Analysis of eeg signals during epileptic and alcoholic states using ar modeling techniques. *Irbm*, 29(1):44–52, 2008.

[21] Oliver Faust, U Rajendra Acharya, Hojjat Adeli, and Amir Adeli. Wavelet-based eeg processing for computer-aided seizure detection and epilepsy diagnosis. *Seizure*, 26:56–64, 2015.

[22] Robert S Fisher, Walter Van Emde Boas, Warren Blume, Christian Elger, Pierre Genton, Phillip Lee, and Jerome Engel Jr. Epileptic seizures and epilepsy: definitions proposed by the international league against epilepsy (ilae) and the international bureau for epilepsy (ibe). *Epilepsia*, 46(4):470–472, 2005.

[23] Kosuke Fukumori, Hoang Thien Thu Nguyen, Noboru Yoshida, and Toshihisa Tanaka. Fully data-driven convolutional filters with deep learning models for epileptic spike detection. In *ICASSP 2019-2019 IEEE international conference on acoustics, speech and signal processing (ICASSP)*, pages 2772–2776. IEEE, 2019.

[24] Andrew J Gabor and Masud Seyal. Automated interictal eeg spike detection using artificial neural networks. *Electroencephalography and clinical Neurophysiology*, 83(5):271–280, 1992.

[25] Sheng Ge, Qing Yang, Ruimin Wang, Pan Lin, Junfeng Gao, Yue Leng, Yuankui Yang, and Haixian Wang. A brain-computer interface based on a few-channel eeg-fnirs bimodal system. *IEEE Access*, 5:208–218, 2017.

[26] Guila Glosser, Lynne C Cole, Jacqueline A French, Andrew J Saykin, and Michael R Sperling. Predictors of intellectual performance in adults with intractable temporal lobe epilepsy. *Journal of the International Neuropsychological Society*, 3(3):252–259, 1997.

[27] Jeffrey Alan Golden. Deep learning algorithms for detection of lymph node metastases

from breast cancer: helping artificial intelligence be seen. *Jama*, 318(22):2184–2186, 2017.

[28] J Gotman and P Gloor. Automatic recognition and quantification of interictal epileptic activity in the human scalp eeg. *Electroencephalography and clinical neurophysiology*, 41(5):513–529, 1976.

[29] Jean Gotman. Automatic recognition of epileptic seizures in the eeg. *Electroencephalography and clinical Neurophysiology*, 54(5):530–540, 1982.

[30] Christian Hoppe, Annkathrin Poepel, and Christian E Elger. Epilepsy: accuracy of patient seizure counts. *Archives of neurology*, 64(11):1595–1599, 2007.

[31] David H Hubel and TN Wiesel. Shape and arrangement of columns in cat's striate cortex. *The Journal of physiology*, 165(3):559–568, 1963.

[32] Ramy Hussein, Hamid Palangi, Z Jane Wang, and Rabab Ward. Robust detection of epileptic seizures using deep neural networks. In *2018 IEEE International Conference on Acoustics, Speech and Signal Processing (ICASSP)*, pages 2546–2550. IEEE, 2018.

[33] KP Indiradevi, Elizabeth Elias, PS Sathidevi, S Dinesh Nayak, and K Radhakrishnan. A multi-level wavelet approach for automatic detection of epileptic spikes in the electroencephalogram. *Computers in biology and medicine*, 38(7):805–816, 2008.

[34] Zafer Iscan, Zümray Dokur, and Tamer Demiralp. Classification of electroencephalogram signals with combined time and frequency features. *Expert Systems with Applications*, 38(8):10499–10505, 2011.

[35] Aysa Jafarifarmand and Mohammad Ali Badamchizadeh. Artifacts removal in eeg signal using a new neural network enhanced adaptive filter. *Neurocomputing*, 103:222–231, 2013.

[36] Gopal Chandra Jana, Ratna Sharma, and Anupam Agrawal. A 1D-CNN-spectrogram based approach for seizure detection from EEG signal. *Procedia Computer Science*, 167:403–412, 2020. Publisher: Elsevier.

[37] Xiao Jiang, Gui-Bin Bian, and Zean Tian. Removal of artifacts from eeg signals: a review. *Sensors*, 19(5):987, 2019.

[38] Alexander Rosenberg Johansen, Jing Jin, Tomasz Maszczyk, Justin Dauwels, Sydney S Cash, and M Brandon Westover. Epileptiform spike detection via convolutional neural networks. In *2016 IEEE International Conference on Acoustics, Speech and Signal Processing (ICASSP)*, pages 754–758. IEEE, 2016.

[39] HKMCC Kandar, Sanjay Kumar Das, Lakshmikanta Ghosh, and Bijan Kumar Gupta. Epilepsy and its management: A review. *Journal of PharmaSciTech*, 1(2):20–26, 2012.

[40] Simin Khalilpour, Amin Ranjbar, Mohammad Bagher Menhaj, and Afshin Sandooghdar. Application of 1-D CNN to predict epileptic seizures using EEG records. In *2020 6th International Conference on Web Research (ICWR)*, pages 314–318. IEEE, 2020.

[41] Aida Khorshidtalab, Momoh-Jimoh E Salami, and Mahyar Hamedi. Robust classification of motor imagery eeg signals using statistical time–domain features. *Physiological measurement*, 34(11):1563, 2013.

[42] Taeho Kim, Phuc Nguyen, Nhat Pham, Nam Bui, Hoang Truong, Sangtae Ha, and Tam Vu. Epileptic seizure detection and experimental treatment: a review. *Frontiers in Neurology*, 11:701, 2020.

[43] William F Kindel, Elijah D Christensen, and Joel Zylberberg. Using deep learning to reveal the neural code for images in primary visual cortex. *arXiv preprint arXiv:1706.06208*, 2017.

[44] Manousos A Klados, Christos Papadelis, Christoph Braun, and Panagiotis D Bamidis. Reg-ica: a hybrid methodology combining blind source separation and regression techniques for the rejection of ocular artifacts. *Biomedical Signal Processing and Control*, 6(3):291–300, 2011.

[45] Cheng-Wen Ko and Hsiao-Wen Chung. Automatic spike detection via an artificial neural network using raw eeg data: effects of data preparation and implications in the limitations of online recognition. *Clinical neurophysiology*, 111(3):477–481, 2000.

[46] Sancgeetha Kulaseharan, Azad Aminpour, Mehran Ebrahimi, and Elysa Widjaja. Identifying lesions in paediatric epilepsy using morphometric and textural analysis of magnetic resonance images. *NeuroImage: Clinical*, 21:101663, 2019.

[47] KG Anjana Lakshmi, SN Nissa Surling, and O Sheeba. A novel approach for the removal of artifacts in eeg signals. In *2017 International Conference on Wireless Communications, Signal Processing and Networking (WiSPNET)*, pages 2595–2599. IEEE, 2017.

[48] Yann LeCun, Yoshua Bengio, and Geoffrey Hinton. Deep learning. *nature*, 521(7553):436–444, 2015.

[49] Jiseon Lee, Junhee Park, Sejung Yang, Hani Kim, Yun Seo Choi, Hyeon Jin Kim, Hyang Woon Lee, and Byung-Uk Lee. Early seizure detection by applying frequency-based algorithm derived from the principal component analysis. *Frontiers in neuroinformatics*, 11:52, 2017.

[50] Weixia Liang, Haijun Pei, Qingling Cai, and Yonghua Wang. Scalp EEG epileptogenic zone recognition and localization based on long-term recurrent convolutional network. *Neurocomputing*, 396:569–576, 2020.

[51] Zachary C Lipton, John Berkowitz, and Charles Elkan. A critical review of recurrent neural networks for sequence learning. *arXiv preprint arXiv:1506.00019*, 2015.

[52] Brian Litt and Javier Echauz. Prediction of epileptic seizures. *The Lancet Neurology*, 1(1):22–30, 2002. Publisher: Elsevier.

[53] Jianguo Liu and Blake Woodson. Deep learning classification for epilepsy detection using a single channel electroencephalography (eeg). In *Proceedings of the 2019 3rd International Conference on Deep Learning Technologies*, pages 23–26, 2019.

[54] Kristina Malmgren, Markus Reuber, and Richard Appleton. Differential diagnosis of epilepsy. *Oxford textbook of epilepsy and epileptic seizures*, pages 81–94, 2012.

[55] C Marque, C Bisch, R Dantas, S Elayoubi, V Brosse, and C Perot. Adaptive filtering for ecg rejection from surface emg recordings. *Journal of electromyography and kinesiology*, 15(3):310–315, 2005.

[56] Carlos Mateo Domingo and Juan Antonio Talavera Martín. Bridging the gap between the short-time fourier transform (stft), wavelets, the constant-q transform and multi-resolution stft. 2020.

[57] Ralph Meier, Heike Dittrich, Andreas Schulze-Bonhage, and Ad Aertsen. Detecting epileptic seizures in long-term human eeg: a new approach to automatic online and real-time detection and classification of polymorphic seizure patterns. *Journal of clinical neurophysiology*, 25(3):119–131, 2008.

[58] Deb K Pal, Amanda W Pong, and Wendy K Chung. Genetic evaluation and counseling for epilepsy. *Nature Reviews Neurology*, 6(8):445–453, 2010.

[59] Michael P Pound, Jonathan A Atkinson, Alexandra J Townsend, Michael H Wilson, Marcus Griffiths, Aaron S Jackson, Adrian Bulat, Georgios Tzimiropoulos, Darren M Wells, Erik H Murchie, et al. Deep machine learning provides state-of-the-art performance in image-based plant phenotyping. *Gigascience*, 6(10):gix083, 2017.

[60] Ashis Pradhan. Support vector machine-a survey. *International Journal of Emerging Technology and Advanced Engineering*, 2(8):82–85, 2012.

[61] Mirjana Prpa and Philippe Pasquier. Brain-computer interfaces in contemporary art: a state of the art and taxonomy. *Brain art*, pages 65–115, 2019.

[62] Osvaldo A Rosso, Susana Blanco, Juliana Yordanova, Vasil Kolev, Alejandra Figliola, Martin Schürmann, and Erol Başar. Wavelet entropy: a new tool for analysis of short duration brain electrical signals. *Journal of neuroscience methods*, 105(1):65–75, 2001.

[63] S. Roy, I. Kiral-Kornek, and S. Harrer. Deep learning enabled automatic abnormal EEG identification. In *International Conference of the IEEE Engineering in Medicine and Biology Society (EMBC)*, pages 2756–2759, 2018.

[64] Subhrajit Roy, Isabell Kiral-Kornek, and Stefan Harrer. Chrononet: a deep recurrent neural network for abnormal eeg identification. In *Conference on Artificial Intelligence in Medicine in Europe*, pages 47–56. Springer, 2019.

[65] Tolulope T Sajobi, Colin B Josephson, Richard Sawatzky, Meng Wang, Oluwaseyi Lawal, Scott B Patten, Lisa M Lix, and Samuel Wiebe. Quality of life in epilepsy: Same questions, but different meaning to different people. *Epilepsia*, 62(9):2094–2102, 2021.

[66] Tuuli M Salmenpera and John S Duncan. Imaging in epilepsy. *Journal of Neurology, Neurosurgery & Psychiatry*, 76(suppl 3):iii2–iii10, 2005.

[67] Rubén San-Segundo, Manuel Gil-Martín, Luis Fernando D'Haro-Enríquez, and José Manuel Pardo. Classification of epileptic eeg recordings using signal transforms and convolutional neural networks. *Computers in biology and medicine*, 109:148–158, 2019.

[68] R Sankar and J Natour. Automatic computer analysis of transients in eeg. *Computers in biology and medicine*, 22(6):407–422, 1992.

[69] Monika Sheoran, Sanjeev Kumar, and Seema Chawla. Methods of denoising of electroencephalogram signal: a review. *International Journal of Biomedical Engineering and Technology*, 18(4):385–395, 2015.

[70] Susan S Spencer. The relative contributions of mri, spect, and pet imaging in epilepsy. *Epilepsia*, 35:S72–S89, 1994.

[71] SP Sridhar. *A Study on Clinical and Biochemical Correlation between Various Types of Seizures and Pseudoseizures*. PhD thesis, Stanley Medical College, Chennai, 2019.

[72] Vairavan Srinivasan, Chikkannan Eswaran, Sriraam, and N. Artificial neural network based epileptic detection using time-domain and frequency-domain features. *Journal of Medical Systems*, 29(6):647–660, 2005.

[73] James L Stone and John R Hughes. Early history of electroencephalography and establishment of the american clinical neurophysiology society. *Journal of Clinical Neurophysiology*, 30(1):28–44, 2013.

[74] Abdulhamit Subasi, Jasmin Kevric, and M. Abdullah Canbaz. Epileptic seizure detection using hybrid machine learning methods. *Neural Computing and Applications*, 31(1):317–325, January 2019.

[75] Abdulhamit Subasi, M Kemal Kiymik, Ahmet Alkan, and Etem Koklukaya. Neural network classification of eeg signals by using ar with mle preprocessing for epileptic seizure detection. *Mathematical and computational applications*, 10(1):57–70, 2005.

[76] Kevin T Sweeney, Tomás E Ward, and Seán F McLoone. Artifact removal in physiological signals—practices and possibilities. *IEEE transactions on information technology in biomedicine*, 16(3):488–500, 2012.

[77] Sachin S Talathi. Deep recurrent neural networks for seizure detection and early seizure detection systems. *arXiv preprint arXiv:1706.03283*, 2017.

[78] E Tessy, PP Muhammed Shanir, and Shaleena Manafuddin. Time domain analysis of epileptic eeg for seizure detection. In *2016 International Conference on Next Generation Intelligent Systems (ICNGIS)*, pages 1–4. IEEE, 2016.

[79] Marleen C Tjepkema-Cloostermans, Rafael CV de Carvalho, and Michel JAM van Putten. Deep learning for detection of focal epileptiform discharges from scalp eeg recordings. *Clinical neurophysiology*, 129(10):2191–2196, 2018.

[80] Ömer Türk and Mehmet Siraç Özerdem. Epilepsy detection by using scalogram based convolutional neural network from eeg signals. *Brain sciences*, 9(5):115, 2019.

[81] Alexandros T Tzallas, Markos G Tsipouras, Dimitrios G Tsalikakis, Evaggelos C Karvounis, Loukas Astrakas, Spiros Konitsiotis, and Margaret Tzaphlidou. Automated epileptic seizure detection methods: a review study. *Epilepsy-histological, electroencephalographic and psychological aspects*, pages 75–98, 2012.

[82] Elif Derya Übeyli. Analysis of eeg signals by combining eigenvector methods and multiclass support vector machines. *Computers in Biology and Medicine*, 38(1):14–22, 2008.

[83] Elif Derya Übeyli. Lyapunov exponents/probabilistic neural networks for analysis of eeg signals. *Expert Systems with Applications*, 37(2):985–992, 2010.

[84] Elif Derya Übeyli. Recurrent neural networks employing lyapunov exponents for analysis of ecg signals. *Expert systems with applications*, 37(2):1192–1199, 2010.

[85] Nicole van Klink, Anne Mooij, Geertjan Huiskamp, Cyrille Ferrier, Kees Braun, Arjan Hillebrand, and Maeike Zijlmans. Simultaneous meg and eeg to detect ripples in people with focal epilepsy. *Clinical Neurophysiology*, 130(7):1175–1183, 2019.

[86] Pieter Van Mierlo, Margarita Papadopoulou, Evelien Carrette, Paul Boon, Stefaan Vandenberghe, Kristl Vonck, and Daniele Marinazzo. Functional brain connectivity from eeg in epilepsy: Seizure prediction and epileptogenic focus localization. *Progress in neurobiology*, 121:19–35, 2014.

[87] David Victorson, Jose E Cavazos, Gregory L Holmes, Anthony T Reder, Valerie Wojna, Cindy Nowinski, Deborah Miller, Sarah Buono, Allison Mueller, Claudia Moy, et al. Validity of the neurology quality-of-life (neuro-qol) measurement system in adult epilepsy. *Epilepsy & Behavior*, 31:77–84, 2014.

[88] Lasitha Vidyaratne, Alexander Glandon, Mahbubul Alam, and Khan M Iftekharuddin. Deep recurrent neural network for seizure detection. In *2016 International Joint Conference on Neural Networks (IJCNN)*, pages 1202–1207. IEEE, 2016.

[89] K Vijayalakshmi and Appaji M Abhishek. Spike detection in epileptic patients eeg data using template matching technique. *International Journal of Computer Applications*, 2(6):5–8, 2010.

[90] Yusen Wang, Wenlong Liao, and Yuqing Chang. Gated recurrent unit network-based short-term photovoltaic forecasting. *Energies*, 11(8):2163, 2018.

[91] Xiaoyan Wei, Lin Zhou, Ziyi Chen, Liangjun Zhang, and Yi Zhou. Automatic seizure detection using three-dimensional cnn based on multi-channel eeg. *BMC medical informatics and decision making*, 18(5):71–80, 2018.

[92] Scott B Wilson and Ronald Emerson. Spike detection: a review and comparison of algorithms. *Clinical Neurophysiology*, 113(12):1873–1881, 2002.

[93] Jie Yang and Mohamad Sawan. From seizure detection to smart and fully embedded seizure prediction engine: A review. *IEEE Transactions on Biomedical Circuits and Systems*, 14(5):1008–1023, 2020.

[94] Xinghua Yao, Qiang Cheng, and Guo-Qiang Zhang. Automated classification of seizures against nonseizures: A deep learning approach. *arXiv preprint arXiv:1906.02745*, 2019.

[95] Ozan Yardimci and Barış Ç Ayyıldız. Comparison of svm and cnn classification methods for infrared target recognition. In *Automatic Target Recognition XXVIII*, volume 10648, page 1064804. International Society for Optics and Photonics, 2018.

Chapter 2

Efficient Epileptic Seizure Detection Using CNN-Aided Factor Graphs

2.1 Introduction

Epilepsy is one of the most common neurological disorders affecting about 50 million people worldwide. This disorder is associated with recurrent episodes of abnormal neural activity in the central nervous system known as epileptic seizures [1]. Based on the area where seizure starts and the intensity of the brain's abnormal signals, patients with epileptic seizures may suffer from different symptoms, including auras, muscle contraction, and loss of consciousness [19] that they affect the patients' private and professional life. For instance, some activities such as swimming, bathing, and climbing a ladder become dangerous as a seizure during that activity might result in unpredictable injuries and even death. Therefore, early detection of epileptic seizures can notably improve the patient's quality of life.

The most common tool used to detect seizures is EEG [30]. While other various techniques, such as magnetic resonance imaging (MRI) [13], magnetoencephalography (MEG) [29], and positron emission tomography (PET) [20] are sometimes used in conjunction to EEG, EEG is widely preferred as it is economical, portable, non-invasive and shows clear rhythms in the frequency domain [28]. However, the review of EEG signals is a time-consuming process, as a neurologist needs to monitor the recording. Expertise is needed to detect seizures as each case is quite variable, with different channels involved, while the spectral content of the rhythmic

activity varies across individuals and signals and is mostly contaminated by physiological and non-physiological interference [7]. As such, automatic seizure detection is a valuable clinical tool to address this issue and reduce the dependency on human experts.

Many machine learning studies have been developed for automatic seizure detection problems. One of the most common approaches applies a support vector machine (SVM), which is mainly followed by additional preprocessing steps such as discrete wavelet transform (DWT) and fast Fourier transform (FFT) to extract more features of EEG signals [27, 2, 22, 15]. In the past decade, DL techniques have become very popular in various applications, including the analysis of time series EEG signals. Therefore, different DL models have been investigated and tested in the area of seizure detection. For instance, Khalilpour et al. [10] applied a 1D CNN to EEG signals of five patients to predict preictal and interictal states of the brain. In [9], the spectrogram of EEG measurements was used as input to a 1D CNN. The authors in [24] utilized DWT to represent the EEG segments, which is used as input to a 1D CNN. Moreover, they combine the DWT of the current, previous, and next block for predicting the label of the current block, which helps exploit the temporal correlations. Another common DL architecture is 2D CNN. Boonyakitanont et al. [3] applied 2D CNN to 24 recordings from 23 patients, where the signals are segmented into 4-second blocks. They showed state-of-the-art performance in terms of detection accuracy.

Most of these prior techniques divide the EEG recording into blocks and treat these blocks independently. This does not take advantage of the temporal correlations that exist between consecutive blocks. While there are methods based on CNN-RNN architectures [23, 16] that can mitigate this issue, it is well known that RNNs have high computational complexity for training. Another method used for exploiting temporal correlations is HMM [14]. HMMs belong to the family of factorizable joint distributions which admit low-complexity inference via factor graph methods [17]. Despite the proliferation of seizure detection algorithms, having a computationally efficient algorithm that can generalize to different patients and perform seizure detection reliably in a real-time manner is lacking.

In this work, we propose a computationally efficient epileptic seizure detection algorithm based on a hybrid model-based/data-driven approach using CNN-aided factor graphs. First, we carefully design a 1D CNN for estimating the probability that a 4-second block of EEG is

a seizure block. Our goal is to design a network that is applied to the EEG signals directly, without feature engineering using transforms such as DWT or FFT. When using such feature engineering, one must carefully select the parameters of the transforms, and the performance of the trained model can vary considerably based on these parameters. Moreover, while these transforms typically provide information about the frequency component of the EEG signals, they are not necessarily impactful for capturing the dependence of the EEG signals across different channels. Such dependence can be indicative of an epileptic seizure. Our proposed 1D CNN is designed to be able to capture the long-term dependence between EEG channels and operates on the signals directly with minimal processing.

To exploit the temporal correlation between consecutive blocks for further improvement, we use factor graph inference, specifically using HMM models to capture temporal correlations among the signals. The number of floating-point operations (FLOPs) during inference indicates that our proposed hybrid method is more efficient than previous works. Based on the FLOPs results, our algorithm shows a two times reduction compared to the baseline model. Despite this decrease in computation, our method achieves up to 5% absolute improvement in performance measures such as precision, recall, and F1-score in a 6-fold leave-4-patients-out evaluation.

The rest of this chapter is organized as follows. In Section 2.2 we describe the problem statement, the dataset that is used for model development and evaluation, and the baseline models. Then, in Section 2.3 we describe our proposed method, which is evaluated and compared to prior methods in Section 2.4. Finally, Section 2.5 provides concluding remarks.

2.2 Background, Dataset, and Baseline Models

In this section, we first discuss the seizure detection problem. We then describe the dataset that is used for our hybrid model-based/data-driven algorithm development and evaluation. Finally, we conclude this section by presenting the baseline methods that are used for comparison in this work.

2.2.1 Seizure Detection Using EEG Signals

EEG is the electrical recording of the brain activities which is the most popular diagnostic and analytical tool for epileptic seizures. In seizure detection problem, there are some basic terms as follows:

- Ictal state, which is the time when the seizure occurs (from start to end).

- Preictal state is a period of time just before a seizure occurs.

- Interictal state refers to the period between seizures.

- Postictal state is a period of time just after the seizure ends.

During reading an EEG by a neurologist, the detection of ictal spikes is sometimes difficult to accomplish due to their similarity to waves that are part of normal EEG or artifacts and the wide variability in spike morphology and background between patients. For instance, abnormalities like breach rhythm (normal rhythm seen with skull defects) can have focal, sharply contoured morphology, and they might be inferred as epileptic seizures. As such, having an automatic system to detect and predict seizures will resolve these issues.

2.2.2 Data Description

In this section we detail the data used in our study of hybrid model-based/data-driven epileptic seizure detection. We first describe the raw EEG data, after which we describe the pre-processing carried out prior to its usage for training and inference.

2.2.2.1 EEG Data

The dataset used in this study is the public CHB-MIT Scalp EEG Database collected at the Children's Hospital Boston and consists of EEG recordings from pediatric subjects with intractable seizures [6][1]. Recordings were collected from 23 subjects: 5 males aged 3-22 years, 17 females aged 1.5- 19 years, and one anonymous subject. Each case contains 9 to 42 continuous European Data Format (EDF) files from a single subject. The duration of the recordings in

---

[1]This database is available online at PhysioNet (`https://physionet.org/physiobank/database/chbm it/`)

each file varies between one to four hours. All signals were sampled at a frequency of 256 Hz with 16-bit resolution. Since case 21 was obtained 1.5 years after case 1 from the same female subject, we consider case 21 as a separate patient; therefore, our experiment includes 24 subjects. Please note that since we are evaluating the algorithms using a 6-fold leave-4-patients-out method, this might negligibly affect only one of the folds.

2.2.2.2 Data Pre-Processing

The dataset contains 664 EDF files from all patients, where the files are annotated using seizure start and end times. Each patient has at least two EDF files that contain seizure episodes. For the CHB-MIT database, seizure classes (focal or generalized seizure) are not specified. To have a more balanced sample from seizures and decrease the chance of overfitting, we only selected EDF files that have at least one seizure episode. Moreover, since the length of the seizures is very short (from 7 seconds to 753 seconds) compared to the overall recording (from 959 seconds to 14427 seconds) in the EDF files, we shorten the recording to 3 times the seizure duration before and 3 times the seizure duration after the seizure. Therefore, our data has 6 seconds of non-seizure for every second of seizure. It should be noted that, for every EDF file that has more than one seizure, we apply the previous scheme to each seizure duration to obtain desirable samples and consider the output as a new recording for the observed patient.

From the EEG channels, we use the 18 bipolar montages: FP1-F7, F7-T7, T7-P7, P7-O1, FP1-F3, F3-T3, T3-P3, P3-O1, FP2-F4, F4-C4, C4-P4, P4-O2, FP2-F8, F8-T8, T8-P8, P8-O2, FZ-CZ, CZ-PZ. A notch filter is used to remove 60 Hz line noise from each EEG signal. Then 4-second blocks, with 1024 sample points per block, are used as moving windows with a step size of 1 second. The value of 4 seconds was chosen to provide a good trade-off between the number of samples in a block and the stationarity of the observed signals over a block [11]. We have observed that when the width of the window is increased, the seizure detection procedure results in up to 3% reduction in performance measures. We now describe some of the prior seizure detection algorithms developed using this dataset, which will be used as baselines in this work.

2.2.3   Baseline Methods

We consider two recent works that presented a state-of-the-art performance on the CHB-MIT dataset as baselines in this study [3, 8]. The method in [3] is designed to take the EEG signals as input without applying any type of transforms. Therefore, we employ the same structure used in [3] where the input shape for the model is (18,1024,1), which implies considering each block as an image with the size of (18,1024) and channel dimension of 1. The method in [8] takes a graphical image of the EEG recording as input rather than the EEG measurements. This type of image-based feature was shown to achieve better detection performance compared to other features-based methods in seizure detection such as spectrogram or periodogram in a recent study [4].

2.3   Methodology

Our hybrid model-based/data-driven algorithm combines a carefully designed CNN, which estimates the presence of seizure in a 4-second block, with factor graph inference to exploit the temporal correlation between the blocks. We begin this section by describing the CNN architecture, followed by the factor graph-based inference step.

2.3.1   1D CNN Architecture

2D CNNs, as utilized in the baseline methods detailed in Subsection 2.2.3, exploit the notion of *locality*, exhibited by natural images, which implies that the level of correlation between different elements typically grows the closer they are in the image. However, in EEG segment matrices, each element represents a single EEG measurement, which is likely to be correlated with all the remaining measurements taken at that time instance, regardless of their row index in the matrix representation. This structure makes 1D CNNs, which combines all measurements taken from different channels at a given time instance, more suitable compared to 2D CNNs used in [3]. That allows the network to better learn the correlations between different channels since the channel measurements can become highly correlated during seizures.

In order to have a comparable configuration with the baseline models that showed the best

Input	Conv1	Conv2	Conv3	Conv4	Conv5	Conv6
EEG dataset (1025×18)	8×Conv1D(10) 8×Conv1D(22) BN, ReLU MaxPool(1×2)	8×Conv1D(10) 8×Conv1D(22) BN, ReLU MaxPool(1×2)	8×Conv1D(10) 8×Conv1D(22) BN, ReLU MaxPool(1×2)	16×Conv1D(10) 16×Conv1D(22) BN, ReLU MaxPool(1×2)	16×Conv1D(10) 16×Conv1D(22) BN, ReLU MaxPool(1×2)	8×Conv1D(1) Dropout(0.25)

Figure 2.1: Proposed 1D CNN architecture.

results for performance measures, we use the same number of layers where the input shape for this model is (1024,18). The inputs to our 1D CNN are EEG signals with minimal prepossessing, which only removes the 60 Hz component of the signals. The baseline models detailed in Subsection 2.2.3 use a kernel size of 3 and 2. Given the number of layers, this results in a receptive field of approximately 30 milliseconds. Since this is not enough to capture low-frequency components of the signal as well as the long-term correlations between the EEG channels, we design our kernel size to be much larger, which results in a receptive field that covers approximately 1 second of the data. Fig. 2.1 shows the complete architecture of the proposed 1D CNN.

As will be shown in Section 2.4, these simple changes, namely choosing the kernel size carefully and using a 1D CNN, improve the results significantly compared to the baseline CNN model in [3]. This is because the network can capture a wider range of frequency components in the signal and also better capture the correlations between the EEG channels. An additional advantage of using 1D CNNs stems from their reduced complexity during inference compared to their 2D counterparts. Although we have increased the receptive field of the network by increasing the kernel size for our proposed 1D CNN architecture compared to [3], the number of floating point operations (FLOPs) during inference (i.e., the number of floating point multiplication and summation operations) for the proposed method is almost down by a factor of 2 compared to [3] and by a factor of 20 compared to [8] as summarized in Table 2.1. For training the networks on the CHB-MIT dataset we use the ADAM optimizer with a learning rate of 0.001, batch size of 128, and 10 epochs of training. While we did not extensively fine-tune these parameters for any of the models, we did not observe a significant difference in performance as we changed these parameters for the models.

Table 2.1: Computational complexity in FLOPs for all models

	Mega FLOPs
2D CNN [3]	14.5
2D CNN [8]	200
1D CNN	9.81
1D CNN+FG	9.81
1D CNN+GRU	29.4

2.3.2   Factor Graph Based Inference

The 1D CNN model outputs an estimate of the probability that a given 4-seconds block corresponds to a seizure. This probability is based solely on its input EEG segment block and does not account for the fact that the presence of a seizure in a given block is likely to also reflect on its preceding and subsequent blocks. To incorporate this temporal correlation, we combine the probability estimates over multiple blocks by assuming that the underlying temporal correlation can be represented using a factor graph and utilize the sum-product method for inference [12]. In the following, we first describe how the underlying dynamics of the seizure detection setup can be represented as a factor graph, after which we discuss the sum-product algorithm and elaborate on its combinations with the proposed 1-D CNN model.

2.3.2.1   Factor Graph Representation of Underlying Dynamics

Factor graphs provide a visual representation of a multivariate function, typically a joint distribution measure, which can be factorized into a partition of local functions [17]. These partitions capture the inherent statistical relationship among variables affecting each partition. To represent a multivariate function as a factor graph, every partition and every variable must be associated with a unique node. Edges connect function nodes to variables nodes if and only if the function is explicitly dependent on the corresponding variable. We adopt the Forney style representation of factor graphs, where variable nodes are replaced by edges [5]. This graphical representation enables desired quantities to be computed at reduced complexity via message passing over the factor graph [17].

To implement factor graphs inference, we first fix the graph's structure, i.e., the intercon-
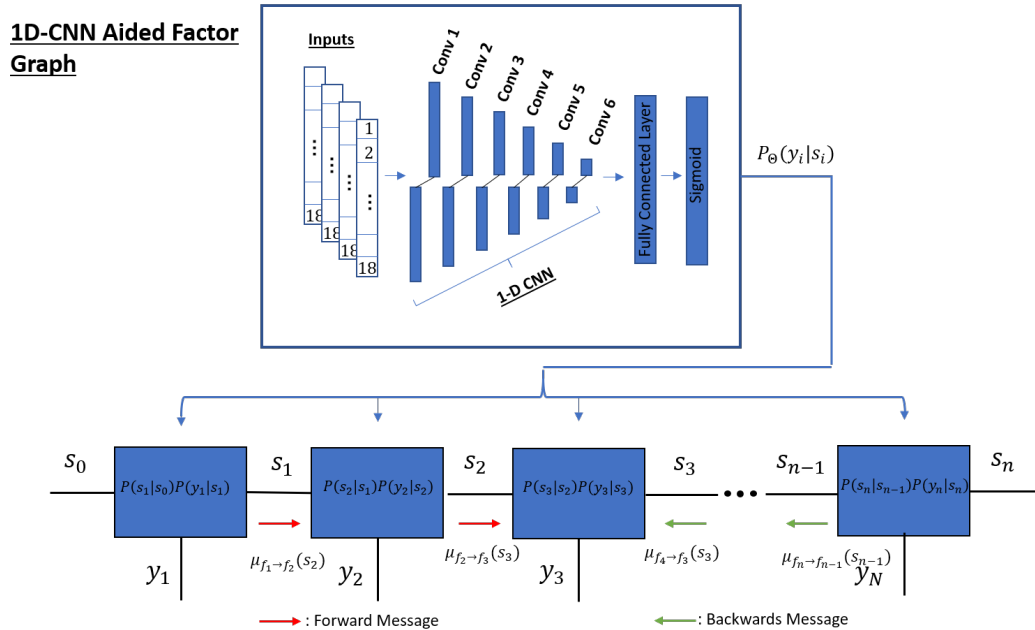
Figure 2.2: Factor Graph of a HMM with function nodes computed using a 1-D CNN.

nection between its nodes, which encapsulates our knowledge on the underlying statistical relationships for the seizure detection problem. A key feature preceding epileptic seizures is the de-synchronization of its rhythmic activity [18]. To capture this behavior in our model study, we adopt a first-order HMM. The Markovian architecture focuses on the temporal characteristics associated with epileptic seizure episodes, highlights the effects of temporal correlations in seizure detection, and facilitates efficient classification at reduced complexity. The resulting factor graph under this model is illustrated in Fig. 2.2.

To formulate this mathematically, let $\boldsymbol{y} = \{y_1, y_2, \cdots, y_N\}$, and $\boldsymbol{s} = \{s_1, s_2, \cdots, s_N\}$ describe the observed EEG measurements and latent seizure states, respectively, over N consecutive 4-seconds blocks. The latent states takes binary values, i.e., $s_i \in \{0, 1\}$ corresponding to the presence or absence of a seizure. We assume that these states satisfy the Markovian property and use $P(s_i|s_{i-1})$ to denote the transition probability. The transition probabilities are chosen using fine-tuning between the values of 0 and 1 with steps of 0.1. In particular, we set $P(s_i = 1|s_{i-1} = 0)$ to correspond to a 10.46% of switching from non-seizure to seizure, and 17.9% for transitioning in the opposite direction. Ideally, one would like the transition probability matrix to reflect the true transitions probabilities between seizure and non-seizure state.

However, the negligible seizure occurrences throughout the recording of EEG episodes produce a highly unbalanced transition probability. Empirically, such transition probabilities did not facilitate accurate inference; hence hyper-parameter optimization of these probabilities was adopted, so that superior performance could be achieved. To close, we assume each EEG measurement depends only on its corresponding seizure state. Under this postulated HMM, the joint probability density function of the measurements and the states can be written as:

$$P(\boldsymbol{s}, \boldsymbol{y}) = \prod_{i=1}^{N} P(s_i|s_{i-1})P(y_i|s_i). \tag{2.1}$$

2.3.2.2 The Sum-Product Algorithm

Having established the mathematical foundation and suitable factor graph representation, the objective is to distinguish between seizure and non-seizures states. Classification of these states is achieved through accurate inference of the marginal distribution $P(s_i, \boldsymbol{y})$, which is the metric used to compute the maximum a-posteriori probability detector. In principle, evaluating $P(s_i, \boldsymbol{y})$ from (2.1) involves *marginalization*; a task whose computational burden scales exponentially with N. However, by employing factor graph inference via the sum-product algorithm, the same computation scales only linearly with N, making this operation computationally feasible for the problem at hand.

The sum-product method relates the desired marginal probability to a product of "messages", where for each $k \in \{1, \ldots, N\}$ we write

$$P(s_k, \boldsymbol{y}) = \mu_{f_j \to s_k}(s_k) \cdot \mu_{f_{j+1} \to s_k}(s_k). \tag{2.2}$$

The terms $\mu_{f_j \to s_k}(s_k), \mu_{f_{j+1} \to s_k}(s_k)$ in (2.2) are interpreted as the "forward message" and "backward message" respectively, and are computed by [17]

$$\mu_{f_j \to s_k}(s_k) = \sum_{\{s_1, \cdots, s_{k-1}\}} \prod_{i=1}^{n} f_i(y_i, s_i, s_{i-1}), \tag{2.3}$$

and

$$\mu_{f_{j+1} \to s_k}(s_k) = \sum_{\{s_{k+1}, \cdots, s_N\}} \prod_{i=n+1}^{N} f_i(y_i, s_i, s_{i-1}), \tag{2.4}$$

where,

$$f_i(y_i, s_i, s_{i-1}) = P(s_i|s_{i-1})P(y_i|s_i). \tag{2.5}$$

For a Markov chain factor graph structure as in Fig. 2.2, the computational complexity is comprised of evaluating the forward (2.3) and the backward (2.4) messages. Since we exploit temporal correlation with factorization structure, the marginalization is performed for a function with a subset of variables. Therefore, the recursive nature of the computations implies that the number of FLOPs grows linearly with the number of 4-second blocks in a given EEG episode, denoted by N. At the same time, the number of FLOPs also increases with the cardinality of the seizure state, denoted by $|\mathcal{S}|$, as well as the order of the Markov chain. Here, all seizure states are binary; hence $|S| = 2$, and the factor graph is that of a first-order Markov chain. As a result, each message computation requires 4 multiplications and 2 addition operations. The result of these computations over a complete EEG episode requires merely $12N$ FLOPs, which is negligible compared to the complexity of applying the neural network models, as reported in Table 2.1.

2.3.2.3 CNN-Aided Factor Graphs

Implementing the sum-product algorithm requires knowledge of the underlying probability distribution $P(y_i|s_i)$. In the case of seizure detection from EEG measurements, acquiring such a distribution from first principles is unattainable. Accurately characterizing epileptic seizures to high fidelity requires a combination of dynamical features and spatial-temporal features, for example, the entropy, amplitude, synchronization, spectral power, amongst other features associated with epileptic seizure episodes, making the underlying distribution highly complex and intractable. To contend with this difficultly, we follow the work [25], combining DL models and inference algorithm. In particular, we utilize the output of the 1D CNN as an estimate of

the conditional distribution $P(y_i|s_i)$ required in order to compute the function nodes[2]. via (2.5). Combining these approaches yields a hybrid model-based/data-driven detector, in which factor graph inference constitutes a robust final stage incorporating temporal correlation with the CNN outputs as illustrated in Fig. 2.2.

To complete the picture, the detection mechanism requires a comparison measure, i.e., a threshold, which represents a decision boundary for one to distinguish between different seizure states based on the estimated marginal distribution produced by the sum-product method. Treating the threshold as fixed, if the resultant probability of a seizure state yielded by the CNN-aided factor graph exceeds that of the applied threshold, then the system is said to be in a seizure state. Otherwise, the system is said to be in a non-seizure state. As shown in the sequel, this approach allows achieving accurate detection with controllable trade-offs between detection and false alarm.

2.4 Results and Discussion

We now discuss our evaluation results in this section. We begin by defining the performance metrics we employed for evaluation followed by the results and the discussions.

2.4.1 Evaluation Method and Performance Metrics

We apply 6-fold leave-4-patient-out cross-validation to evaluate the performance and the generalizability of our hybrid model-based/data-driven approach. Specifically, 4 patients are kept for testing and 20 patients for training in each fold. The dataset used for evaluation, similar to train data, is segmented into 4-second blocks with a moving window of 1 second where each block is labeled. To evaluate the performance of the models trained in each fold, we use the following metrics.

- *F1-score*: is a harmonic mean of recall and precision where the former indicates the proportion of real positive cases that are correctly predicted positive and latter denotes

---

[2]In principle, a CNN classifier is trained with the cross-entropy loss to detect s_i from y_i, which is an estimate of the conditional distribution $P(s_i|y_i)$. Here we use the CNN output as an estimate of the conditional $P(y_i|s_i)$, instead of converting it via Bayes rule as done in [26], in order to avoid instabilities due to dividing by the estimated marginal of the seizure state s_i.

Table 2.2: Summary of Results

	AUC-ROC	AUC-PR	F1 score
2D CNN [3]	0.87 ± 0.05	0.72 ± 0.11	0.85 ± 0.01
2D CNN LOO [8]	N/A	N/A	0.46 ± 0.31
Our 1D CNN	0.89 ± 0.04	0.74 ± 0.1	0.89 ± 0.02
Our 1D CNN-FG	0.90 ± 0.05	0.76 ± 0.11	0.90 ± 0.03
Our 1D CNN-GRU	0.90 ± 0.03	0.76 ± 0.08	0.90 ± 0.03

the proportion of predicted positive cases that are correctly real positives [21]. If the cost of false positives and false negatives are very different, it is better to look at both precision and recall that can be achieved by F1-score.

- *AUC-PR*: is the area under the precision-recall curve where the high area under the curve means the low false-positive rate and low false-negative rate.

- *AUC-ROC* is the area under receiver operating characteristics (ROC) curve, which is performance measurement for classification problems at various threshold settings.

We choose these performance measures since the data is imbalanced (i.e., for every block with seizure, we have 6 blocks with no seizures, and AUC measures are a great indicator of performance over imbalanced data.

2.4.2 Numerical Results

We consider 5 models for comparison. The baselines models from [3, 8], the 1D CNN we proposed, the CNN-aided factor graph, and the 1D CNN with GRU for capturing the temporal correlations. From the baseline models, we implement the exact architecture in [3] and evaluate it using the 6-fold leave-4-patient-out. For [8], since it uses images as features, we just report the results of their leave-one-patient-out (LOO) evaluations from their paper.

Fig. 2.3 shows the average AUC-ROC across the 6 folds, while Table 2.2 summarizes all the results. As can be seen, changing the model from 2D CNN proposed in [3] to our proposed 1D CNN architecture results in approximately 2% improvement across all performance measures. Our hybrid model-based/data-driven CNN-aided factor graph further improves the results by
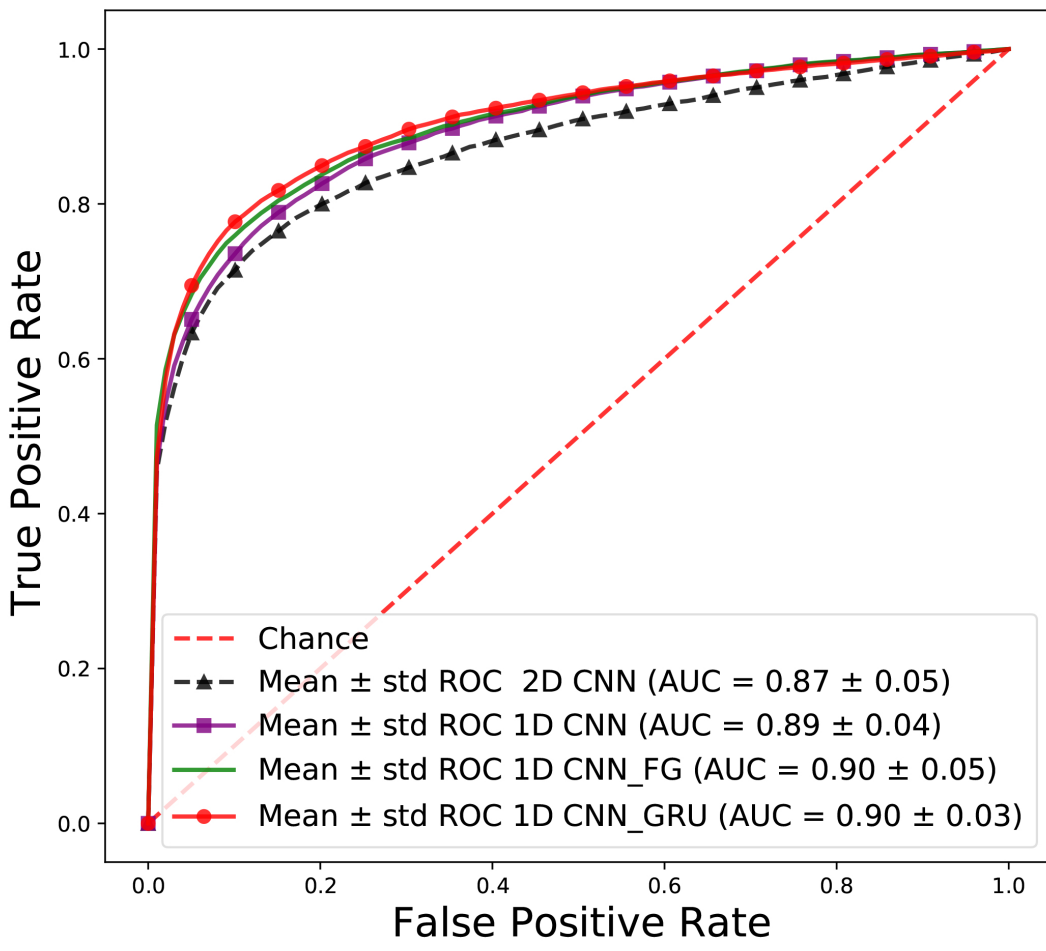
Figure 2.3: Area under ROC curve for all architectures.

as much as 2%. Compared to [8], we perform a leave-4-patient-out evaluation as opposed to leave-one-patient-out. This reduces the number of patients we use for training compared to [8]. Despite this reduction, we achieve a much higher F1 score compared to [8] as shown in Table 2.2. Moreover, while AUC-PR is not reported in [8], the precision of 0.51 ± 0.34 and recall of 0.53 ± 0.25 is reported, which is significantly lower than the performance achieved by our proposed approach.

The 1D CNN with GRU achieves the same performance as our proposed CNN-aided factor graph inference method for all performance metrics. This demonstrates that the hybrid model-based/data-driven approach proposed here can achieve similar performance as purely data-driven methods that employ deep and highly parameterized neural networks. Furthermore, this level of performance is achieved by our CNN-aided factor graph at a fraction of the computational complexity of deep learning-based approaches as summarized in Table 2.1. This makes the proposed method suitable for real-time seizure detection.

2.5   Conclusions

In this study, we proposed a computationally efficient hybrid model-based/data-driven method using CNN-aided factor graphs for seizure detection. First, we carefully designed a 1D CNN for estimating the probability that a 4-second block of EEG recording is a seizure block. We then used this neural network in the factor node of the factor graph for inference. We demonstrated that the proposed method generalizes well to other patients using a 6-fold leave-4-patient-out cross-validation. We also showed that our algorithm achieves up to 5% improvement in performance compared to prior work while maintaining much lower computational complexity. This makes our approach ideal for real-time seizure detection. For future work, we plan to expand our approach to classifying focal and generalized seizures since this is a challenging task in clinical procedures.

References

[1] Epilepsy. `https://www.who.int/news-room/fact-sheets/detail/epilepsy`.

[2] Shaikh Rezwan Rafid Ahmad, Samee Mohammad Sayeed, Zaziba Ahmed, Nusayer Masud Siddique, and Mohammad Zavid Parvez. Prediction of epileptic seizures using support vector machine and regularization. In *2020 IEEE Region 10 Symposium (TENSYMP)*, pages 1217–1220. IEEE, 2020.

[3] Poomipat Boonyakitanont, Apiwat Lek-uthai, Krisnachai Chomtho, and Jitkomut Songsiri. A Comparison of Deep Neural Networks for Seizure Detection in EEG Signals. *bioRxiv*, page 702654, 2019. Publisher: Cold Spring Harbor Laboratory.

[4] Kyung-Ok Cho and Hyun-Jong Jang. Comparison of different input modalities and network structures for deep learning-based seizure detection. *Scientific Reports*, 10(1):122, January 2020.

[5] G. D. Forney. Codes on graphs: Normal realizations. *IEEE Trans. Inf. Theory*, 47:520–548, 2001.

[6] Ary L Goldberger, Luis AN Amaral, Leon Glass, Jeffrey M Hausdorff, Plamen Ch Ivanov, Roger G Mark, Joseph E Mietus, George B Moody, Chung-Kang Peng, and H Eugene Stanley. PhysioBank, PhysioToolkit, and PhysioNet: components of a new research resource for complex physiologic signals. *circulation*, 101(23):e215–e220, 2000. Publisher: Am Heart Assoc.

[7] Meysam Golmohammadi, Saeedeh Ziyabari, Vinit Shah, Silvia Lopez de Diego, Iyad Obeid, and Joseph Picone. Deep architectures for automated seizure detection in scalp EEGs. *arXiv preprint arXiv:1712.09776*, 2017.

[8] Catalina Gomez, Pablo Arbelaez, Miguel Navarrete, Catalina Alvarado-Rojas, Michel Le Van Quyen, and Mario Valderrama. Automatic seizure detection based on imaged-EEG signals through fully convolutional networks. *Scientific Reports*, 10(1):21833, December 2020.

[9] Gopal Chandra Jana, Ratna Sharma, and Anupam Agrawal. A 1D-CNN-spectrogram based approach for seizure detection from EEG signal. *Procedia Computer Science*, 167:403–412, 2020. Publisher: Elsevier.

[10] Simin Khalilpour, Amin Ranjbar, Mohammad Bagher Menhaj, and Afshin Sandooghdar. Application of 1-D CNN to predict epileptic seizures using EEG records. In *2020 6th International Conference on Web Research (ICWR)*, pages 314–318. IEEE, 2020.

[11] Wlodzimierz Klonowski. Everything you wanted to ask about eeg but were afraid to get the right answer. *Nonlinear biomedical physics*, 3(1):1–5, 2009.

[12] Frank R Kschischang, Brendan J Frey, and Hans-Andrea Loeliger. Factor graphs and the sum-product algorithm. 47(2):498–519, 2001.

[13] Sancgeetha Kulaseharan, Azad Aminpour, Mehran Ebrahimi, and Elysa Widjaja. Identifying lesions in paediatric epilepsy using morphometric and textural analysis of magnetic resonance images. *NeuroImage: Clinical*, 21:101663, 2019. Publisher: Elsevier.

[14] Miran Lee, Inchan Youn, Jaehwan Ryu, and Deok-Hwan Kim. Classification of both seizure and non-seizure based on EEG signals using hidden Markov model. In *2018 IEEE International Conference on Big Data and Smart Computing (BigComp)*, pages 469–474. IEEE, 2018.

[15] Chaosong Li, Weidong Zhou, Guoyang Liu, Yanli Zhang, Minxing Geng, Zhen Liu, Shang Wang, and Wei Shang. Seizure Onset Detection Using Empirical Mode Decomposition and Common Spatial Pattern. *IEEE Transactions on Neural Systems and Rehabilitation Engineering*, 29:458–467, 2021. Publisher: IEEE.

[16] Weixia Liang, Haijun Pei, Qingling Cai, and Yonghua Wang. Scalp EEG epileptogenic zone recognition and localization based on long-term recurrent convolutional network. *Neurocomputing*, 396:569–576, 2020.

[17] Hans-Andrea Loeliger. An introduction to factor graphs. 21(1):28–41, 2004.

[18] Florian Mormann, Thomas Kreuz, Ralph G Andrzejak, Peter David, Klaus Lehnertz, and Christian E Elger. Epileptic seizures are preceded by a decrease in synchronization. *Epilepsy research*, 53(3):173–185, 2003. Publisher: Elsevier.

[19] Chulkyun Park, Gwangho Choi, Junkyung Kim, Sangdeok Kim, Tae-Joon Kim, Kyeongyuk Min, Ki-Young Jung, and Jongwha Chong. Epileptic seizure detection for multi-channel EEG with deep convolutional neural network. In *2018 International Conference on Electronics, Information, and Communication (ICEIC)*. IEEE, 2018.

[20] Nikoletta Pianou and Sofia Chatziioannou. Imaging with PET/CT in Patients with Epilepsy. In *Epilepsy Surgery and Intrinsic Brain Tumor Surgery*, pages 45–50. Springer, 2019.

[21] David MW Powers. Evaluation: from precision, recall and F-measure to ROC, informedness, markedness and correlation. *arXiv preprint arXiv:2010.16061*, 2020.

[22] S Raghu, Natarajan Sriraam, Shyam Vasudeva Rao, Alangar Sathyaranjan Hegde, and Pieter L Kubben. Automated detection of epileptic seizures using successive decomposition index and support vector machine classifier in long-term EEG. *Neural Computing and Applications*, 32(13):8965–8984, 2020. Publisher: Springer.

[23] S. Roy, I. Kiral-Kornek, and S. Harrer. Deep learning enabled automatic abnormal EEG identification. In *International Conference of the IEEE Engineering in Medicine and Biology Society (EMBC)*, pages 2756–2759, 2018.

[24] Roneel V Sharan and Shlomo Berkovsky. Epileptic seizure detection using multi-channel EEG wavelet power spectra and 1-D convolutional neural networks. In *2020 42nd Annual International Conference of the IEEE Engineering in Medicine & Biology Society (EMBC)*, pages 545–548. IEEE, 2020.

[25] Nir Shlezinger, Nariman Farsad, Yonina C Eldar, and Andrea J Goldsmith. Learned factor graphs for inference from stationary time sequences. *arXiv preprint arXiv:2006.03258*, 2020.

[26] Nir Shlezinger, Nariman Farsad, Yonina C Eldar, and Andrea J Goldsmith. ViterbiNet: A deep learning based Viterbi algorithm for symbol detection. *IEEE Trans. Wireless Commun.*, 19(5):3319–3331, 2020.

[27] Itaf Ben Slimen, Larbi Boubchir, Zouhair Mbarki, and Hassene Seddik. EEG epileptic seizure detection and classification based on dual-tree complex wavelet transform and machine learning algorithms. *Journal of biomedical research*, 34(3):151, 2020. Publisher: Education Department of Jiangsu Province.

[28] Abdulhamit Subasi, Jasmin Kevric, and M. Abdullah Canbaz. Epileptic seizure detection using hybrid machine learning methods. *Neural Computing and Applications*, 31(1):317–325, January 2019.

[29] Nicole van Klink, Anne Mooij, Geertjan Huiskamp, Cyrille Ferrier, Kees Braun, Arjan Hillebrand, and Maeike Zijlmans. Simultaneous MEG and EEG to detect ripples in people with focal epilepsy. *Clinical Neurophysiology*, 130(7):1175–1183, 2019. Publisher: Elsevier.

[30] Gaetano Zazzaro, Salvatore Cuomo, Angelo Martone, R Valentino Montaquila, Gerardo Toraldo, and Luigi Pavone. EEG signal analysis for epileptic seizures detection by applying data mining techniques. *Internet of Things*, page 100048, 2019. Publisher: Elsevier.

Chapter 3

CNN-Aided Factor Graphs with Estimated Mutual Information Features for Seizure Detection

3.1 Introduction

Epilepsy is a highly common neurological disorder, causing recurrent episodes of involuntary movement known as epileptic seizures [13]. Based on the place in the brain where seizure starts and the intensity of the abnormal signals, patients with epileptic seizures may suffer from different symptoms such as auras, repetitive muscle contraction, and loss of consciousness. [16]. Epileptic seizures severely affect the patient's quality of life and can have other social and economic impacts; for instance, some activities, including swimming, bathing, and climbing a ladder, become dangerous as a seizure during that activity might result in unpredictable injuries and even death. Therefore, early detection of seizures can notably improve the patient's quality of life. A leading tool for seizure identification is based on EEG monitoring, being economical, portable, and non-invasive [26]. However, the review of EEG recordings is a time-consuming expert-dependent process due to contamination by physiological and non-physiological resources [6], and similarity of epileptic spikes to normal EEG waveforms.

The challenges associated with EEG monitoring gave rise to a growing interest in ma-

chine learning aided automatic seizure detection. A common approach is to train a model, typically a CNN, applied to features extracted from the Wavelet or Fourier transform of the signal [24, 1, 18, 11, 21, 7], typically involving careful feature engineering. Additional methods process the raw EEG signals directly. These include the application of CNNs [8, 3] to 4-second EEG blocks, providing instantaneous prediction without exploiting temporal correlation between blocks, as well as processing the complete signal using RNNs [19, 12], which tend to be challenging to properly train. The challenges associated with previous works motivates the formulation of a reliable automatic seizure detection algorithm which generalizes to different patients, benefits from both temporal and inter-channel correlation, and is computationally efficient facilitating its application in real-time.

In this work, we propose a data-driven automatic seizure detection system coined MICAL. MICAL combines computationally efficient 1D CNNs with principled methods for benefiting from temporal and inter-channel correlation. Following [20], we exploit the temporal correlation by imposing a Markovian model on the latent seizure activity [10], using the CNN output not as seizure estimates, but as messages conveyed as a form of learned factor graph inference [23, 9, 22]. To exploit the inter-channel correlation during the ictal (i.e., the seizure) state in a manner that accounts for the high-order joint statistics of the channels, we also use an estimate of the MI between each of the EEG channels. This is achieved using neural MI estimation methods [25], whose estimates are used as features. The MI features along with features learned by the 1D-CNN are then used for learning the factor nodes for factor graph inference. Our numerical evaluations, which use the CHB-MIT dataset [5], demonstrate how each of the ingredients combined in MICAL contributes to its reliability, allowing it to achieve improved accuracy and generalization performance compared to previous algorithms.

The rest of this chapter is organized as follows. In Section 3.2 we describe the problem statement and review necessary preliminaries. Then, in Section 3.3 we describe the proposed MICAL algorithm; Section 3.4 presents a numerical study, while Section 3.5 provides concluding remarks.

3.2 Problem Statement and Preliminaries

3.2.1 Seizure Detection Problem

Based on the dataset used in this study, seizure detection refers to the identification and local-ization of ictal discharges from EEG recordings of patients with epilepsy [4]. To formulate this mathematically, let $X = \{X_1, X_2, \cdots, X_N\}$ be the EEG recordings of a patient, where N represents the number of channels. Each measured channel X_i is comprised of n consecutive blocks, e.g., blocks of 1-second recordings, and we write $X_i = [x_{t_1}^{(i)}, x_{t_2}^{(i)}, \cdots, x_{t_n}^{(i)}]$, where $x_t^{(i)}$ is the signal corresponding to the i-th EEG channel during the t-th block. The seizure state for each block is represented as a binary vector $s = [s_{t_1}, \ldots s_{t_n}]$, where $s_t \in \{0, 1\}$ models whether or not a seizure occurs in the t-th block. Our goal is to design a system which maps the EEG recordings X into an estimate of s, which is equivalent to finding the time indices where seizure occurs. Explicitly modeling the relationship between the EEG signals X and the seizure states s is likely to be intractable. Nonetheless, it is known that the recordings exhibit both inter-channel correlations as well as temporal correlation. The former stems from the fact that when a seizure starts, the seizure activity propagates to other areas in the brain [17]. When a seizure happens, a sharp wave discharges in one or more EEG channels and the patterns of other channels recordings are affected. This manifests high dependence between different channels, i.e., between $x_t^{(i)}$ and $x_t^{(j)}$, when t is at the beginning and during ictal phase. Temporal correlation results from the fact that seizures typically span multiple recording blocks, and thus the probability of observing a seizure at time instance t depends on the presence of a seizure in the previous block, such that the entries of s can be approximated as obeying a Markovian structure [10]. Our proposed solution, detailed in Section 3.3, exploits this statistical structure using factor graph inference briefly summarized next.

3.2.2 Factor Graph Inference

Factor graphs are a representation of factorizable multi-variable functions, such as probabil-ity distributions, as a bipartite graph. These graphical models facilitate inference at reduced complexity via message passing algorithms, such as the sum-product methods [14].

Consider an observed sequence $Y = [y_1, \ldots, y_n]$ encapsulating a latent state sequence $s = [s_1, \ldots, s_n]$ whose entries take values in a finite set $\mathcal{S}$, as a form of a HMM. In such cases, the joint distribution of y, s obeys

$$P(s, y) = \prod_{k=1}^{n} P(s_k|s_{k-1})P(y_k|s_k), \tag{3.1}$$

which can be represented as factor graph with variable nodes $\{s_k\}_{k=1}^{n}$ and function nodes $\{f_k\}_{k=1}^{n}$, where $f_k(s_k, s_{k-1}) := P(s_k|s_{k-1})P(y_k|s_k)$.

The factor graph representation allows one to compute the maximum a-posteriori probability (MAP) decision rule with a complexity that only grows linearly with n as opposed to exponentially with n. This is achieved by evaluating the marginal distribution $P(s_k, y)$ for each $k \in \{1, \ldots n\}$ via message passing over the factor graph. In this case, the forward messages are recursively updated via

$$\mu_{f_k \to s_k}(s_k) = \sum_{\{s_1, \cdots, s_{i-1}\}} \prod_{j=1}^{k} f_j(s_j, s_{j-1}), \tag{3.2}$$

and the backward messages via

$$\mu_{f_{k+1} \to s_k}(s_k) = \sum_{\{s_{k+1}, \cdots, s_n\}} \prod_{j=k+1}^{n} f_j(s_j, s_{j-1}). \tag{3.3}$$

Then, the desired marginal distribution, which is maximized by the MAP rule, is given by

$$P(s_k, y) = \mu_{f_k \to s_k}(s_k) \cdot \mu_{f_{k+1} \to s_k}(s_k). \tag{3.4}$$

Intuitively (3.2)-(3.3) are interpreted as an aggregate of neighboring information. Once all neighbors have communicated (i.e., messages have propagated the entirety of the graph) the product of the forwards and backward messages determines the marginal probability.
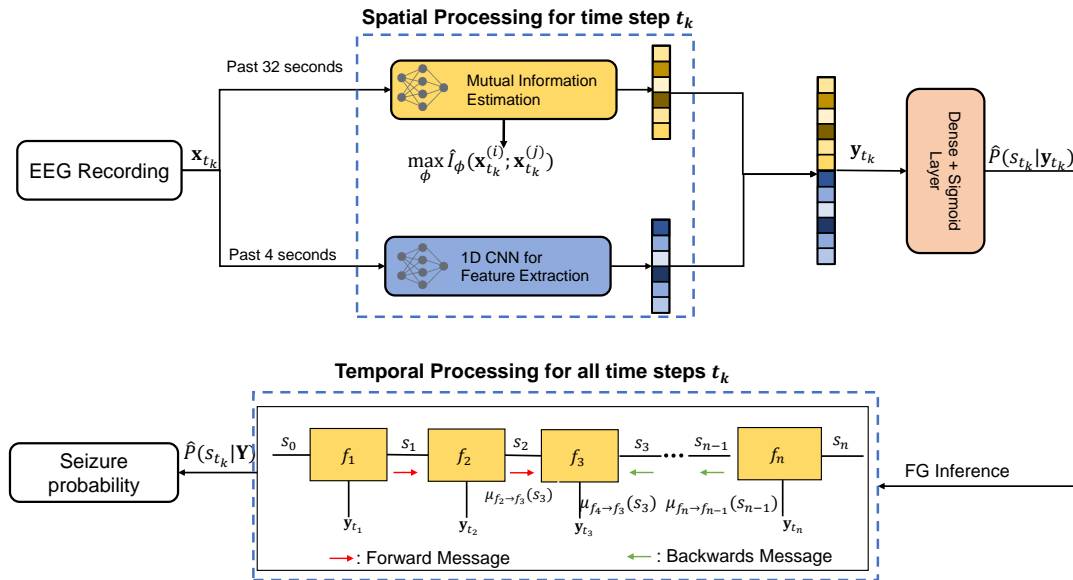
Figure 3.1: MICAL illustration.

3.3 MICAL Seizure Detection Algorithm

In this section, we present the proposed MICAL algorithm. MICAL is comprised of three main components: neural MI estimator quantifying the instantaneous dependence between different channels at each EEG block to capture the inter-channel correlation (see Subsection 3.3.1); a 1D CNN which generates a latent representation of the raw EEG block plus a soft estimate of the seizure state using the joint features from the 1D-CNN and the neural MI estimator (see Subsection 3.3.2); and factor graph inference utilizing the soft estimates as learned function nodes to incorporate temporal correlation (see Subsection 3.3.3). A high-level illustration of the flow of MICAL is depicted in Fig. 3.1.

3.3.1 Neural Mutual Information Estimation

MI is a measure of the statistical dependence between two random variables. Unlike the popular cross-correlation measure of similarity, MI represents higher-order joint statistics, and is thus able to capture non-linear relationship between samples, which are likely to occur in EEG signals during seizure. The MI between the random variables x_1, x_2 taking values in $\mathcal{X} \times \mathcal{X}$ with

a joint distribution $P_{X_1X_2}$ and marginals P_{X_1} and P_{X_2} is defined as

$$I(X_1; X_2) = D_{\text{KL}}(P_{X_1X_2}\|P_{X_1}P_{X_2}), \tag{3.5}$$

where D_{KL} is the Kulback-Leibler (KL) divergence that shows how one distribution is different from the other.

A key challenge in using MI as a measure of statistical depends stems from the challenge in estimating (3.5) from realizations of the random quantities [15]. Nonetheless, it was recently shown that neural networks can be trained to estimate the MI, based on the Donsker-Varadhan representation

$$D_{KL}(P_{X_1X_2}\|P_{X_1}P_{X_2}) = \sup_{T:\mathcal{X}\times\mathcal{X}\mapsto\mathbb{R}} \mathbb{E}_{P_{X_1X_2}}[T(x_1, x_2)] - \log\left(\mathbb{E}_{P_{X_1}P_{X_2}}\left[e^{T(x_1,x_2)}\right]\right), \tag{3.6}$$

and training a neural model with parameters $\boldsymbol{\phi}$ denoted $T_{\boldsymbol{\phi}}$ to maximize the right hand side of (3.6) [2]. To overcome limitations associated with the estimation variance, the work [25] proposed the Smoothed MI Lower-bound Estimator (SMILE), which learns to estimate MI by training a neural network to maximize the objective

$$\hat{I}_{\boldsymbol{\phi}}(X_1; X_2) = \mathbb{E}_{P_{X_1X_2}}\left[T_{\boldsymbol{\phi}}(x_1, x_2)\right] - \log\mathbb{E}_{P_{X_1}P_{X_2}}\left[\text{clip}(e^{T_{\boldsymbol{\phi}}(x_1,x_2)}, e^{-\tau}, e^{\tau})\right], \tag{3.7}$$

where $\text{clip}(v, l, u) := \max(\min(v, u), l)$ and τ is a hyperparameter. The resulting neural estimator was shown to learn to reliably predict MI under various distributions.

In MICAL, we apply SMILE to estimate $I(\boldsymbol{x}_t^{(i)}; \boldsymbol{x}_t^{(j)})$ at each block t for each channel pair i, j. Since MI is symmetric, i.e., $I(\boldsymbol{x}_t^{(i)}; \boldsymbol{x}_t^{(j)}) = I(\boldsymbol{x}_t^{(j)}; \boldsymbol{x}_t^{(i)})$, we only estimate the MI for $j > i$. We set $T_{\boldsymbol{\phi}}$ to be a fully-connected network with two hidden layers and ReLU activations, and train it with $\tau = 0.9$ in the objective (3.7). The resulting neural estimator, which learns to capture statistical dependence, is numerically shown to reflect on the presence of seizure, satisfying the underlying hypothesis of high correlation among recordings during seizure state. This is illustrated in Fig. 3.2, where it is observed that the trained estimator outputs higher MI values during seizure compared to non-seizure blocks.
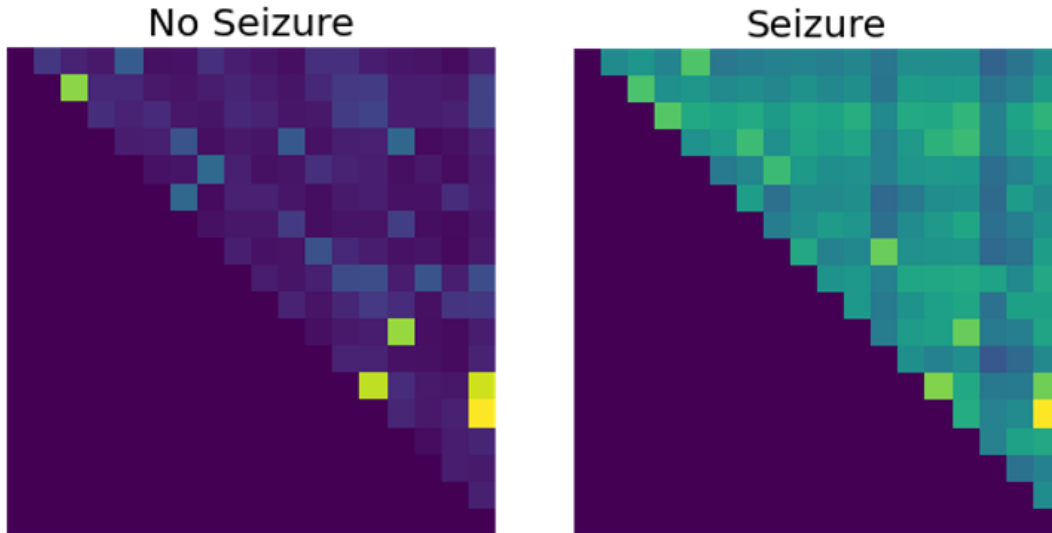
Figure 3.2: Neural MI estimation for seizure and non-seizure.

3.3.2 1D CNN

In parallel to neural MI estimation, each raw EEG signals block is also processed using a dedicated 1D CNN to extract relevant features from the block. The resulting vector y_t, representing the stacking of these extracted features and the estimated MI at EEG block t, is used to produce a probabilistic estimate of the presence of a seizure.

We develop a 1D CNN architecture to extract meaningful features from raw EEG signals and combine these features with the MI estimation results. Compared to 2D CNNs, specifically, the baseline model proposed by Boonyakitanont et al. [3], 1D CNN can evaluate all EEG channels at a given time instance, but in 2D CNNs only the channel indexes that are close together are processed together.

To have a comparable configuration with the baseline model, we use the same number of filters. Unlike previous studies, we design the kernel size such that our 1D CNN will have a high receptive field of 1 second of the recording, compared to approximately 33 ms in prior works. This feature of the architecture leads to capturing low-frequency components of the signals and long-term temporal correlation within the 4-second blocks in EEG signals. The details of the proposed CNN model is shown in Fig 3.1.

3.3.3 Factor Graph Inference

Using the MI estimates and the features from 1D CNN, the seizure state probability from each 4-second block is treated independently. The resulting prediction thus does not exploit the presence of temporal correlation, which is known to be present in EEG-based seizure detection. Therefore, as proposed in [23] for sleep state tracking, we exploit the presence of temporal correlation by utilizing the block-wise soft decisions not for prediction but as learned function nodes in a factor graph.

We incorporate temporal correlation by assuming that the relationship between the extracted features $y_1, \ldots, y_n$ and the underlying seizure state $s_1, \ldots, s_n$ can be represented as an HMM. Similar modelling was shown to faithfully capture the temporal statistics in EEG-based seizure detection [10]. For such models, one can compute the MAP rule with linear complexity using sum-product inference over the resulting factor graph, as described in Subsection 3.2.2. However, to evaluate the messages (3.2)-(3.3), one must be able to compute the function nodes $\{f_k\}_{k=1}^n$, given by

$$f_k(s_{t_k}, s_{t_{k-1}}) = P(s_{t_k}|s_{t_{k-1}})P(y_{t_k}|s_{t_k}). \tag{3.8}$$

In MICAL, we utilize the block-wise soft decisions as estimates of the conditional distribution $P(y_{t_k}|s_{t_k})$. The transition probability $P(s_{t_k}|s_{t_{k-1}})$, which is essentially comprised of two values, can be obtained from histogram, or manually tuned as we do in our numerical study in Section 3.4. The obtained marginal distributions (3.4) are compared to a pre-defined threshold T for detection. The resulting seizure detection algorithm is summarized as Algorithm 1.

3.4 Numerical Results

We evaluate MICAL[1] using the CHB-MIT dataset [5]. The data is comprised of scalp EEG recordings from 24 pediatric subjects with intractable seizures, sampled at a frequency of 256 Hz, where seizure start and end times are labeled. In order to balance and denoise the dataset, a few simple pre-processing steps are included. Sample recordings with at least one seizure are selected, and a notch filter is applied to remove the noise from the power line. Due to

---

[1]The source code and the complete set of hyperparameters can be found online at `https://github.com/bsalafia/CNN-Aided-Factor-Graphs-with-Estimated-Mutual-Information-Features-for-Seizure-Detection-MICAL.git`

Algorithm 1: MICAL seizure detection

---

1 **Inputs:** SMILE and 1D CNN networks, estimated $P(s_{t_k}|s_{t_{k-1}})$, EEG signals X, threshold T

   Feature extraction:

2 **for** $k = 1, \ldots n$ **do**

3   Apply SMILE to estimate $\hat{I}_\phi(x_{t_k}^{(i)}; x_{t_k}^{(j)})$, $j > i$;

4   Apply 1D CNN to obtain combined features y_{t_k} and obtain soft decision;

5 **end**

   Factor graph inference:

6 Compute $\{f_k\}$ from soft decisions via (3.8);

7 **for** $k = 1, \ldots n$ **do**

8   Compute $\mu_{f_{t_k} \to s_k}(\{0, 1\})$ via (3.2);

9   Compute $\mu_{f_{t_{n-k+2}} \to s_{n-k+1}}(\{0, 1\})$ via (3.3);

10 **end**

11 Detect seizure at t_k if $\mu_{f_{t_k} \to s_k}(1)\mu_{f_{t_{k+1}} \to s_k}(1) > T$.

---

the short seizure duration, for each recording file, we reduce non-seizure samples to 10 times before and 10 times after seizure time. Therefore, for every second of seizure data, there are 20 seconds of non-seizure data. The seizures is estimated for every second. To estimate the probability of seizure over the t-th second, the past 32 seconds of recording is used to solve the optimization that estimates MI. This window size was selected by experimenting with window lengths ranging from 16 seconds to 64 seconds and choosing the window length that yields the best results. Therefore, the window size of 32 seconds has demonstrated the best results over the dataset. The past 4 seconds of recording is used as input to the 1D CNN for estimating the features. The value of 4 seconds is selected to satisfy a good trade off between the number of samples in a block and the stationarity of the observed signals over a block.

In our experiments, five models are used for comparison. The 2D CNN used in [3] and spectrogram detector of [7] as two baseline models since they reported the best results compared to prior work. For MICAL, we tune the transition probability to $P(s_{t_k} = 1|s_{t_{k-1}} = 1) = 89.54\%$ and $P(s_{t_k} = 1|s_{t_{k-1}} = 0) = 17.90\%$. To evaluate the contribution of each of the individual components of MICAL, we evaluate inference based solely on 1D CNN features (without the MI features or factor graph inference), as well as when its outputs are processed with an RNN comprised of GRU cells to learn to exploit temporal correlation rather than using factor graph inference. All detectors use decision threshold of $T = 0.5$.

For considering variability among patients, 6-fold leave-4-patients-out evaluation is conducted. To examine the performance of the proposed hybrid algorithm, three metrics are measured: area under ROC curve (AUC-ROC) which shows the capability to distinguish between seizure and non-seizure samples, area under precision recall curve (AUC-PR) that is the indicative of success and failure rates, and F1 score representing the hormonal mean between precision and recall.

	AUC-ROC	AUC-PR	F1 score
2D CNN [3]	0.78 ± 0.08	0.37 ± 0.17	0.88 ± 0.03
Spectrogram [7]	0.77 ± 0.07	0.37 ± 0.1	0.92 ± 0.03
1D CNN	0.82 ± 0.04	0.42 ± 0.12	0.91 ± 0.02
1D CNN-GRU	0.82 ± 0.03	0.44 ± 0.10	0.90 ± 0.06
MICAL	**0.83 ± 0.04**	**0.50 ± 0.13**	**0.93 ± 0.01**

Table 3.1: Summary of results

The results for three performance measures are summarized in Table 3.1. The represented values for all metrics show the average across 6 folds. It is observed in Table 3.1 that the 1D CNN used by MICAL achieves almost 5% improvement compared with the baseline models, specifically for AUC-ROC and AUC-PR. While adding GRU to the 1D CNN has no significant effect on the model performance, the incorporation of MI estimation and factor graph inference by MICAL yields the highest performance measures, 0.83 and 0.50 for AUC-ROC and AUC-PR, respectively and 0.93 for F1 score. This implies that including only the temporal aspect of EEG recordings is not enough to have an accurate seizure detection, and the results indicate that our algorithm admits the hypothesis of existing high correlation among signals during seizure states. Furthermore, exploiting temporal correlations in a principled manner through factor graphs is shown to facilitate learning an accurate detector, compared to using a black-box RNNs, at a much reduced computational complexity. It should be noted that the metric results for 2D CNN baseline model for Table 3.1 are different from Table 2.2 as for each EDF file, there are 20 seconds of no-seizure samples instead of 6 seconds, resulting in a more imbalanced dataset for training.

3.5   Conclusion

We proposed MICAL, which is a data-driven EEG-based seizure detector designed to exploit both inter-channel and temporal correlations. For this, MICAL estimates the MI between each pair of EEG channels to capture the non-linear correlation among recordings observed during seizure times. The estimated MI is combined with a carefully designed 1D CNN to provide a soft estimate for each signal block. Instead of using these features for prediction, they are utilized to evaluate the function nodes of an underlying factor graph, allowing it to infer at linear-complexity while exploiting temporal features between EEG blocks. We demonstrate that MICAL achieves notable improved performance compared to previously proposed methods.

References

[1] Shaikh R Ahmad et al. Prediction of epileptic seizures using support vector machine and regularization. In *2020 IEEE Region 10 Symposium*, pages 1217–1220.

[2] Mohamed Ishmael Belghazi et al. Mutual information neural estimation. In *International Conference on Machine Learning*, pages 531–540. PMLR, 2018.

[3] Poomipat Boonyakitanont et al. A comparison of deep neural networks for seizure detection in EEG signals. *bioRxiv*, page 702654, 2019.

[4] Prabhu D Emmady and Arayamparambil C Anilkumar. EEG, Abnormal Waveforms. *StatPearls*, 2020.

[5] Ary L Goldberger et al. PhysioBank, PhysioToolkit, and PhysioNet: components of a new research resource for complex physiologic signals. *circulation*, 101(23):e215–e220, 2000.

[6] Meysam Golmohammadi et al. Deep architectures for automated seizure detection in scalp EEGs. *arXiv preprint arXiv:1712.09776*, 2017.

[7] Gopal Chandra Jana, Ratna Sharma, and Anupam Agrawal. A 1D-CNN-spectrogram based approach for seizure detection from EEG signal. *Procedia Computer Science*, 167:403–412, 2020.

[8] Simin Khalilpour et al. Application of 1-D CNN to predict epileptic seizures using EEG records. In *2020 International Conference on Web Research*, pages 314–318.

[9] Patrick Knobelreiter et al. Belief propagation reloaded: Learning BP-layers for labeling problems. In *Proceedings of the IEEE/CVF Conference on Computer Vision and Pattern Recognition*, pages 7900–7909, 2020.

[10] Miran Lee et al. Classification of both seizure and non-seizure based on EEG signals using hidden Markov model. In *2018 IEEE International Conference on Big Data and Smart Computing (BigComp)*, pages 469–474.

[11] Chaosong Li et al. Seizure onset detection using empirical mode decomposition and common spatial pattern. 29:458–467, 2021.

[12] Weixia Liang et al. Scalp EEG epileptogenic zone recognition and localization based on long-term recurrent convolutional network. *Neurocomputing*, 396:569–576, 2020.

[13] Brian Litt and Javier Echauz. Prediction of epileptic seizures. *The Lancet Neurology*, 1:22–30, 2002.

[14] Hans-Andrea Loeliger. An introduction to factor graphs. 21(1):28–41, 2004.

[15] Liam Paninski. Estimation of entropy and mutual information. *Neural computation*, 15(6):1191–1253, 2003.

[16] Chulkyun Park et al. Epileptic seizure detection for multi-channel EEG with deep convolutional neural network. In *2018 International Conference on Electronics, Information, and Communication (ICEIC)*.

[17] Antonio Quintero-Rincón et al. A new algorithm for epilepsy seizure onset detection and spread estimation from eeg signals. In *Journal of Physics: Conference Series*, volume 705, page 012032, 2016.

[18] S Raghu et al. Automated detection of epileptic seizures using successive decomposition index and support vector machine classifier in long-term EEG. *Neural Computing and Applications*, 32(13):8965–8984, 2020.

[19] S. Roy, I. Kiral-Kornek, and S. Harrer. Deep learning enabled automatic abnormal EEG identification. In *International Conference of the IEEE Engineering in Medicine and Biology Society*, pages 2756–2759, 2018.

[20] Bahareh Salafian et al. Efficient epileptic seizure detection using CNN-aided factor graphs. *arXiv preprint arXiv:2108.02372*, 2021.

[21] Roneel Sharan and Shlomo Berkovsky. Epileptic seizure detection using multi-channel EEG wavelet power spectra and 1-D convolutional neural networks. In *2020 International Conference of the IEEE Engineering in Medicine & Biology Society*, pages 545–548.

[22] Nir Shlezinger et al. Data-driven factor graphs for deep symbol detection. In *IEEE International Symposium on Information Theory*, pages 2682–2687, 2020.

[23] Nir Shlezinger et al. Learned factor graphs for inference from stationary time sequences. *arXiv preprint arXiv:2006.03258*, 2020.

[24] Itaf Ben Slimen et al. EEG epileptic seizure detection and classification based on dual-tree complex wavelet transform and machine learning algorithms. *Journal of biomedical research*, 34(3):151, 2020.

[25] Jiaming Song and Stefano Ermon. Understanding the limitations of variational mutual information estimators. *arXiv preprint arXiv:1910.06222*, 2019.

[26] Abdulhamit Subasi, Jasmin Kevric, and M. Abdullah Canbaz. Epileptic seizure detection using hybrid machine learning methods. *Neural Computing and Applications*, 31(1):317–325, January 2019.

Chapter 4

Mutual Information-based CNN-Aided Learned Factor Graphs (MICAL) for Seizure Detection

4.1   Introduction

Epilepsy is a chronic neurological disorder which is accompanied by sudden and unforeseen occurrence of signs or symptoms as a result of abnormal electrical activity in the brain that may cause seizures [17]. According to World Health Organization, about 50 million people worldwide are diagnosed with epilepsy [1]. The extensive sudden discharges in neural brain activity due to epileptic seizures can lead to life-threatening impacts such as involuntary movements, sensations, and emotions and may cause a temporary loss of awareness and even death [51].

4.1.1   Diagnostic Tests for Epileptic Seizure

There are many different tests used to see whether a person has the form of epilepsy and if so, what type of seizures the patient is suffering from. These approaches comprise of two main categories, experimental tests, and imaging and monitoring. The first group includes reviewing medical history [41], performing blood tests to observe the metabolic or genetic disorders associated with the seizures [44, 30] or underlying health conditions that could be the triggers

of epileptic seizures [30]. Imaging and monitoring are the most popular tools in detecting epileptic seizures. In this regard, various screening techniques such as magnetoencephalogram (MEG) [66], computed tomography (CT) [52], positron emission tomography (PET) [57], and magnetic resonance imaging (MRI) [34] have been employed. Among these techniques, EEG is the most powerful method as it shows clear rhythmic electrical activities of the neurons [59]. There are two types of EEG recording strategies: invasive EEG (ECOG) [71] and scalp EEG. ECOG is usually used when a patient is diagnosed by refractory surgery as it provides direct measurement of brain electrical activity by implanting electrodes on the cortex [67]. Scalp EEG has been done by locating multiple electrodes on the scalp of individuals that are connected to a monitoring device through many wires [71]. This technique is widely preferred as it is non-invasive, economical, and portable. From clinical point of view, a neurologist can analyze abnormalities in EEG signals through visual inspection to understand the presence or the level of epileptic seizures. However, this observation is based on long-term records [63] which is a time-consuming task and subject to inter-observer variability [7]. Moreover, EEGs are usually exposed to be contaminated by undesired artifact resources that can interfere with neural information and cause misdiagnose in epileptic seizures [28]. Therefore, to address the issues related to EEG monitoring, several automatic seizure detection approaches have been explored. These techniques are divided into spike detection, feature engineering, and non-feature-based design. In the following subsections, we first discuss the seizure detection problem. We then explain previous studies that have been accomplished for automatic seizure detection techniques, and ultimately, we detail our proposed method.

4.1.2   Seizure Detection Problem Using EEG Signals

In seizure detection problem, there are few basic terms as follows:

- Ictal state which is the time when the seizure occurs (from start to end).

- Preictal state is a period of time just before a seizure occurs.

- Interictal state refers to the period between seizures.

- Postictal state is a period of time just after the seizure ends.

In this study, seizure detection refers to the identification and localization of ictal discharges from EEG recordings of patients with epileptic seizures [14]. One traditional way to analyze EEG signals for seizure detection is visually monitoring the recordings by an expert. However, for more objective analysis and reproducible results, visual reviewing is a time-consuming process. In addition, this process is usually accompanied by human errors due to the subjective nature of the analysis, ictal spikes morphology as well as similarity of these signals to the normal waves or artifacts. Therefore, automatic seizure detection is a key technology to overcome the difficulties in monitoring EEG recordings. Mathematically, let $X = \{X_1, X_2, \cdots, X_N\}$ be the EEG signals of a patient, where N represents the number of channels and X_i refers to information measured for i-th channel. The goal of an automatic seizure detection system is to find time indices from EEG recordings X when seizures occur. In Subsection 4.1.3 to 4.1.5, we describe some methods that have been previously proposed in seizure detection.

4.1.3   Spike Detection

A number of spike detection methods have been previously developed. Basically, these methods aim at detection of the presence of interictal spikes in the multichannel EEG recording with high sensitivity and selectivity [64] and they are divided into different categories including template matching [54, 69], mimetic analysis [21, 22], power spectral analysis [15], wavelet analysis [24] and artificial neural networks (ANNs) [33, 19, 3].However, these methods mainly depend upon the expert definition of EEG characteristics such as slop, duration, height, and sharpness, which are not sufficient enough to represent an epileptic seizure spike, and it can result in a highly false detection rate [70].

4.1.4   Feature-Based Design

There are number of features that influence the seizure detection performance. Feature extraction methods can be divided to time-domain features, frequency-domain features, time and frequency features (discretely), and time-frequency domain features (simultaneously).

4.1.4.1 Feature Extraction

Time-domain analysis Time-domain analysis works with stationary signals, whereas biosignals are non-stationary. Hence, the first step for performing this technique is considering the signal as multiple stationary segments. Previous studies have been used slope sign change, Willison amplitude, and Lyapunov exponents. Using Lyapunov exponents with a probabilistic neural network (PNN) was proposed by Übeyli et al. [65] where Lyapunov exponents determine the stability of any steady-state behavior, including chaotic solutions [65]. Khorshidtalab et al. [31] assessed applying a time-domain feature extractor based on modified Willison amplitude (WAMP) and slope sign change (SSC) with predefined threshold followed by two different classifiers such as SVM and fuzzy C-means (SFCM).

Frequency-domain analysis The frequency-domain analysis is categorized into three groups: fast Fourier transform (FFT), Eigenvector, and Autoregressive (AR). The authors in [37] used FFT and PCA to partition the signals into five sub-band frequencies and find a linear combination of frequency features with the maximum variance, respectively. Eigenvector techniques through power spectral density (PSD) are used to calculate signal frequency and power from artifact-dominated measurements . AR methods estimate the power spectrum density (PSD) of the EEG using a parametric approach [6]. The two Yule-Walker and Burg's techniques are usually employed to estimate AR models [60, 16].

Time and frequency features Iscan et al. [25] applied combined time and frequency features to classify healthy and epileptic EEG signals. Time-domain features were extracted by using cross-correlation and frequency-domain features by computing the PSD. Srinivasan et al. [58] observed three frequency-domain features (dominant frequency, average power in the primary energy zone, and normalized spectral entropy) and two time-domain features (spike rhythmicity and relative spike amplitude) to detect the seizure.

Time-frequency domain analysis Time-frequency domain analysis extracts features from a signal in both time and frequency domains simultaneously. Time-frequency distribution (TFD) and wavelet transform analysis (WT) is the most popular techniques in this area [32]. Boashash

et al. [9] performed the optimal subset of TF features using the wrapper method with sequential forward feature selection (SFFS) on multi-channel recordings via channel fusion and feature fusion approaches. The application of discrete wavelet transform (DWT) was done by Subasi et al. [59]. They first used a dynamic wavelet network to decompose EEGs into the frequency sub-bands; then, an ANN was applied to output two classes of normal and epileptic states. Rosso et al. [49] introduced a new tool based on wavelet entropy using orthogonal discrete wavelet transform (ODWT). ODWT comprises three parameters: relative wavelet energy, wavelet entropy (WE), and relative wavelet entropy (RWE).

Deep learning-based feature extraction   The classifier used in most of the abovementioned techniques was SVM. However, these methods are suitable for the problems where classes are distributed linearly. As such, recent studies are focused on using DL algorithms as they can learn the features of their input even in the presence of non-linear behaviour [73]. The authors in [53] first generated three different features based on Fourier, wavelet, and empirical mode decomposition transforms. They then applied a shallow 2D CNN and concluded that Fourier transforms achieved the best results. Another wavelet-based deep learning approach was performed in [5]. In this method, DWT was used to extract time-frequency domain features in five sub-band frequencies, and then a 2D CNN architecture was employed to learn the features from predefined coefficients. Applying 1D CNN to time-frequency features was observed in [12, 18]. In the proposed method, first DWT of signals was processed and a 1D CNN architecture then generated the probability distribution over labels.

4.1.5   Non-feature Based Design

Developing a feature-based technique requires careful engineering and considerable domain expertise to design an extractor that transforms the raw data into a suited internal representation [36]. However, this strategy is difficult since various types of patterns appear when a seizure occurs [32]. Unlike feature engineering algorithms, deep-learning models are representation learning methods with multiple levels of representation obtained by composing simple but non-linear modules that each transform representation at one level (starting with the raw input) into a representation at a higher level [36]. The two main DL structures which applied to

raw EEG data are CNN and RNN. Below, we summarize some of the previous studies focused on these scopes.

4.1.5.1 Convolutional Neural Network (CNN)

This class of DL models is extensively used for epileptic seizure detection. In [29], after using a notch filter, a 1D CNN with few convolutional layers was employed to detect interictal epileptiform spikes due to seizures. Acharya et al. [2] applied a 3-layer CNN architecture to the normalized EEG signals. A 2D CNN architecture was implemented in [39] where dataset contains of five different cases. Boonyakitanont et al. [10] proposed a detection scheme using raw EEG records divided into 4-second blocks followed by a deep 2D CNN architecture to learn the features from EEG signals. They showed the state-of-the-art performance based on detection accuracy via per-patient training.

4.1.5.2 Recurrent neural networks

Although CNNs are popular for seizure detection, these models are not able to exploit temporal correlation. Hence, many recent studies have been focused on RNNs architectures. The investigation of RNNs performance was explored in [68, 72]. However, these models usually encounter vanishing gradient when dealing with long-term dependent signals. Therefore, to overcome this limitation, recent studies are mostly considered LSTM and gated recurrent unit (GRU). Hussein et al. [23] used a deep recurrent neural network, particularly LSTM to the segmented EEG signals to learn the most robust features from recordings. Aristizabal et al. [4] developed another LSTM-based seizure detection technique for six pairs of EEG signals. The performance of GRU was observed in [61]. In this model, the GRU-hidden unites were used to classify EEG to three classes including healthy, inter-ictal and ictal states. Roy et al. [50] proposed an architecture termed ChronoNet formed of stacking multiple 1D convolution layers followed by GRU layers. The combination of a CNN structure with an RNN model such as LSTM was pursued in [62]. In their study, five different archetypes including 1D CNNs, 2D CNNs, LSTMs, 1D CNNs with LSTMs and 2D CNNs with LSTMs were implemented. Their evaluation results indicated that the model consisting of 2D CNNs with LSTMs showed the best performance.

4.2   Motivation and Proposed algorithm

Despite the proliferation of non-feature based models, there are two major limitations in applying these approaches for seizure detection: CNNs are not able to exploit temporal correlation and RNNs suffer from high computational complexity during training. Moreover, most of the existing methods have been built based on limited EEG data taken from few patients that makes these models less practical in clinical applications. The challenges associated with previous works motivate us to introduce a generalized and hybrid model-based/data-driven approach that is capable of capturing temporal correlation efficiently as well as the inter-channel correlation among EEG channels during seizure times. The inter-channel correlation results from the impact of seizures on electrical brain activity. When a seizure occurs in one or more EEG channels, the patterns of other channel recordings are affected, and it represents as high dependence between signals at the beginning and during ictal state [11, 48]. Fig. 4.1 demonstrates the signal patterns during seizure vs. no-seizure states. Temporal correlation results from the fact that seizures typically span multiple recording blocks, and thus the probability of observing a seizure for input block depends on the presence of the seizure in the previous blocks. To include these two correlations, we propose an automatic seizure detection system called MICAL. In order to implement MICAL, we develop our previous study on CNN-aided factor graphs in which we exploited the temporal correlation by adopting a first-order HMM on the latent seizure activity [38], using the CNN output as messages conveyed to a form of learned factor graph inference. Fig 4.2 illustrates MICAL structure. We first train a neural MI network to estimate instantaneous dependence among EEG channels that leads to capturing inter-channel correlation. The MI estimations combined with 1D CNN latent representations are then used for learning factor graph inference node. Employing factor graphs results in exploiting temporal correlation at reduced complexity via HMM and message passing based on sum-product algorithm. In the following sections, we first explain each component of the proposed method, followed by a data description. We then observe algorithm performance and finally mention discussion and conclusion.
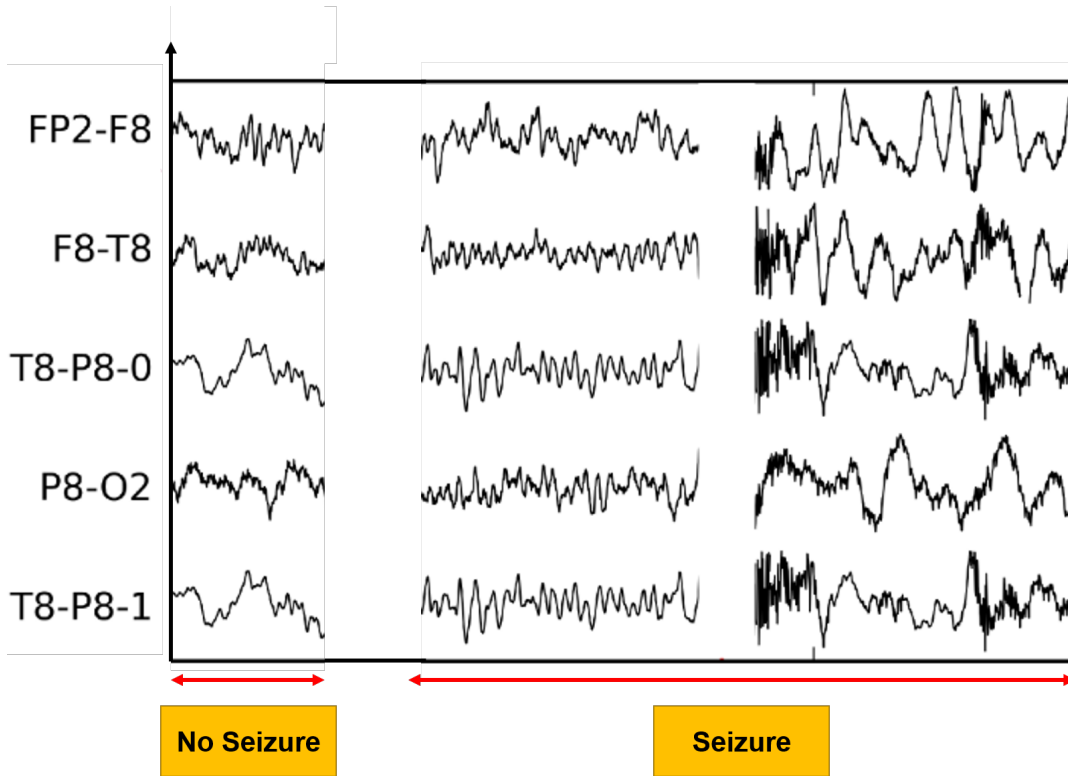
Figure 4.1: Inter-channel correlation during seizure vs. no-seizure [27].

4.2.1 Neural Mutual Information Estimation

In order to compute inter-channel correlation among recordings, the most popular approach is cross-correlation which is a measure of similarity between one signal and the time-delayed version of other signals; however, this method is unable to capture nonlinear correlation between samples. Unlike cross-correlation, MI represents higher-order joint statistics and is thus able to capture non-linear relationships between samples, which are likely to occur in EEG signals during the seizure. MI can quantify the dependencies between random variables. Mathematically, it can be formulated as (4.1):

$$I(X_1; X_2) = \int_{\mathcal{X}_1 \times \mathcal{X}_2} \log\left(\frac{d\mathbb{P}_{X_1 X_2}}{d\mathbb{P}_{X_1} \otimes \mathbb{P}_{X_2}}\right) d\mathbb{P}_{X_1 X_2} \tag{4.1}$$

where $\mathbb{P}_{X_1 X_2}$ is the joint probability distribution and $\mathbb{P}_{X_1}$ and $\mathbb{P}_{X_2}$ are marginals. X_1 and X_2 represent two random variables where in the case of seizure detection, they can be interpreted
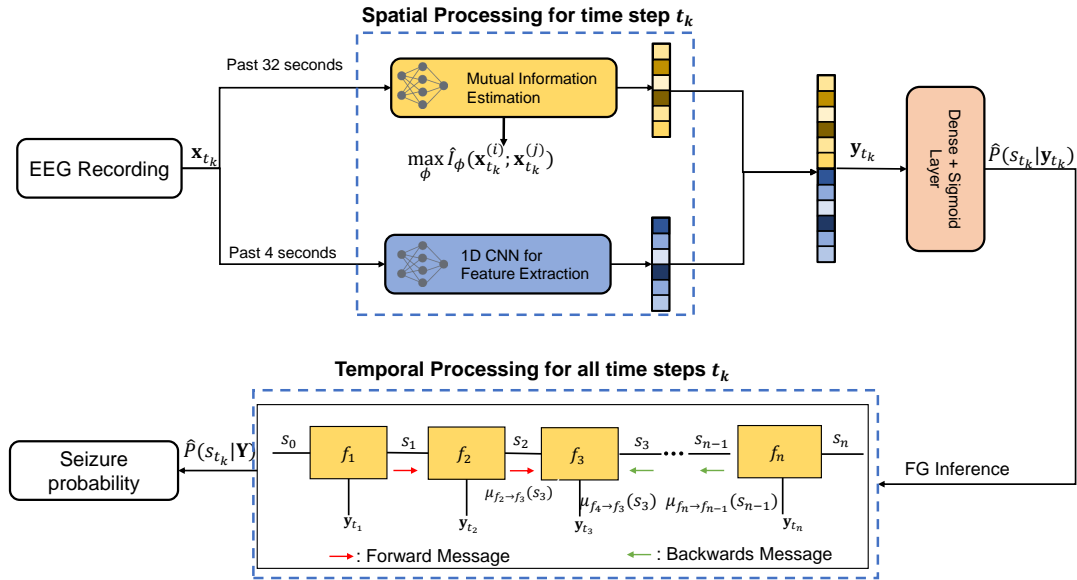
Figure 4.2: MICAL illustration.

as the recordings for two different channels.

A general estimator for MI computation is equivalent to the Kullback-Leibler (KL) divergence between the joint and the product of the marginals of two random variables X_1 and X_2 [35]:

$$I(X_1, X_2) = D_{KL}(\mathbb{P}_{X_1 X_2} \| \mathbb{P}_{X_1} \otimes \mathbb{P}_{X_2}) \tag{4.2}$$

where D_{KL} is defined as:

$$D_{KL}(\mathbb{P} \| \mathbb{Q}) := \mathbb{E}_{\mathbb{P}} \left[\log \frac{d\mathbb{P}}{d\mathbb{Q}} \right] \tag{4.3}$$

Although MI is a more accurate measure of high correlation among channels recording during seizure compared to cross-correlation, the exact calculation based on (4.1) and (4.3) for EEG samples which do not have specific probability distribution is challenging [45]. To address this issue, Belghazi et al. [8] proposed a general-purpose Mutual Information Neural Estimator (MINE). A key technical aspect of MINE is dual representations of the KL-divergence, which is based on Donsker-Varadhan representation [13]. This representation leads to the following

lower-bound where the supremum is taken over all functions T such that the two expectations are finite.

$$D_{KL}(\mathbb{P}\|\mathbb{Q}) \geq \sup_{T \in \mathcal{F}} \mathbb{E}_{\mathbb{P}}[T] - \log\left(\mathbb{E}_{\mathbb{Q}}\left[e^T\right]\right) \tag{4.4}$$

Using both (4.3) and dual representation of KL-divergence, the idea is to choose $\mathcal{F}$ to be the set of functions $T_\theta : \mathcal{X}_1 \times \mathcal{X}_2 \to \mathbb{R}$ parametrized by a deep neural network with parameters $\theta \in \Theta$ and moving average gradient ascent to find the optimal parameters. This network is called a statistics network, where the bound is calculated as:

$$I(X_1; X_2) \geq I_\theta(X_1, X_2) \tag{4.5}$$

and the neural information measure, $I_\theta(X_1, X_2)$ is defined as:

$$I_\theta(X_1, X_2) = \sup_{\theta \in \Theta} \mathbb{E}_{\mathbb{P}_{X_1 X_2}}[T_\theta] - \log\left(\mathbb{E}_{\mathbb{P}_{X_1} \otimes \mathbb{P}_{X_2}}\left[e^{T_\theta}\right]\right) \tag{4.6}$$

It should be noted, the most critical limitation of MINE is the variance can exponentially grow by ground truth which results in poor bias-variance trade-offs. In order to solve the bias problem, Song et al. [56] considered T as the invertible function of the density ratio. To achieve this purpose, they used variational f-divergence proposed by Nyugen et al. [43] leading to the following lower-bound for MI estimation: (Nyugen et al. (NWJ)). $\forall P, Q \in \mathcal{P}(\mathcal{X})$ such that $P \ll Q$,

$$D_{KL}(\mathbb{P}\|\mathbb{Q}) = \sup_{T \in L^\infty(Q)} \left\{\mathbb{E}_{\mathbb{P}}[T] - \log\left(\mathbb{E}_{\mathbb{Q}}\left[e^{T-1}\right]\right) := I_{NWJ}(T)\right\} \tag{4.7}$$

and $D_{KL}(\mathbb{P}\|\mathbb{Q}) = I_{NWJ}(T)$ when $T = \log\frac{dP}{dQ} + 1$ which leads to unbiased mini-batch estimator. To address the issue of high variance, the partition function is clipped and the following
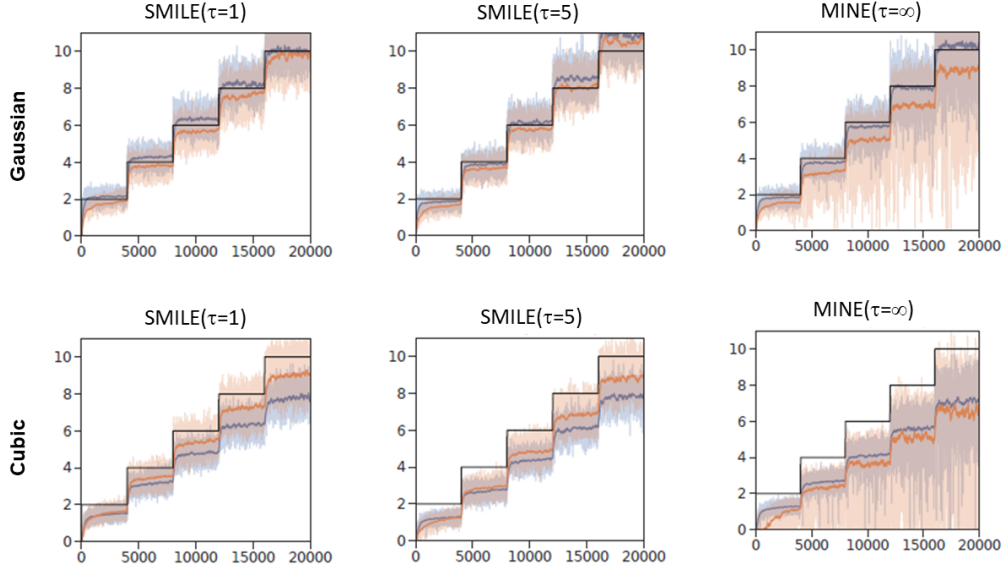
Figure 4.3: Performance of mutual information estimation approaches on Gaussian (top row) and Cubic (bottom row) for SMILE and MINE. (black line is ground truth, blue and orange graphs are estimated MI and shadows show the variance.) [56]

estimator with smooth partition function is achieved [56]:

$$\hat{I}_\theta(X_1;X_2) = \mathbb{E}_{P_{X_1 X_2}}\left[T_\theta(x_1, x_2)\right] - \log \mathbb{E}_{P_{X_1} P_{X_2}}\left[\mathrm{clip}(e^{T_\theta(x_1, x_2)}, e^{-\tau}, e^\tau)\right], \qquad (4.8)$$

Where, $clip(v, l, u) = max(min(v, u), l)$.

Therefore, in [56], T_θ is a neural network that estimates the log-density ratio with hyperparameter τ. This approach is called the Smoothed Mutual Information "Lower-bound" Estimator (SMILE).

To investigate the performance of SMILE, the mutual information estimation on two toy tasks based on Gaussian and Cubic distributions are compared with the ground truth MI. Fig. 4.3 indicates the effect of employing SMILE on estimated MI for number of iterations. As shown, the MINE estimator represents high bias and high variance, while employing SMILE reduces the bias and variance values and makes the estimated MI similar to the ground truth.

In a nutshell, MICAL uses SMILE to estimate $I(x_t^{(i)}; x_t^{(j)})$ at each block t for each channel pair i, j. Since MI is symmetric, i.e., $I(x_t^{(i)}; x_t^{(j)}) = I(x_t^{(j)}; x_t^{(i)})$, we only estimate the MI for
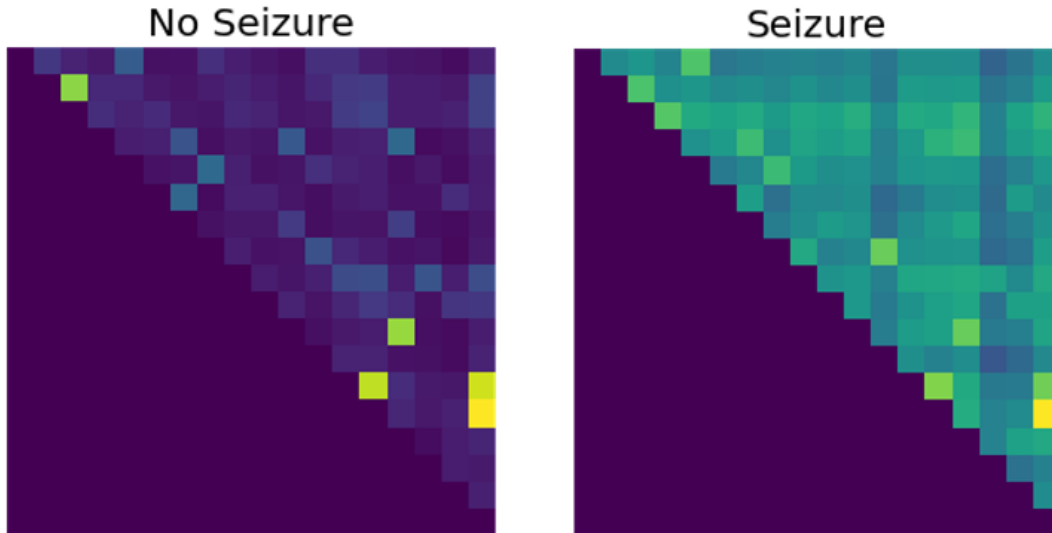
Figure 4.4: Neural MI estimation for seizure and non-seizure.

$j > i$. T_θ is set to be a fully-connected network with two hidden layers and ReLU activations, and train it with $\tau = 0.9$ in the objective (4.8). The resulting neural estimator, which learns to capture statistical dependence, is numerically shown to reflect on the presence of seizure, satisfying the underlying hypothesis of high correlation among recordings during seizure state. This is illustrated in Fig. 4.4, where it is observed that the trained estimator outputs higher MI values during seizure compared to non-seizure blocks.

4.2.2 1D CNN

Parallel to MI estimator, we design and employ a 1D CNN in order to produce latent representation of raw EEG signals. For having a comparable configuration with the baseline model [10], the same number of layers, including convolutions, pooling, dropout, and fully connected layers, are chosen. As shown in Fig. 4.5, we design kernel size in a way that we can obtain a high receptive field compared to prior works. Our proposed 1D CNN is able to cover almost 1 second of the data while previous researches showed only 30 milliseconds. Having high receptive field results in capturing long term correlation as well as capturing low-frequency components of EEG signals. Moreover, unlike 2D CNN where measurements closer to the filters are considered to be processed, 1D CNN can operate on all EEG channels at a given time instance. Details of the proposed CNN are indicated in Fig. 4.5.

Input	Conv1	Conv2	Conv3	Conv4	Conv5	Conv6
EEG dataset (1025×18)	8×Conv(10) 8×Conv(22) BN, ReLU MaxPool(1×2)	8×Conv(10) 8×Conv(22) BN, ReLU MaxPool(1×2)	8×Conv(10) 8×Conv(22) BN, ReLU MaxPool(1×2)	16×Conv(10) 16×Conv(22) BN, ReLU MaxPool(1×2)	16×Conv(10) 16×Conv(22) BN, ReLU MaxPool(1×2)	8×Conv(1) Dropout(0.25)

Figure 4.5: Proposed 1D CNN architecture.

Algorithm 2: MICAL seizure detection

---

1 **Inputs:** SMILE and 1D CNN networks, estimated $P(s_{t_k}|s_{t_{k-1}})$, EEG signals X, threshold T

  Feature extraction:

2 **for** $k = 1, \ldots n$ **do**

3 $\quad$ Apply SMILE to estimate $\hat{I}_\theta(x_{t_k}^{(i)}; x_{t_k}^{(j)})$, $j > i$;

4 $\quad$ Apply 1D CNN to obtain combined features y_{t_k} and obtain soft decision;

5 **end**

  Factor graph inference:

6 Compute $\{f_i\}$ from soft decisions via (4.14);

7 **for** $k = 1, \ldots n$ **do**

8 $\quad$ Compute $\mu_{f_{t_k} \to s_k}(\{0, 1\})$ via (4.12);

9 $\quad$ Compute $\mu_{f_{t_{n-k+2}} \to s_{n-k+1}}(\{0, 1\})$ via (4.13);

10 **end**

11 Detect seizure at t_k if $\mu_{f_{t_k} \to s_k}(1)\mu_{f_{t_{k+1}} \to s_k}(1) > T$.

4.2.3 Factor Graph Inference

Predicting seizure solely based on combined features from MI estimator and 1D CNN does not take into account past and future EEG blocks. Therefore, we utilize block-wise soft decisions as learned function nodes in a factor graph to incorporate the presence of temporal correlation. We follow our proposed factor graphs from a previously developed algorithm for sleep stage detection for time sequence data [55]. Factor graph represents the factorization of local functions of several variables, typically forming a graphical structure of joint distribution measures [40]. For instance, function $f(u, w, x, y, z)$ can be factorized as:

$$f(u, w, x, y, z) = f_1(u, w, x)f_2(x, y, z)f_3(z) \tag{4.9}$$

The factor graph illustration for this factorization is shown in Fig. 4.6.

A factor graph consists of nodes and variables where for every factor and variable, there are
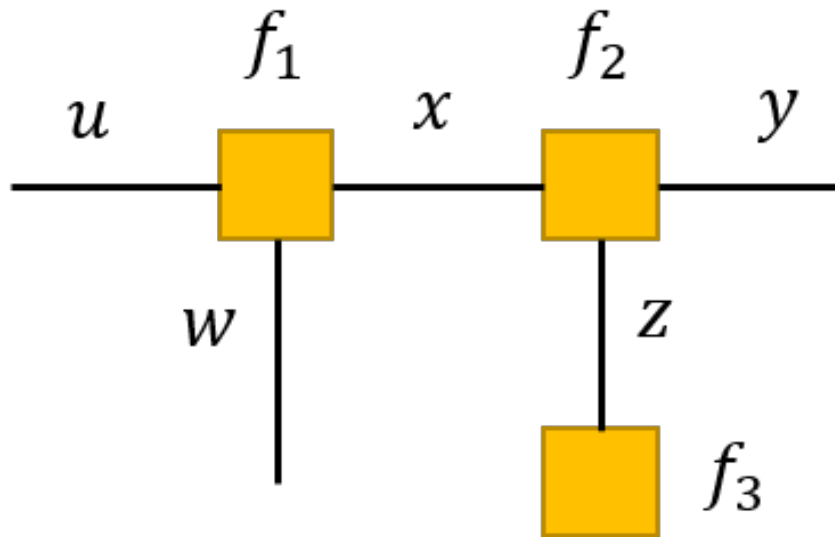
Figure 4.6: Simple factor graph structure.

unique nodes and unique edges, respectively. In addition, a factor node is connected to a variable edge if and only if the factor is a function of the variable. Implicitly, no variable appears in more than two factors. As indicated in Fig.4.2, we employ Forney style representation where variable nodes are replaced by edges. The key advantage of this style is that it can be decoded by the sum-product method used in the factor graph. To implement factor graph inference, the first step is to create the structure of the graph, i.e. interconnection between nodes. For this purpose, we use the underlying property of seizure mechanism where the generation of seizure is closely associated with abnormal synchronization of neurons [42]. To incorporate this feature in our model, we adopt the first-order HMM. HMM is widely used in modeling time series data, and it is mostly based on the probabilistic method. HMM can be represented as a chain model where future and current states are determined by previous state [38]. The Markovian architecture leads to exploiting temporal correlation in seizure detection procedures at reduced complexity and makes the model well-suited in real-time applications. Mathematically, we assume $\boldsymbol{y} = \{y_1, y_2, \cdots, y_N\}$ as extracted features and latent seizure states $\boldsymbol{s} = \{s_1, s_2, \cdots, s_N\}$ over N consecutive blocks that can be related by an HMM. The latent state supposed to satisfy the Marchovian property carries binary values of $s_i \in \{0, 1\}$, and it shows the presence or absence of seizure in a block. Under HMM assumption, the joint probability distribution between

extracted features and the states can be formulated as:

$$P(\boldsymbol{s}, \boldsymbol{y}) = \prod_{i=1}^{N} P(s_i|s_{i-1})P(y_i|s_i). \tag{4.10}$$

where $P(s_i|s_{i-1})$ represents transition probability which is a control parameter, and it is manually set to be 89.54% for switching from no-seizure to seizure and 17.9% for the opposite situation. The next step towards seizure detection is classifying the states based on HMM. This requires to achieve marginal distribution $P(s_i, \boldsymbol{y})$ from (4.10); however, the marginalisation task as a metric to compute the maximum a-posteriori probability detector is computationally expensive since it grows exponentially with the block size. Therefore, a factor graph inference-based sum-product algorithm is employed to calculate the same process linearly to overcome this limitation. The sum-product method establishes the relationship between marginal probability and the product of messages. Where for each $k \in \{1, \ldots, N\}$, it can be written as:

$$P(s_k, \boldsymbol{y}) = \mu_{f_j \to s_k}(s_k) \cdot \mu_{f_{j+1} \to s_k}(s_k). \tag{4.11}$$

In (4.11), $\mu_{f_j \to s_k}(s_k)$ is interpreted as forward message:

$$\mu_{f_j \to s_k}(s_k) = \sum_{\{s_1, \cdots, s_{k-1}\}} \prod_{i=1}^{n} f_i(y_i, s_i, s_{i-1}), \tag{4.12}$$

and $\mu_{f_{j+1} \to s_k}(s_k)$ as the backward message is achieved by:

$$\mu_{f_{j+1} \to s_k}(s_k) = \sum_{\{s_{k+1}, \cdots, s_N\}} \prod_{i=n+1}^{N} f_i(y_i, s_i, s_{i-1}), \tag{4.13}$$

where $f_i(y_i, s_i, s_{i-1})$ is function node and it is given by:

$$f_i(y_i, s_i, s_{i-1}) = P(s_i|s_{i-1})P(y_i|s_i). \tag{4.14}$$

The resultant marginal distributions (4.11) are compared to a predefined threshold T of 0.5 for

detection. According to (4.14), implementing sum-product algorithm requires the knowledge of probability distribution $P(y_i|s_i)$. In practice, obtaining this statistical model that relates observations and time series is a highly complex process. As such, we follow the work in [55] which relies on a hybrid model and data-driven approach. We, therefore, use joint features of MI estimator and 1D CNN as the soft estimate of probability distributions to learn function nodes in the factor graph. Algorithm 2 summarizes the steps in MICAL seizure detection.

4.2.4 Data description

4.2.4.1 EEG Data

The dataset used in this work is the publicly available CHB-MIT Database collected at the Children's Hospital Boston. CHB-MIT consists of scalp EEG recordings from pediatric subjects with intractable seizures [20][1]. Recordings belong to 24 cases with ages from 1.5 to 22. Each patient contains 9 to 42 EDF files from a single subject. All signals were sampled at 256 samples per second with 16-bit resolution, and seizure start and end times are labeled. Moreover, the International 10-20 system of EEG electrode positions and nomenclature was used for these recordings. As indicated in Fig.4.7, letters represent the area of the brain under electrodes e.g., F- Frontal lobe and T - Temporal lobe. Also, Even numbers refer to the right side of the head, and odd numbers denote the left side of the head.

4.2.4.2 EEG Pre-processing

Unlike prior works, we consider simple pre-processing steps for our proposed algorithm that makes it well-suited for real-time applications. Since seizures duration (from 7 seconds to 753 seconds) compared to overall recording (from 959 seconds to 14427 seconds) is very short and to have a balanced dataset, first EDf files that include at least one seizure are selected. Each recording is then shortened to 10 times the seizure duration before and 10 times the seizure duration after the seizure. Therefore, for every second of seizure data, there are 20 seconds of non-seizure data. From EEG channels, the 18 bipolar montages are chosen: FP1-F7, F7-T7,

---

[1]This database is available online at PhysioNet (`https://physionet.org/physiobank/database/chbmit/`)
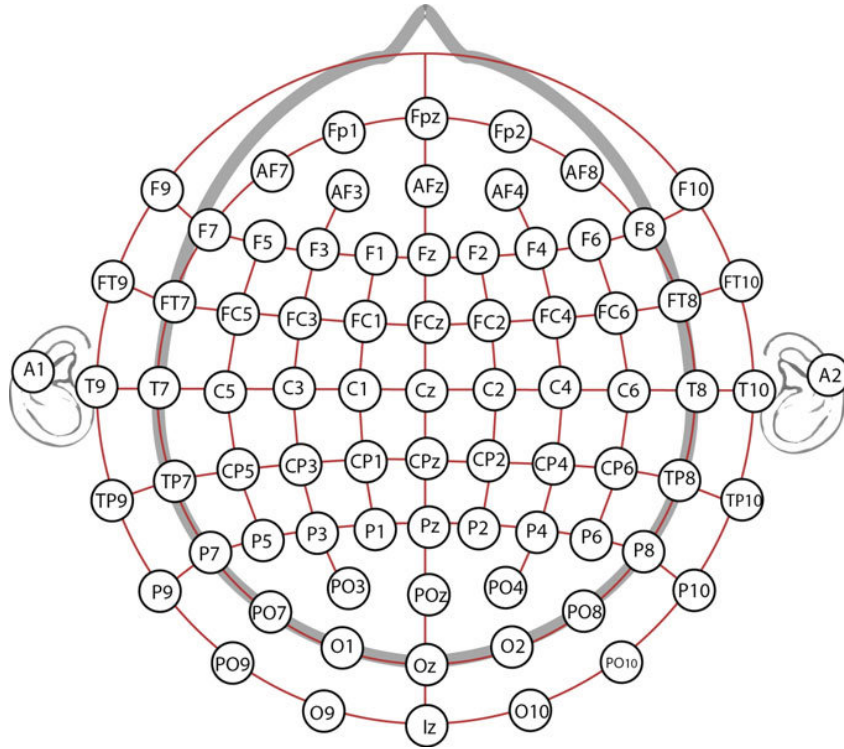
Figure 4.7: Electrode Placement according to the International 10-20 System[47].

T7-P7, P7-O1, FP1-F3, F3-T3, T3-P3, P3-O1, FP2-F4, F4-C4, C4-P4, P4-O2, FP2-F8, F8-T8, T8-P8, P8-O2, FZ-CZ, CZ-PZ. Hereafter, a notch filter is applied to remove 60 Hz line noise from each EEG signal. To estimate the probability of seizure over the t-th second, the past 32 seconds of recording is used to solve the optimization that estimates MI. This window size is large enough to incorporate the correlation among measurements during ictal state and demonstrates the best results over the dataset. In addition, the past 4 seconds of recording is used as input to the 1D CNN for estimating meaningful features from EEG blocks. The value of 4 seconds is selected to satisfy a good trade-off between the number of samples in a block and the stationarity of the observed signals over a block.

4.3   Results and Discussion

To evaluate the performance of models for the experiments, four following metrics are measured:

- *AUC-ROC*: is the area under receiver operating characteristics (ROC) curve, which shows

the capability of the model to distinguish between seizure and no-seizure samples.

- *AUC-PR*: is the area under the precision-recall curve which represents success and failure rates meaning that the high area under the curve shows a low false-positive rate and low false-negative rate.

- *F1 score*: is a harmonic mean of recall and precision where former indicates the proportion of real positive cases that are correctly predicted positive and latter denotes the ratio of predicted positive cases that are correctly real positive [46].

- *Confusion matrix*: shows a summary of predicted results for a model. The number of true and false predictions are represented with count values and broken down by each class.

	AUC-ROC	AUC-PR	F1 score
2D CNN [10]	0.78 ± 0.08	0.37 ± 0.17	0.88 ± 0.03
Spectrogram [26]	0.77 ± 0.07	0.37 ± 0.1	0.92 ± 0.03
1D CNN	0.82 ± 0.04	0.42 ± 0.12	0.91 ± 0.02
1D CNN-GRU	0.82 ± 0.03	0.44 ± 0.10	0.90 ± 0.06
MICAL	**0.83 ± 0.04**	**0.50 ± 0.13**	**0.93 ± 0.01**

Table 4.1: Summary of results

MICAL is generalized well across all patients as we conduct a 6-fold-leave-4-patient-out evaluation. Hence, for each fold, four different patients are kept out for the test. In our experiment, we consider 5 different configurations for comparison, including two baseline models, since they showed the best results compared to previous studies. One model is related to non-feature-based design, and the other is based on a deep learning-based feature extraction algorithm. The 2D CNN was employed to raw EEG signals in [10] and Jana et al. [26] proposed an architecture comprised of spectrogram detection and a 1D CNN. To observe the effect of each component in MICAL, we use our proposed 1D CNN without MI estimator and factor graphs as well as apply GRU to our CNN to have another model that mitigates temporal correlation.

Fig 4.8 shows average values of ROC across all 6 folds and Table 4.1 summarizes the results for three performance measures. Our proposed CNN results in Table 4.1 show that applying 1D
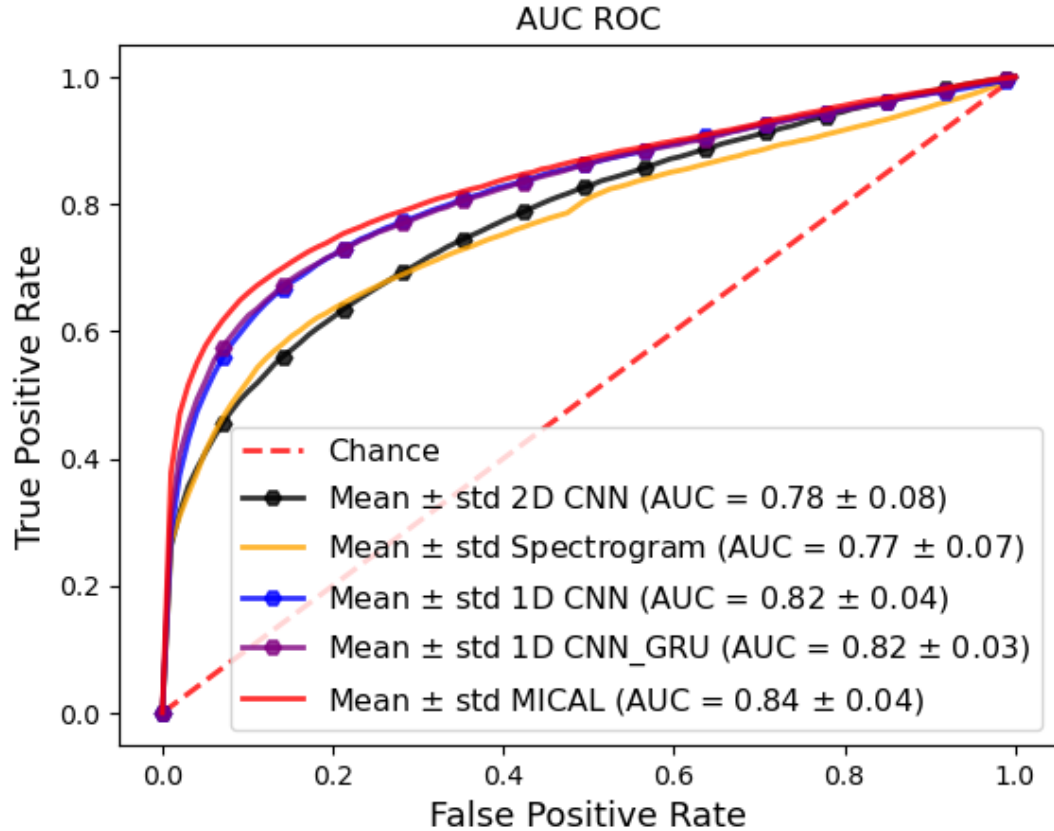
Figure 4.8: Area under ROC curve for all architectures.

CNN can improve the performance by as much as 5% compared to [26, 10]. Despite exploiting temporal correlation by 1D CNN-GRU model, it is important to note that adding this RNN black box to 1D CNN does not make a significant change in the results. However, the best performance is achieved by MICAL which highlights the impact of MI estimation as well as factor graph on the accuracy of the seizure detection system. As shown, MICAL yields an F1 score of 0.93 and 0.83 and 0.50 for AUC-ROC and AUC-PR, respectively. From a clinical perspective, specifically, AUC-PR shows the highest value for MICAL that implies the lowest false-negative and lowest false positive rates compared to other configurations. Furthermore, comparing the confusion matrices of MICAL with baseline models in Fig.4.9, our algorithm performs better than [26, 10], specifically MICAL decreases the false positive rate.
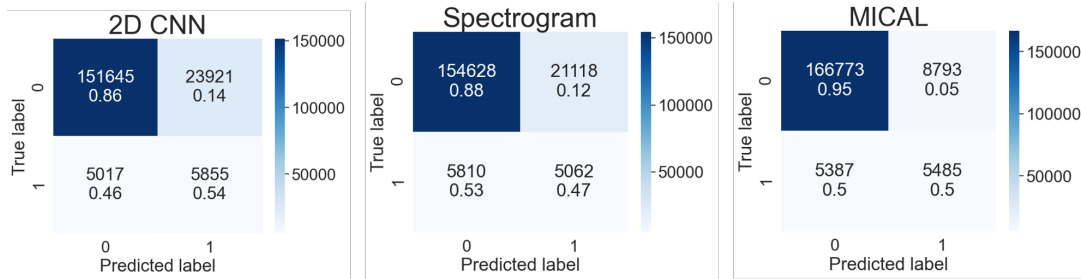
Figure 4.9: Confusion matrices for two baseline models and MICAL.

4.4 Conclusions

In this work, we introduced MICAL which is a hybrid model-based data-driven detector. MICAL is able to exploit inter-channel correlation as a result of seizure occurrence through MI estimation. Our proposed approach also benefits from capturing temporal correlation efficiently via factor graph inference. The neural MI estimator used in MICAL computes the MI between each pair of EEG channels, and it satisfies the underlying hypothesis of existing highly non-linear correlation during seizure states. Moreover, applying factor graph to the soft estimate of joint features from MI estimator and our design 1D CNN leads to exploring the temporal correlation of EEG blocks at reduced complexity and high accuracy. MICAL delivers the best performance results compared to previously observed models.

References

[1] Epilepsy. `https://www.who.int/news-room/fact-sheets/detail/epilepsy`.

[2] U Rajendra Acharya, Shu Lih Oh, Yuki Hagiwara, Jen Hong Tan, and Hojjat Adeli. Deep convolutional neural network for the automated detection and diagnosis of seizure using eeg signals. *Computers in biology and medicine*, 100:270–278, 2018.

[3] Nurettin Acir, Ibrahim Oztura, Mehmet Kuntalp, Baris Baklan, and Cuneyt Guzelis. Automatic detection of epileptiform events in eeg by a three-stage procedure based on artificial neural networks. *IEEE Transactions on Biomedical Engineering*, 52(1):30–40, 2004.

[4] David Ahmedt-Aristizabal, Clinton Fookes, Kien Nguyen, and Sridha Sridharan. Deep classification of epileptic signals. In *2018 40th Annual International Conference of the IEEE Engineering in Medicine and Biology Society (EMBC)*, pages 332–335. IEEE, 2018.

[5] Rohan Akut. Wavelet based deep learning approach for epilepsy detection. *Health information science and systems*, 7(1):1–9, 2019.

[6] Amjed S Al-Fahoum and Ausilah A Al-Fraihat. Methods of eeg signal features extraction using linear analysis in frequency and time-frequency domains. *International Scholarly Research Notices*, 2014, 2014.

[7] Umar Asif, Subhrajit Roy, Jianbin Tang, and Stefan Harrer. Seizurenet: Multi-spectral deep feature learning for seizure type classification. In *Machine Learning in Clinical Neuroimaging and Radiogenomics in Neuro-oncology*, pages 77–87. Springer, 2020.

[8] Mohamed Ishmael Belghazi, Aristide Baratin, Sai Rajeshwar, Sherjil Ozair, Yoshua Bengio, Aaron Courville, and Devon Hjelm. Mutual information neural estimation. In *International Conference on Machine Learning*, pages 531–540. PMLR, 2018.

[9] Boualem Boashash and Samir Ouelha. Automatic signal abnormality detection using time-frequency features and machine learning: A newborn eeg seizure case study. *Knowledge-Based Systems*, 106:38–50, 2016.

[10] Poomipat Boonyakitanont, Apiwat Lek-uthai, Krisnachai Chomtho, and Jitkomut Songsiri. A Comparison of Deep Neural Networks for Seizure Detection in EEG Signals. *bioRxiv*, page 702654, 2019. Publisher: Cold Spring Harbor Laboratory.

[11] Mary AB Brazier. Spread of seizure discharges in epilepsy: anatomical and electrophysiological considerations. *Experimental neurology*, 36(2):263–272, 1972.

[12] Xuhui Chen, Jinlong Ji, Tianxi Ji, and Pan Li. Cost-sensitive deep active learning for epileptic seizure detection. In *Proceedings of the 2018 ACM International Conference on Bioinformatics, Computational Biology, and Health Informatics*, pages 226–235, 2018.

[13] Monroe D Donsker and SR Srinivasa Varadhan. Asymptotic evaluation of certain markov process expectations for large time, i. *Communications on Pure and Applied Mathematics*, 28(1):1–47, 1975.

[14] Prabhu D Emmady and Arayamparambil C Anilkumar. EEG, Abnormal Waveforms. *StatPearls [Internet]*, 2020. Publisher: StatPearls Publishing.

[15] Themis P Exarchos, Alexandros T Tzallas, Dimitrios I Fotiadis, Spiros Konitsiotis, and Sotirios Giannopoulos. Eeg transient event detection and classification using association rules. *IEEE Transactions on Information Technology in Biomedicine*, 10(3):451–457, 2006.

[16] Oliver Faust, RU Acharya, Alastair R Allen, and CM Lin. Analysis of eeg signals during epileptic and alcoholic states using ar modeling techniques. *Irbm*, 29(1):44–52, 2008.

[17] Robert S Fisher, Walter Van Emde Boas, Warren Blume, Christian Elger, Pierre Genton, Phillip Lee, and Jerome Engel Jr. Epileptic seizures and epilepsy: definitions proposed by the international league against epilepsy (ilae) and the international bureau for epilepsy (ibe). *Epilepsia*, 46(4):470–472, 2005.

[18] Kosuke Fukumori, Hoang Thien Thu Nguyen, Noboru Yoshida, and Toshihisa Tanaka. Fully data-driven convolutional filters with deep learning models for epileptic spike detection. In *ICASSP 2019-2019 IEEE international conference on acoustics, speech and signal processing (ICASSP)*, pages 2772–2776. IEEE, 2019.

[19] Andrew J Gabor and Masud Seyal. Automated interictal eeg spike detection using artificial neural networks. *Electroencephalography and clinical Neurophysiology*, 83(5):271–280, 1992.

[20] Ary L Goldberger, Luis AN Amaral, Leon Glass, Jeffrey M Hausdorff, Plamen Ch Ivanov, Roger G Mark, Joseph E Mietus, George B Moody, Chung-Kang Peng, and H Eugene Stanley. PhysioBank, PhysioToolkit, and PhysioNet: components of a new research resource for complex physiologic signals. *circulation*, 101(23):e215–e220, 2000. Publisher: Am Heart Assoc.

[21] J Gotman and P Gloor. Automatic recognition and quantification of interictal epileptic activity in the human scalp eeg. *Electroencephalography and clinical neurophysiology*, 41(5):513–529, 1976.

[22] Jean Gotman. Automatic recognition of epileptic seizures in the eeg. *Electroencephalography and clinical Neurophysiology*, 54(5):530–540, 1982.

[23] Ramy Hussein, Hamid Palangi, Z Jane Wang, and Rabab Ward. Robust detection of epileptic seizures using deep neural networks. In *2018 IEEE International Conference on Acoustics, Speech and Signal Processing (ICASSP)*, pages 2546–2550. IEEE, 2018.

[24] KP Indiradevi, Elizabeth Elias, PS Sathidevi, S Dinesh Nayak, and K Radhakrishnan. A multi-level wavelet approach for automatic detection of epileptic spikes in the electroencephalogram. *Computers in biology and medicine*, 38(7):805–816, 2008.

[25] Zafer Iscan, Zümray Dokur, and Tamer Demiralp. Classification of electroencephalogram signals with combined time and frequency features. *Expert Systems with Applications*, 38(8):10499–10505, 2011.

[26] Gopal Chandra Jana, Ratna Sharma, and Anupam Agrawal. A 1D-CNN-spectrogram based approach for seizure detection from EEG signal. *Procedia Computer Science*, 167:403–412, 2020. Publisher: Elsevier.

[27] Imene Jemal, Amar Mitiche, and Neila Mezghani. A study of eeg feature complexity in epileptic seizure prediction. *Applied Sciences*, 11(4):1579, 2021.

[28] Xiao Jiang, Gui-Bin Bian, and Zean Tian. Removal of artifacts from eeg signals: a review. *Sensors*, 19(5):987, 2019.

[29] Alexander Rosenberg Johansen, Jing Jin, Tomasz Maszczyk, Justin Dauwels, Sydney S Cash, and M Brandon Westover. Epileptiform spike detection via convolutional neural networks. In *2016 IEEE International Conference on Acoustics, Speech and Signal Processing (ICASSP)*, pages 754–758. IEEE, 2016.

[30] HKMCC Kandar, Sanjay Kumar Das, Lakshmikanta Ghosh, and Bijan Kumar Gupta. Epilepsy and its management: A review. *Journal of PharmaSciTech*, 1(2):20–26, 2012.

[31] Aida Khorshidtalab, Momoh-Jimoh E Salami, and Mahyar Hamedi. Robust classification of motor imagery eeg signals using statistical time–domain features. *Physiological measurement*, 34(11):1563, 2013.

[32] Taeho Kim, Phuc Nguyen, Nhat Pham, Nam Bui, Hoang Truong, Sangtae Ha, and Tam Vu. Epileptic seizure detection and experimental treatment: a review. *Frontiers in Neurology*, 11:701, 2020.

[33] Cheng-Wen Ko and Hsiao-Wen Chung. Automatic spike detection via an artificial neural network using raw eeg data: effects of data preparation and implications in the limitations of online recognition. *Clinical neurophysiology*, 111(3):477–481, 2000.

[34] Sancgeetha Kulaseharan, Azad Aminpour, Mehran Ebrahimi, and Elysa Widjaja. Identifying lesions in paediatric epilepsy using morphometric and textural analysis of magnetic resonance images. *NeuroImage: Clinical*, 21:101663, 2019.

[35] Solomon Kullback. *Information theory and statistics*. Courier Corporation, 1997.

[36] Yann LeCun, Yoshua Bengio, and Geoffrey Hinton. Deep learning. *nature*, 521(7553):436–444, 2015.

[37] Jiseon Lee, Junhee Park, Sejung Yang, Hani Kim, Yun Seo Choi, Hyeon Jin Kim, Hyang Woon Lee, and Byung-Uk Lee. Early seizure detection by applying frequency-based algorithm derived from the principal component analysis. *Frontiers in neuroinformatics*, 11:52, 2017.

[38] Miran Lee, Inchan Youn, Jaehwan Ryu, and Deok-Hwan Kim. Classification of both seizure and non-seizure based on EEG signals using hidden Markov model. In *2018 IEEE International Conference on Big Data and Smart Computing (BigComp)*, pages 469–474. IEEE, 2018.

[39] Jianguo Liu and Blake Woodson. Deep learning classification for epilepsy detection using a single channel electroencephalography (eeg). In *Proceedings of the 2019 3rd International Conference on Deep Learning Technologies*, pages 23–26, 2019.

[40] Hans-Andrea Loeliger. An introduction to factor graphs. 21(1):28–41, 2004.

[41] Kristina Malmgren, Markus Reuber, and Richard Appleton. Differential diagnosis of epilepsy. *Oxford textbook of epilepsy and epileptic seizures*, pages 81–94, 2012.

[42] Florian Mormann, Thomas Kreuz, Ralph G Andrzejak, Peter David, Klaus Lehnertz, and Christian E Elger. Epileptic seizures are preceded by a decrease in synchronization. *Epilepsy research*, 53(3):173–185, 2003.

[43] XuanLong Nguyen, Martin J Wainwright, and Michael I Jordan. Estimating divergence functionals and the likelihood ratio by convex risk minimization. *IEEE Transactions on Information Theory*, 56(11):5847–5861, 2010.

[44] Deb K Pal, Amanda W Pong, and Wendy K Chung. Genetic evaluation and counseling for epilepsy. *Nature Reviews Neurology*, 6(8):445–453, 2010.

[45] Liam Paninski. Estimation of entropy and mutual information. *Neural computation*, 15(6):1191–1253, 2003.

[46] David MW Powers. Evaluation: from precision, recall and F-measure to ROC, informedness, markedness and correlation. *arXiv preprint arXiv:2010.16061*, 2020.

[47] Mirjana Prpa and Philippe Pasquier. Brain-computer interfaces in contemporary art: a state of the art and taxonomy. *Brain art*, pages 65–115, 2019.

[48] Antonio Quintero-Rincón, Marcelo Pereyra, Carlos D'Giano, Hadj Batatia, and Marcelo Risk. A new algorithm for epilepsy seizure onset detection and spread estimation from eeg signals. In *Journal of Physics: Conference Series*, volume 705, page 012032. IOP Publishing, 2016.

[49] Osvaldo A Rosso, Susana Blanco, Juliana Yordanova, Vasil Kolev, Alejandra Figliola, Martin Schürmann, and Erol Başar. Wavelet entropy: a new tool for analysis of short duration brain electrical signals. *Journal of neuroscience methods*, 105(1):65–75, 2001.

[50] Subhrajit Roy, Isabell Kiral-Kornek, and Stefan Harrer. Chrononet: a deep recurrent neural network for abnormal eeg identification. In *Conference on Artificial Intelligence in Medicine in Europe*, pages 47–56. Springer, 2019.

[51] Tolulope T Sajobi, Colin B Josephson, Richard Sawatzky, Meng Wang, Oluwaseyi Lawal, Scott B Patten, Lisa M Lix, and Samuel Wiebe. Quality of life in epilepsy: Same questions, but different meaning to different people. *Epilepsia*, 62(9):2094–2102, 2021.

[52] Tuuli M Salmenpera and John S Duncan. Imaging in epilepsy. *Journal of Neurology, Neurosurgery & Psychiatry*, 76(suppl 3):iii2–iii10, 2005.

[53] Rubén San-Segundo, Manuel Gil-Martín, Luis Fernando D'Haro-Enríquez, and José Manuel Pardo. Classification of epileptic eeg recordings using signal transforms and convolutional neural networks. *Computers in biology and medicine*, 109:148–158, 2019.

[54] R Sankar and J Natour. Automatic computer analysis of transients in eeg. *Computers in biology and medicine*, 22(6):407–422, 1992.

[55] Nir Shlezinger, Nariman Farsad, Yonina C Eldar, and Andrea J Goldsmith. Learned factor graphs for inference from stationary time sequences. *arXiv preprint arXiv:2006.03258*, 2020.

[56] Jiaming Song and Stefano Ermon. Understanding the limitations of variational mutual information estimators. *arXiv preprint arXiv:1910.06222*, 2019.

[57] Susan S Spencer. The relative contributions of mri, spect, and pet imaging in epilepsy. *Epilepsia*, 35:S72–S89, 1994.

[58] Vairavan Srinivasan, Chikkannan Eswaran, Sriraam, and N. Artificial neural network based epileptic detection using time-domain and frequency-domain features. *Journal of Medical Systems*, 29(6):647–660, 2005.

[59] Abdulhamit Subasi, Jasmin Kevric, and M. Abdullah Canbaz. Epileptic seizure detection using hybrid machine learning methods. *Neural Computing and Applications*, 31(1):317–325, January 2019.

[60] Abdulhamit Subasi, M Kemal Kiymik, Ahmet Alkan, and Etem Koklukaya. Neural network classification of eeg signals by using ar with mle preprocessing for epileptic seizure detection. *Mathematical and computational applications*, 10(1):57–70, 2005.

[61] Sachin S Talathi. Deep recurrent neural networks for seizure detection and early seizure detection systems. *arXiv preprint arXiv:1706.03283*, 2017.

[62] Marleen C Tjepkema-Cloostermans, Rafael CV de Carvalho, and Michel JAM van Putten. Deep learning for detection of focal epileptiform discharges from scalp eeg recordings. *Clinical neurophysiology*, 129(10):2191–2196, 2018.

[63] Ömer Türk and Mehmet Siraç Özerdem. Epilepsy detection by using scalogram based convolutional neural network from eeg signals. *Brain sciences*, 9(5):115, 2019.

[64] Alexandros T Tzallas, Markos G Tsipouras, Dimitrios G Tsalikakis, Evaggelos C Karvounis, Loukas Astrakas, Spiros Konitsiotis, and Margaret Tzaphlidou. Automated epileptic seizure detection methods: a review study. *Epilepsy-histological, electroencephalographic and psychological aspects*, pages 75–98, 2012.

[65] Elif Derya Übeyli. Lyapunov exponents/probabilistic neural networks for analysis of eeg signals. *Expert Systems with Applications*, 37(2):985–992, 2010.

[66] Nicole van Klink, Anne Mooij, Geertjan Huiskamp, Cyrille Ferrier, Kees Braun, Arjan Hillebrand, and Maeike Zijlmans. Simultaneous meg and eeg to detect ripples in people with focal epilepsy. *Clinical Neurophysiology*, 130(7):1175–1183, 2019.

[67] Pieter Van Mierlo, Margarita Papadopoulou, Evelien Carrette, Paul Boon, Stefaan Vandenberghe, Kristl Vonck, and Daniele Marinazzo. Functional brain connectivity from eeg in epilepsy: Seizure prediction and epileptogenic focus localization. *Progress in neurobiology*, 121:19–35, 2014.

[68] Lasitha Vidyaratne, Alexander Glandon, Mahbubul Alam, and Khan M Iftekharuddin. Deep recurrent neural network for seizure detection. In *2016 International Joint Conference on Neural Networks (IJCNN)*, pages 1202–1207. IEEE, 2016.

[69] K Vijayalakshmi and Appaji M Abhishek. Spike detection in epileptic patients eeg data using template matching technique. *International Journal of Computer Applications*, 2(6):5–8, 2010.

[70] Scott B Wilson and Ronald Emerson. Spike detection: a review and comparison of algorithms. *Clinical Neurophysiology*, 113(12):1873–1881, 2002.

[71] Jie Yang and Mohamad Sawan. From seizure detection to smart and fully embedded seizure prediction engine: A review. *IEEE Transactions on Biomedical Circuits and Systems*, 14(5):1008–1023, 2020.

[72] Xinghua Yao, Qiang Cheng, and Guo-Qiang Zhang. Automated classification of seizures against nonseizures: A deep learning approach. *arXiv preprint arXiv:1906.02745*, 2019.

[73] Ozan Yardimci and Barış Ç Ayyıldız. Comparison of svm and cnn classification methods for infrared target recognition. In *Automatic Target Recognition XXVIII*, volume 10648, page 1064804. International Society for Optics and Photonics, 2018.

Chapter 5

General Discussion and Conclusion

5.1 Summary

Seizure detection based on EEG recording mainly relies on visual inspection by a neurologist or an expert. While many automatic approaches within the literature have been explored for seizure detection, these algorithms are not accurate or reliable enough to replace experts. Therefore, the initial focus of the thesis was to develop and evaluate a new hybrid algorithm that showed considerable improvement compared to prior work at a reduced complexity. The subsequent chapters then described and observed the impact of MI estimation as a measure of dependency among EEG channels. It was shown that MI can capture inter-channel correlations, and can improve the performance of seizure detection when used as features. Our complete MICAL algorithm was shown to perform better than prior work, especially in terms of cross patient generalizability.

5.2 Strengths and Limitations

The specific strengths for each of the individual contributions have already been discussed within their respective chapters, but here we consolidate these observations.

Our proposed MICAL algorithm can achieve state-of-the-art performance compared to prior work by exploiting the temporal and inter-channel correlations that exist in the data. Specifically, for the first time, we propose using MI to measure the inter-channel correlation.

This method can capture correlations even in the presence of a nonlinear relationship between the channels. To capture the temporal correlations, we used factor graphs, which are computationally more efficient than RNNs. We showed that despite being more efficient, the factor graph inference achieves similar performance as RNNs. We employ a 6-fold-leave-4-patient-out evaluation in our evaluations, which focuses on cross-patient generalizability. The preliminary results in this work are promising and demonstrate that it may be possible to train models that can generalize across patients with acceptable performance.

Although MICAL demonstrates very promising preliminary results, more evaluations are required to find and address the limitations of the proposed method. First, the training session of MI estimator can be time-consuming. To overcome this problem, a graph neural network can be used to compute the MI between all pairs of EEG channels simultaneously. Moreover, the number of patients in the CHB-MIT database is not enough for CNN to learn general features across patients. In addition, this limited size also does not allow us to perform large scale evaluation of our model for a more accurate understanding of its generalizability. For example, for some folds, we have observed overfitting where the model fits well to the training set but not the test set. It is hard to understand what is the cause of the overfitting given the limited data size, and the over fitting can be improved on a larger training dataset.

5.3   Future Directions

The work done within the thesis has provided a framework for investigating a hybrid method for seizure detection that can exploit the temporal and inter-channel correlations to achieve better performance. We will use the TUH database to train and evaluate our model on a much larger dataset as part of future work. We will also seek the help of multiple neurologists to label and choose a random set of challenging examples from this dataset. This challenging test set can then be used to better evaluate the performance of our model and prior work.

We also plan to investigate and understand how much better MI estimation is compared to other correlation measures. This can be achieved by using Pearson correlation or discriminate MI estimation as a correlation measure. Moreover, in addition to MI estimation, directed information (DI) can be another feature that can be employed to quantify the pair-wise causal

influence between EEG channels. The results can then be compared to observe MI or DI (or both) is the most influential factor in seizure detection.

While developing our model, we observed that MI estimation among channels started increasing before the ictal state. In addition, factor graph inference through forwarding messages can predict seizure probability for future EEG blocks. Therefore, we will investigate seizure prediction using some of the techniques we developed in this thesis.

Another challenging task in epileptic seizure application is classifying focal and generalized seizures. For this purpose, the TUH database can be used where signals are annotated for seizure and no-seizure as well as the type of seizure (i.e., focal or generalized). For each patient, the channels from which seizure starts are specified in the dataset. We plan to use this information in the TUH dataset and some of the techniques we presented as part of this thesis for developing an algorithm that automatically can classify the type of seizure.

Curriculum Vitae

Name:	Bahareh Salafian
Post-Secondary Education and Degrees:	Isfahan University of Technology Isfahan, Iran 2014 - 2018 B.Sc. (Electrical Engineering) University of Western Ontario London, ON, Canada 2019 - 2021 M.Sc. (Biomedical Engineering)
Honours and Awards:	Western Graduate Research Scholarship University of Western Ontario, London, ON, Canada 2019 - 2021 Ranked top 6% among undergraduate students of ECE Department Isfahan University of Technology, Isfahan, Iran 2018 Ranked top 0.5% among approximately 300,000 participants in the nationwide university entrance exam, Iran, 2014
Related Work Experience:	Graduate Teaching Assistant, Introduction to Electrical Engineering University of Western Ontario, London, ON, Canada, Winter 2020 Teaching Assistant, C and C++ programming Isfahan University of Technology, Isfahan, Iran, Fall 2015 - Winter 2018 Intern and Project Manager Isfahan University of Medical Sciences Isfahan, Iran, Summer 2017

Publications:

B. Salafian, E. Fishel Ben, N. Shlezinger and S. De Ribaupierre, N. Farsad, "Efficient Epileptic Seizure Detection Using CNN-Aided Factor Graphs", *2021 Annual International Conference of the IEEE Engineering in Medicine and Biology Society. IEEE, 2021* [Epub ahead of print].

R. Kafieh, Z. Amini, H. Rabbani, B. K. Baghbaderani, **B. Salafian**, F. Mazaheri, and M. Mokhtari, "Automatic Multifaceted Matlab Package for Analysis of Ocular Images (AMPAO)", *SoftwareX, vol. 10, p. 100339, 2019*

B. Salafian, R. Kafieh, A. Rashno, M. Pourazizi, and S. Sadri, "Automatic Segmentation of ChoroidLayer in EDI OCT Images Using Graph Theory in Neutrosophic Space", *arXiv preprintarXiv:1812.01989, 2018*

Virtual Presentations:

B. Salafian, E. Fishel Ben, N. Shlezinger and S. De Ribaupierre, N. Farsad, "Efficient Epileptic Seizure Detection Using CNN-Aided Factor Graphs", *43th Annual International Conference of the IEEE Engineering in Medicine and Biology Society. IEEE, November, 2021*.

B. Salafian, E. Fishel Ben, N. Shlezinger and S. De Ribaupierre, N. Farsad, "Epileptic Seizure Detection Using CNN-Aided Factor Graphs and Information Theoretic Measures ", *5th International Conference of Basic and Clinical Multimodal Imaging , October, 2021*.

B. Salafian, E. Fishel Ben, N. Shlezinger and S. De Ribaupierre, N. Farsad, "CNN-aided Factor Graphs With Estimated Mutual Information Features For Seizure Detection ", *Biotechnology and Bioengineering Competition, October, 2021*